INSTRUMENTATION OF A RIGID PAVEMENT SYSTEM

FINAL REPORT

OHIO DEPARTMENT OF TRANSPORTATION
U.S. DEPARTMENT OF TRANSPORTATION
FEDERAL HIGHWAY ADMINISTRATION

Principal Investigators:
Shad M. Sargand
Glenn A. Hazen

Graduate Research Assistants:
Christopher C. Bazeley
Joel R. Copley
Michael E. George

CENTER FOR GEOTECHNICAL AND ENVIRONMENTAL RESEARCH
CIVIL ENGINEERING DEPARTMENT
OHIO UNIVERSITY

April 1997

Roger G.

1. Report No.	2. Government Accession No.	3. Recipient's Catalog No.
FHWA/OH-97/001		

4. Title and Subtitle	5. Report Date
INSTRUMENTATION OF A RIGID PAVEMENT SYSTEM	November, 1996
	6. Performing Organization Code
	8. Performing Organization Report No.
7. Author(s)	10. Work Unit No. (TRAIS)
Shad Sargand, Glenn A. Hazen	
9. Performing Organization Name and Address	11. Contract or Grant No.
Ohio University Department of Civil Engineering Athens, OH 45701	State Job No. 14515(0)
	13. Type of Report and Period Covered
12. Sponsoring Agency Name and Address	Final Report
Ohio Department of Transportation 25 S. Front St. Columbus, OH 43215	14. Sponsoring Agency Code

15. Supplementary Notes

Prepared in cooperation with the U.S. Department of Transportation, Federal Highway Administration

16. Abstract

This research focused on development of a comprehensive field instrumentation program to measure the in-situ responses of a concrete pavement system subjected to Falling Weight Deflectometer (FWD) loading and various environmental conditions. Responses measured were slab stresses, vertical slab deflection, temperature gradient through the slab thickness, base and subgrade soil moisture content, and load transfer pressures at the slab-base interface.

Moisture content was found to increase up to 50% once an expansion crack develops. The temperature gradient through the slab was not linear. Deflections were greatest at the joints for environmental and FWD testing. Significant stresses and deflections developed in all lengths of slabs tested. Lowest stresses were recorded in the 21 foot slabs. Strain measuring sensors were able to detect stress relief due to cracking. Load transfer pressures at the slab-base interface and the moisture level of the base and subgrade did not appear to be significant.

Three-dimensional finite element modeling was shown to be effective for calculating deflections and stresses that develop due to changes in environmental factors and non-destructive testing.

17. Key Words	18. Distribution Statement
highway, rigid pavement, instrumentation, stress, deflection, slabs	No Restrictions. This document is available to the public through the National Technical Information Service, Springfield, Virginia 22161

19. Security Classif. (of this report)	20. Security Classif. (of this page)	21. No. of Pages	22. Price
Unclassified	Unclassified		

Table of Contents

List of Figures

List of Tables

APPENDIX

ACKNOWLEDGMENTS

The authors are grateful to the many individuals who contributed to this effort. The cooperation of the Ohio Department of Transportation personnel was essential to the successful completion of this project. The authors wish to especially thank Roger Green for his many helpful comments and suggestions. We also express our sincere appreciation to William Edwards for the administration and coordination provided.

Chapter 1

Introduction

1.1 General Statement

The strength and durability of rigid pavement make it a very appealing option for highway engineers. However, much is still not understood about the behavior of a rigid slab in the field. The temperature differential that forms in the slab due to solar heating can produce high stresses and large deflections that usually are not accounted for in design. Neglecting these environmental effects in design can lead to accelerated deterioration of the structure, resulting in early replacement and/or more frequent maintenance.

This project provided a substantial amount of data on the behavior of rigid pavement under actual field conditions. Over two hundred instruments were placed in nine slabs by Center for Geotechnical and Environmental Research (CGER) personnel. Data on the stresses and displacements caused by thermal factors were collected in every season for various lengths of slabs. Numerous dynamic tests were conducted at the site as well. All data was processed and placed in tabular format. As a final check for accuracy, some of the data was compared with results given by Finite Element Modeling (FEM) software.

1.2 Literature Review

A significant amount of research is being conducted in the transportation field today. In the past few years, many research papers have been published about rigid pavements. The following paragraphs summarize a few articles related to this project.

In their article, *Field Instrumentation and Performance Modeling of Rigid Pavements,*

Raymond S. Rollings and David W. Pittman express the need for more investigation of the effect temperature has on rigid slabs (1). A discussion of the design methods developed by the U.S. Army Corps of Engineers since WWII notes that actual field data have been collected for load transfer between slabs and used to improve the design procedure. Unfortunately, the Corps uses slab thicknesses as their only criteria for joint spacing and slab size. Rollings and Pittman (1) state that a variety of analytical models is available to calculate temperature effects and induced stresses. They encourage further research to collect field data that can be compared with theoretical models to further improve the design process.

Jamshid M. Armaghani, et al., summarize the effects of solar radiation on Portland Cement Concrete (PCC) in their article, *Temperature Response of Concrete Pavements* (2). Thermocouples and horizontal and vertical Linear Variable Differential Transformers (LVDTs) were placed on six twenty-foot slabs at a test road in Florida. The authors made numerous observations by plotting the temperature differential and displacement versus time. They note that maximum and minimum pavement temperatures generally occur one hour after the corresponding ambient air temperature reaches its maximum or minimum. Their results also support the position that the maximum positive or negative vertical displacement at any point on the slab directly corresponds with the maximum or minimum temperature differential. The second fact provides a starting point for finite element modeling of environmental effects on rigid pavement.

A discussion on the use of the finite element method of analysis to analyze the effects of temperature on a rigid pavement slab is presented in the article *Temperature Effects on Rigid Pavements* by Allen, et al., (3). The magnitudes of displacements and stresses found by conventional methods are compared to those found by finite element analysis. Their research finds that actual

temperature induced stresses and displacements are usually not large enough to exceed the maximum allowable; however, they do have an influence on slab behavior when combined with other types of loading (i.e., wheel loading at the corner of a temperature-deformed slab). The authors state that the temperature effects should be accounted for in rigid pavement design, and the temperature differential between the top and bottom of the slab cannot be accurately modeled with a linear temperature gradient.

The value of information collected by a Dynatest Falling Weight Deflectometer (FWD) is addressed in Jacob Uzan's article, *Rigid Pavement Evaluation Using NDT - Case Study* (4). Uzan is able to back calculate the modulus of elasticity (E) of the concrete slab and the modulus of reaction for the base and subgrade by combining data taken at various points on the slab. Although the pavement response can vary as much as 17% from test to test, the data are accurate enough to estimate the properties very closely to what was found in lab tests performed on material samples taken from the site.

A survey method is used by W.R. Hudson and Patrick R. Flannagan to show more damage is done to a roadway by traffic loading than bending stress caused by environmental effects. *An Examination of Environmental Versus Load Effects on Pavements,* outlines the method used to separate damage caused by the two types of loading (5). Fourteen sites are selected from around the United States. Each site consists of two sections, one open to traffic and one not. Care was taken to ensure that a wide spread of freeze/thaw conditions was represented. The amount of damage (rutting, cracking, etc.) on each section was recorded. For each of the fourteen sites, the section with traffic loading showed more damage than the other. Those sites exposed to harsher freeze/thaw cycles showed more damage than those exposed to mild conditions. Data from this study support

the hypothesis that traffic causes more damage than environmental conditions. The study also shows that high environmental stresses can add to the amount of damage caused by other direct types of loading.

Dan F. Adkins and Gary P. Merkley show that temperature changes can be mathematically modeled in a concrete slab. The article, *Mathematical Modeling of Temperature Change in a Concrete Pavement,* begins with a detailed investigation of how heat energy is transferred through a slab (6). The authors note that heating comes primarily through solar radiation. During the winter months there may not be enough daylight hours for radiant heat from the sun to completely thaw moisture in the slab before temperature returns to freezing by convective heat loss. A mathematical model using finite difference to estimate temperature at various depths in a slab is developed in their article. The actual temperature gradients in a concrete divider wall and a saturated concrete cylinder are measured in field and laboratory tests. Similar results are found for the exposed surface of the slab, but the agreement begins to deteriorate as the depth from the surface increases. As much as a 15°F difference can be found for the predicted and actual values at the bottom of the concrete.

1.3 Objectives

All efforts in this investigation will be focused on the following objectives:

- Determine the deflection and induced stress caused by Falling Weight Deflectometer (FWD) and environmental conditions.
- Compare the FWD induced responses found by CGER instrumentation to those registered by the Ohio Department of Transportation (ODOT).
- Present all recorded data in a clear, understandable format.
- Discuss the reasons for various instrumentation failures.

- Compare environmental and FWD results to values predicted by finite element software.
- Discuss conclusions that can be drawn from the data and make recommendations for future research.

Chapter 2

Site Layout and Instrumentation

2.1 Project Background

The test site is located one mile west of the Burkhardt Road exit on State Route 2 near Vermillion, Ohio. Instrumentation was placed in nine slabs on the westbound traffic lane between stations 114+00 and 124+00 during the first weeks of September, 1993. All of the deflection, pressure, and temperature measuring sensors survived placement in excellent operating condition. Ninety-three percent of the soil moisture, and ninety-eight percent of the strain measuring sensors, survived paving in excellent condition as well.

2.2 Site Layout

The site consists of nine slabs along the westbound lane. All of the slabs are in the traffic lane of a divided four-lane highway. Slabs are numbered beginning in the west and proceeding east. Joint spacing varies from 21 to 60 feet. All slabs have a width of 12 feet, are 10 inches thick, and are supported by a 10 inch base of 304 crushed limestone. Figure 2.1 provides a plan view of the site. Instrumentation wires from each slab are buried in a trench leading to the side of the road. All lead wires terminate at nine concrete pads. Plastic 24 or 36 pin harnesses are used to secure the individual wires and allow quick connection to the data acquisition systems.

Pads supported the portable stainless steel cabinet that was used to protect data collection equipment from the weather during environmental testing. Sheet metal covers protected the lead wire terminations on the other eight pads. All of the pads were supplied with electrical power. Data collection equipment was moved from base to base, and while a base was not in use, leads were pro-

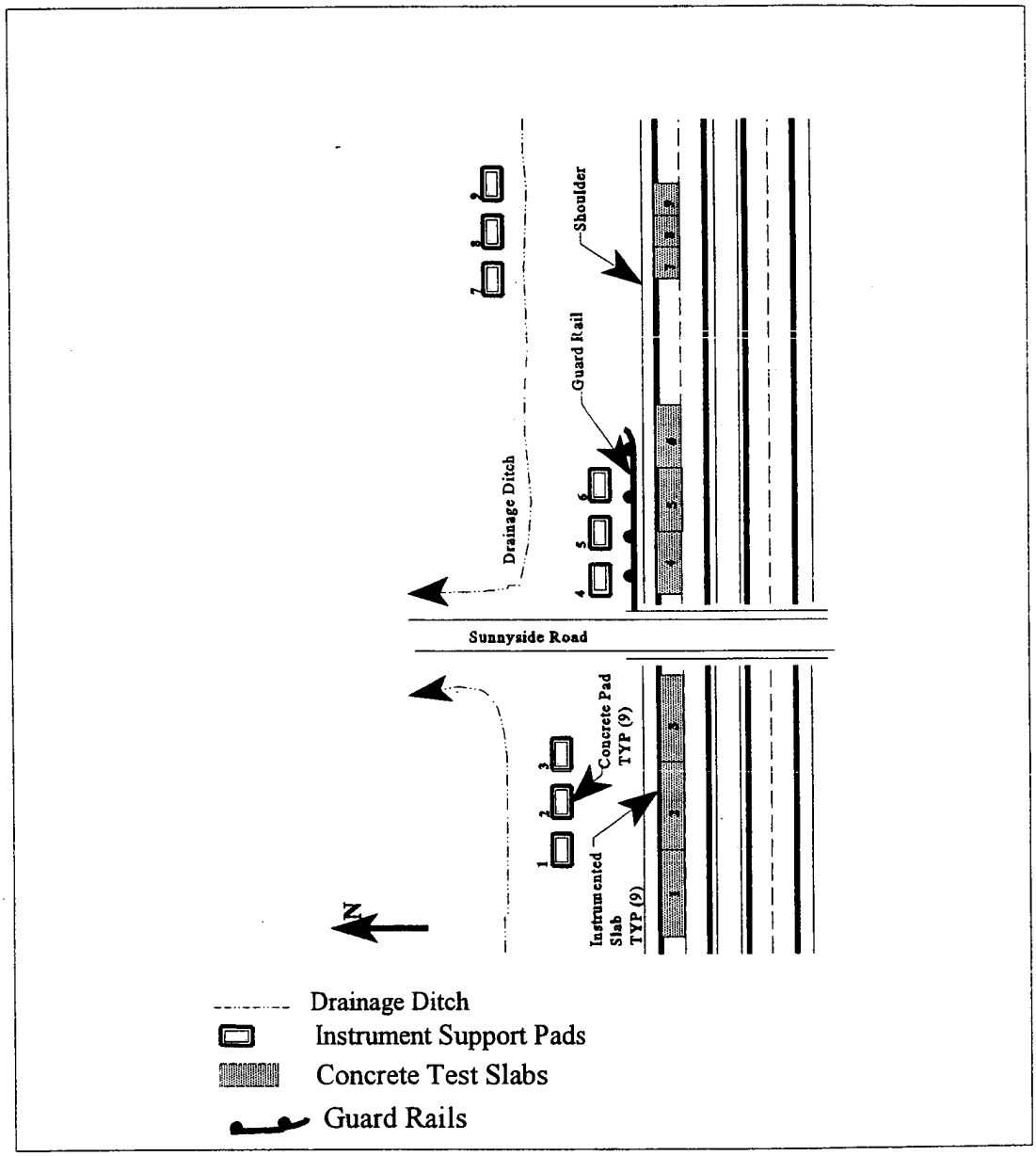

Figure 2.1 Layout of the Rt. 2 site.

tected by sheet metal cover.

2.3 Instrumentation Coordinate System

Due to the large number of gauges buried in the concrete of each slab, it was necessary to establish a coordinate system to keep track of sensor locations. Each slab had its own coordinate system. The origin point of each coordinate system was located mid-way (i.e., longitudinal centerline) along the northern edge of the slab. The northern edge is the edge where the slab contacts the berm. See Appendix A for figures depicting the coordinate system and a summary of instrumentation for the project.

2.4 Instrumentation Selection

This project measured many aspects of slab response. This section describes how they are measured using the selected gauges.

2.4.1 Concrete Slab Temperature Measurement

The temperature gradient through the depth of the slab was measured using J-type thermocouples supplied by Measurement Instruments East, Inc., of Blairsville, Pennsylvania. A J-type thermocouple contains four individual sensors at 0, 3, 6, and 9 inch depths from the tip of the long leg of the tube. The thermocouples were placed in the concrete so that the first sensor was one inch from the finished top of the slab.

2.4.2 Concrete Slab Vertical Displacement Measurement

Vertical deflection of the slab was measured using LVDTs produced by Schlumberger Industries of Buffalo, New York. Each LVDT assembly was placed in the concrete so that the body

was rigidly anchored to the slab. The bottom of the core rested on top of a reference rod cemented well below the slab to base material. Figure 2.2 presents a diagram of an LVDT used on this project. See section 2.6.6 for information on how the reference rod was installed.

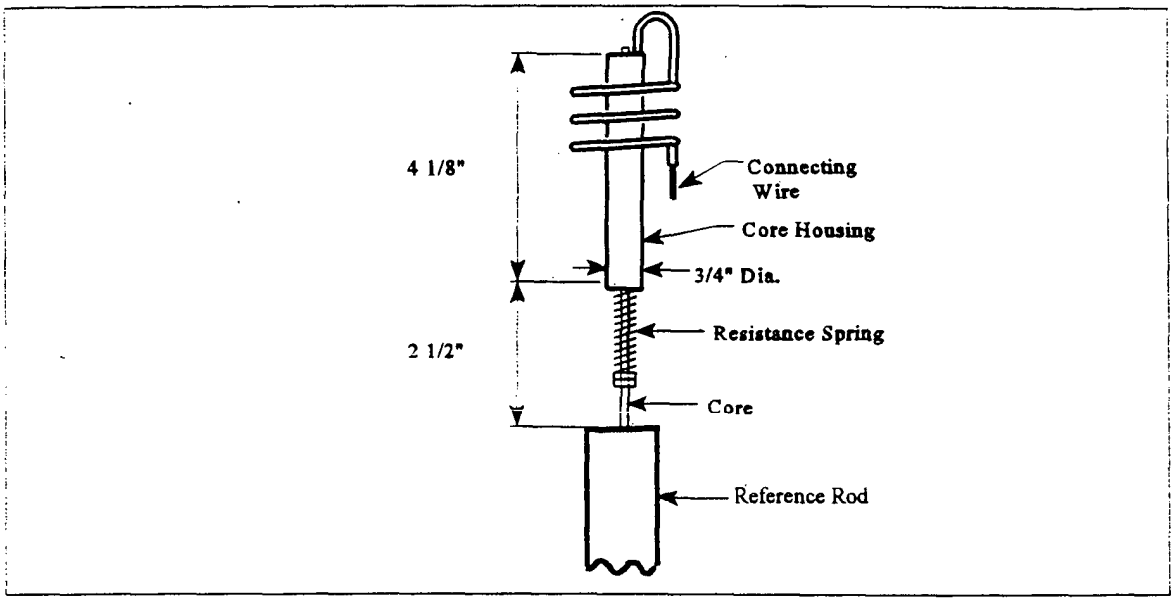

Figure 2.2 Diagram of an LVDT.

All LVDTs used in this project have an average sensitivity of ±0.130 inch/volt at 12 volts excitation. Sensitivity was calibrated by CGER personnel with a digital micrometer. The LVDTs had a linear stroke of ±0.6 inches, and were read as a change in voltage in the ±5 volt range. All LVDTs had an operational temperature range of -36 to 144°F. Each LVDT required a DC power from an outside source during testing.

2.4.3 Concrete Slab Strain Measurement

Strains in the slab were measured using three devices; the KM-100B strain transducer, the PML-60 strain gauge, and the Carlson Strain Meter. Figure 2.3 illustrates each type of strain gauge.

KM-100B strain transducers are manufactured by the Tokyo Sokki Corp. and distributed by Texas Measurements, Inc., of College Station, Texas. The transducers operate as a 350 ohm full

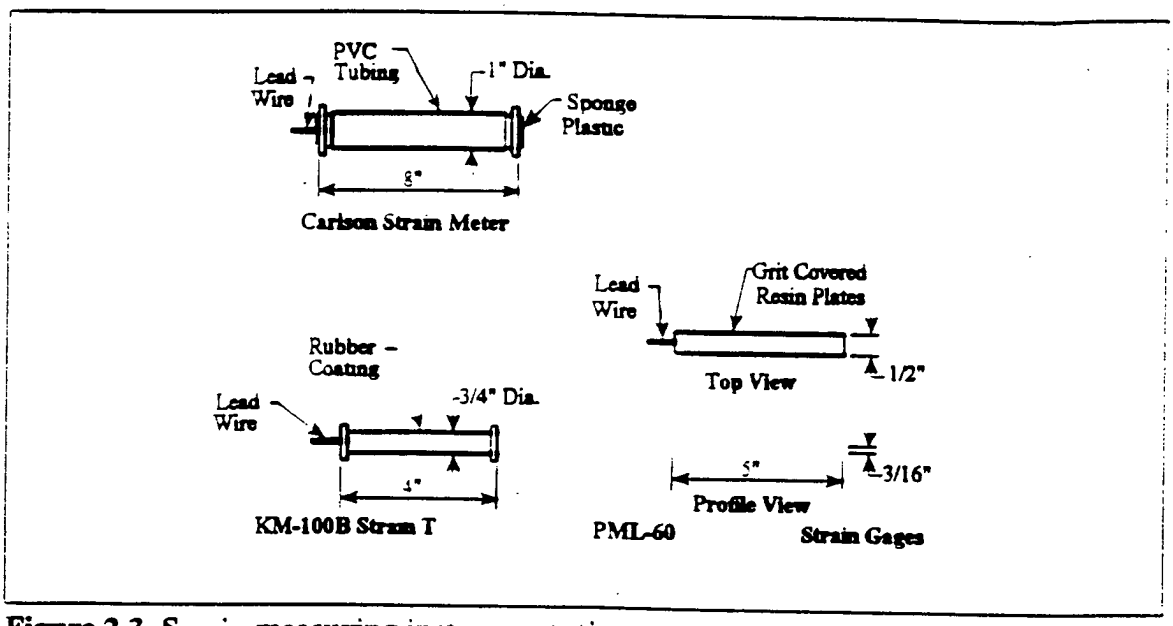

Figure 2.3 S measuring instrumentation.

Wheatstone Bridge configuration. All of the strain transducers used in this project have a gauge factor of approximately 2.0, a strain limit of ±500 microstrains, and an operating temperature range of -4 to 176°F. All strain transducers were located eight inches from the top of the finished slab.

PML-60 embedment strain gauges were also manufactured by the Tokyo Sokki Corp. They use a 120 ohm quarter Wheatstone Bridge configuration. All PML-60s have a gauge factor of 2.12, an operational temperature range of -22 to 144°F, and a strain limit of 2%. The body of the gauge consists of two thin resin plates hermetically sealed and coated with a coarse grit material to ensure adequate bonding with the concrete. PMLs were placed in pairs at 1.5 and 8.5 inch depths. The number and location of PML-60s varied from slab to slab.

B.R. Jones and Associates of Normangee, Texas, distribute the Carlson Strain Meter. The meters were placed five inches from the top of the slab. Two variable resistors were used to measure the deformation of the concrete at that level. The sensing element is an elastic wire, electrical resistance device that acts as both a strain meter and a temperature indicator. The wire is separated

into two coils wrapped around a ceramic core for strain measurement. When the meter is loaded, one resistor is strained more than the other creating a resistance differential. This information is used to calculate both the temperature and the strain using the equation described in Section 4.4.3. The meter is wired in a full Wheatstone Bridge configuration. Accuracy of 0.01 ohms of the total resistance is available.

2.4.4 Slab/Base Interface Pressure Measurement

Two pressure cells measured vertical pressure under each slab; the Model 4810 vibrating wire and the Model 3610 semiconductor. Geokon, Inc., of Lebanon, New Hampshire, manufactured both pressure cells. A diagram of a typical pressure cell is provided in Figure 2.4.

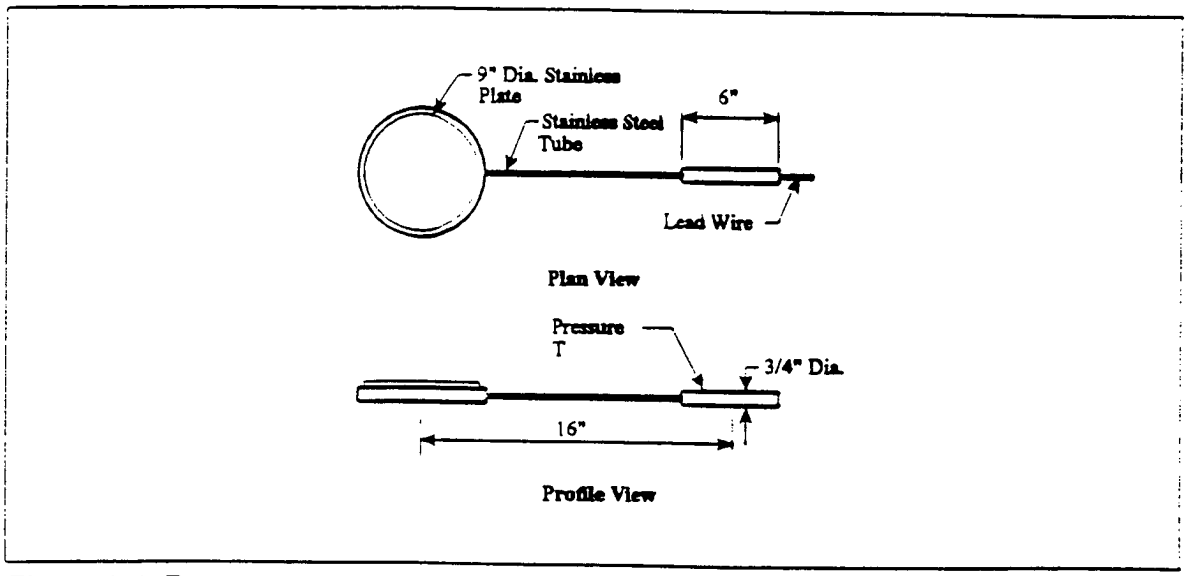

Figure 2.4 Pressure cell diagram.

Both types of pressure cells consist of two nine-inch diameter stainless steel plates separated by a small chamber filled with antifreeze solution. This cavity is connected to a pressure transducer via a thin stainless steel tube. The transducer converts the pressure in the tube into an electrical

signal. Output for a semiconductor cell is the change in voltage read by the transducer. For a vibrating wire pressure cell the output is the frequency of a wire under a load-induced vibration.

Semiconductor pressure cells have a range of measurement from 0 to 10 psi with an output of 0 to 10 volts. Vibrating wire pressure cells have a range of 0 to 25 psi with an output frequency of 1200 to 2000 Hz. Pressure cells were embedded in a 2 inch thick concrete layer with the sensitive face exposed. After laboratory calibration, they were set in a prepared test site.

2.4.5 Soil Moisture Measurement

The volumetric water content of the base and subgrade is found using a two pronged probe manufactured by Campbell Scientific, Inc. Measurement utilizes Time Domain Reflectometry (TDR). This process involves sending a propagation wave along the length of the cable to the probe and measuring the time necessary for the signal to return. The probe consists of two parallel, 12 inch stainless steel rods, two inches apart. Rods were located horizontally at locations where base and subgrade moisture levels were of interest.

2.5 Instrumentation Layout

Every slab contained instruments to measure strain, deflection, pressure, temperature gradient, and soil moisture. The number and placement of these gauges varied from slab to slab. Slabs one, four, and seven had two LVDTs at the longitudinal centerline, while the remaining slabs had three additional LVDTs at the west joint. Sixty foot slabs had 12 PML embedment strain gauges, all 40-foot slabs had 8, and 21-one foot slabs had four. Semiconductor pressure cells are found under slabs one, two, four, five, seven, and eight. Vibrating wire pressure cells were placed under slabs one, three, four, six, seven, and nine.

The remainder of the instrumentation was the same for all slabs. Every slab in the project had two thermocouples, one at the longitudinal centerline and one at the west joint. At the transverse centerline there were two strain transducers and one Carlson strain gauge. Two soil moisture probes were located in the base, one at the longitudinal centerline and one at the west joint. One probe was located in the base material beneath the longitudinal centerline of each slab as well.

Lead wires coming from some of the sensors required splicing to provide enough cable length to reach the concrete pads. Only the LVDTs, strain transducers, and embedment strain gauges required splicing. All splices were sealed using layers of silicone sealant and heat shrink material. Plastic harnesses were used in some cases as extra protection. Splice connections were buried along with the wires and lie directly beneath the shoulder.

All of the wires were routed into a one inch deep trench dug into the base leading to the edge of the roadway. Deepening the trench would have disturbed the compaction of the base material and affected test results. The wires ran from the slab to the pad in a backfilled two foot deep trench. Two pieces of four inch PVC piping were used as conduits to run the wires through the concrete to the top of the pad. All lead wires, except the thermocouples, were collected and placed into harnesses for attachment to data collection equipment at the terminal point. The contractor provided each pad with 120 volts of AC electricity. Figure 2.5 shows a typical cross section of the highway.

2.6 Instrumentation Placement

Installation of all instrumentation occurred in August and September 1993. Placement of the Single Layer Deflectometers (SLDs) and the strain measuring instruments took the majority of the time and required CGER personnel to develop specialized installation hardware.

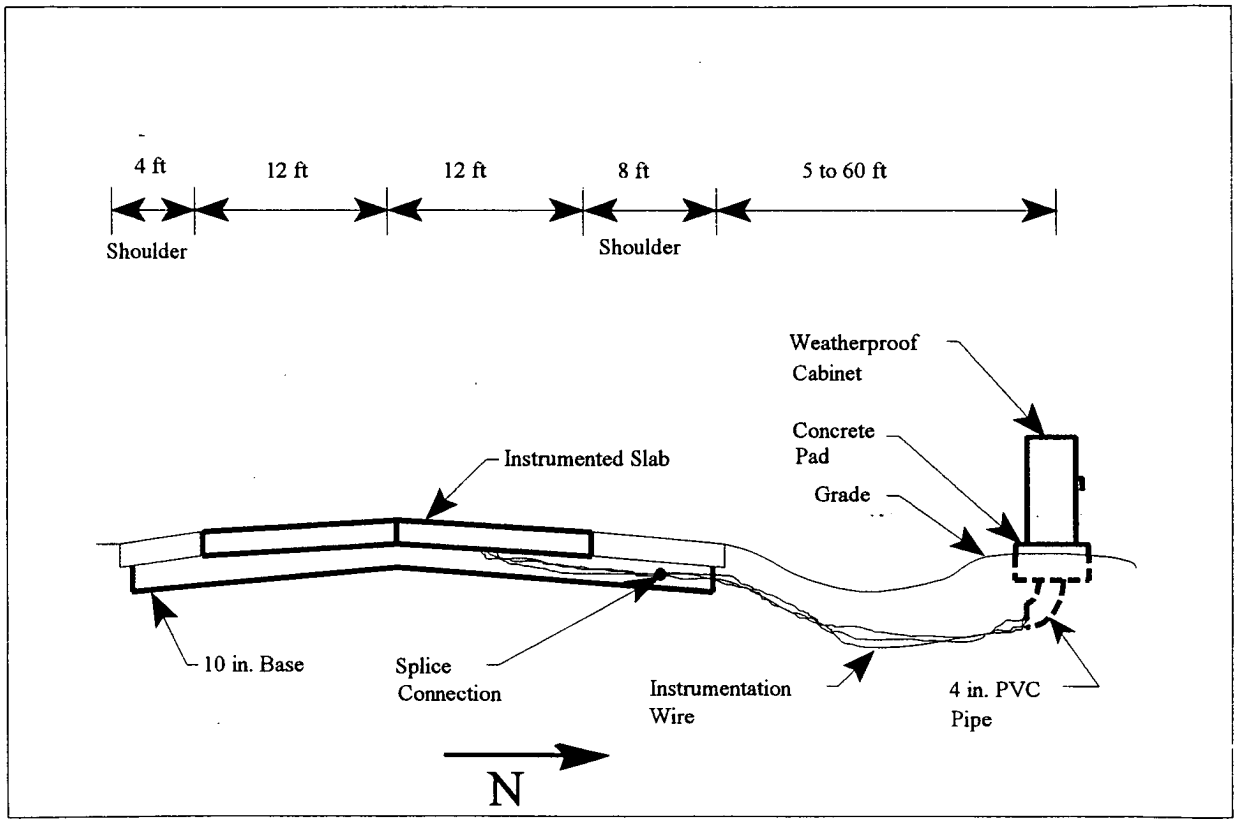

Figure 2.5 Typical site cross section.

2.6.1 Soil Moisture Probe Placement

Soil moisture probes were located to give the soil moisture at critical points in the subgrade. Two probes were placed beneath the center of the slab to give a general idea of the condition of the soil in the base and subgrade. The probe at the west joint was used to measure the effects of infiltration of water through the contraction crack.

Soil moisture probes were located in the base and subgrade. They had to be placed before paving could begin. Probes in the subgrade were set in place before base material was placed and compacted. Cables from the subgrade probes were buried during placement of the base material and later dug up and placed into a trench leading to the concrete pad. The remaining probes were installed after the contractor placed the base material.

2.6.2 Thermocouple Placement

Thermocouples were located at the longitudinal centerline and at the west joint. This placement of the thermocouples allowed comparisons of the strain and displacement data to the temperature gradient of the slab.

All of the thermocouples were installed before paving began. The thermocouples were secured to the wire reinforcing mesh so they would remain in position during paving. Thermocouples were secured with tie wires. The bottom leg of the thermocouple strip rested on the base material. Individual sensors were at depths of 1, 4, 7, and 10 inches, measured from the surface of the concrete slab.

2.6.3 Pressure Cell Placement

Placement of the pressure cells allowed for the measurement of slab/interface pressure due to environmental curling and FWD testing. One pressure cell was located at a corner of the slab

where the pressure should be greatest in concave down bending, and two were located at the longitudinal centerline where the pressure should be greatest during concave up bending.

Each pressure cell was embedded in a small concrete block before being transported to the site. Each block was 12 inches wide, 24 inches long, and 2 inches thick. This was done to ensure that no concrete would seep under the cell and thus decrease the quality of contact between the cell and the base material. Cells were installed in the base material before paving. Prior to pressure cell block placement a small amount of base material was removed and one inch of fine sand was placed underneath the block. Sand provided even pressure distribution on the cell.

2.6.4 Carlson Strain Meter Placement

Each Carlson Strain Meter was tied directly to the reinforcing mesh using a thin steel wire. To ensure the wire did not adversely affect the operation of the gauge, care was taken to locate the wire away from the ends of the gauge, and so attach only to the PVC tube. All slabs had one Carlson Meter in place near the center of the slab at a depth of 5 inches (neutral axis). Strain at the neutral axis is equal to zero for bending. Therefore, the only strain measured by the Carlson strain meter must be the axial strain.

2.6.5 Embedment Strain Gauge and Strain Transducer Placement

The strain transducers were placed at the longitudinal centerline of the slab to measure the maximum bending stress encountered by the slab. The embedment strain gauges were placed to monitor dynamic load at several points in the slab.

Two factors must be accounted for to ensure that the KM-100Bs and the PML-60s properly record the actual strain. First, each gauge must be aligned as close to the longitudinal axis as possible. Second, instrumentation should not disturb the "normal" state of stress around it. Both

factors were dealt with by using an installation process developed by CGER personnel. This installation process used a sheet metal placement box to place and protect sensors. Each placement box was made of 22 gauge, galvanized steel with dimensions 9½ inches high, 10 inches long, and 5 inches wide. The box was open at the top and bottom with a handle placed across the top opening. Figure 2.6 presents a diagram of a placement box.

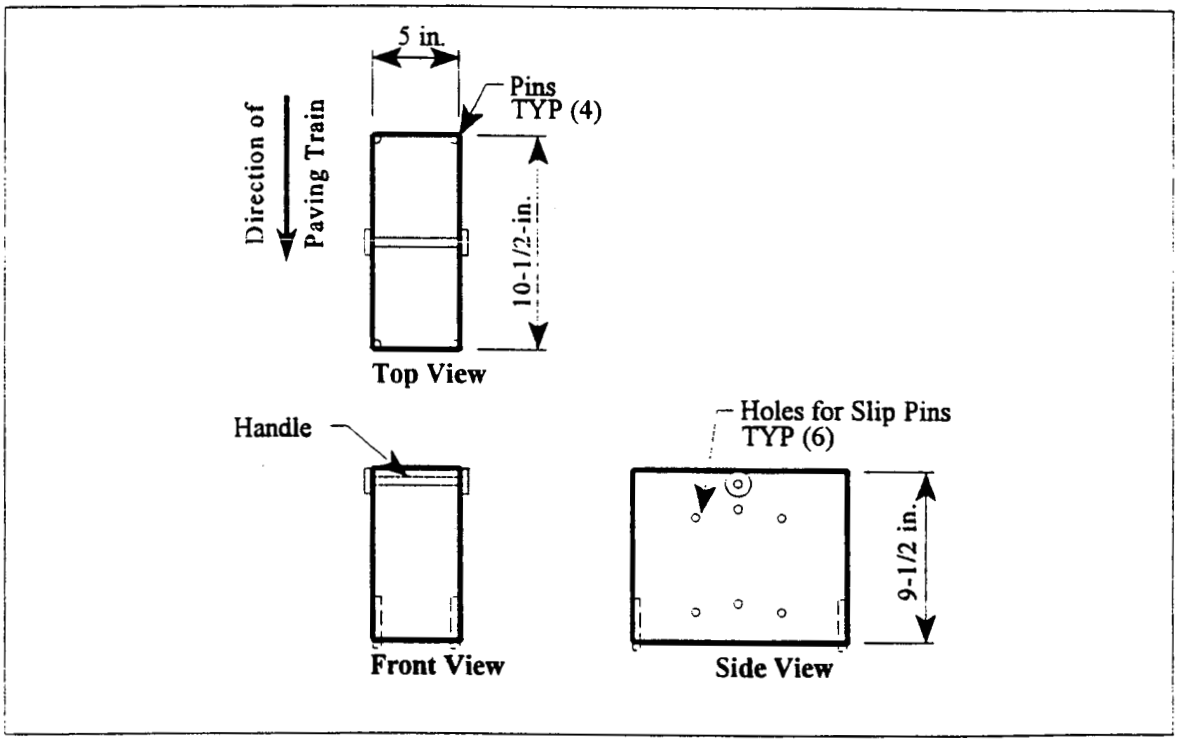

Figure 2.6 Diagram of the strain gage / strain transducer placement box.

The primary reason for using a placement box was to protect the gauge from being moved off line by the lateral force exerted by the paving machine. The placement box resists paving force with support from the surrounding reinforcement mesh and with four steel pins driven into the base material. Pins were located in the front and in the back of the box to resist overturning. The box was inserted in mesh openings and steel pins driven into the base material immediately before paving.

Concrete was taken from the paving machine to fill the box up to the level of the bottom gauge, 1.5 inches from the top of the base. Two pins were inserted through the side of the box and the gauge was placed. A third pin slid over the gauge and concrete was added to fill to the 8½ inch level. The second gauge was then placed using three more pins. Concrete was added to fill the box. A small vibrator was then used to distribute the concrete around the sensors, and the slip pins were removed.

The boxes were removed individually as soon as the finishing machine passed over them, as the paving process progressed. Box removal was done by CGER personnel who rode on the paving train and pulled each box. The contractor's finishing crew smoothed over the disturbance in the concrete, leaving no visible disturbance on the surface of the roadway.

2.6.6 Single Layer Deflectometer (SLD) Installation

SLD is the acronym for Single Layer Deflectometer, a system using an LVDT/reference rod combination designed to measure vertical deflection. The LVDTs were installed in the slabs to measure critical points of deflection. Both the FWD and environmental tests record responses at the same critical points, the joint and the centerline, so that results can be correlated.

The reference rod was installed first for the SLD. A 6 inch diameter hole was augured out of the base material to a depth of 6½ to 7 feet. Loose material was removed from the hole and the bottom was compacted with a spud bar. The reference rod was inserted and plumbed to vertical and 12 to 18 inches of concrete was poured into the hole to attach a base. Two inches of steel rod were left above the grade of the base material to contact the movable core of the LVDT.

To prevent excessive movement of the reference rod and to retain vertical alignment, a two inch PVC pipe was placed coaxially with the rod. A spacer at the top of the pipe was added to keep the rod centered in the pipe. The space between the pipe and the side of the hole was backfilled with

sand. LVDTs, housed in a steel casing, were embedded in the concrete, directly over the reference rod. The casing consisted of three parts: two segments of four inch diameter steel pipe, and a six inch square steel plate welded to the pipes. The plate served as a platform for the LVDT and eliminated "punching out" of the housing under traffic loading. An LVDT was attached to the plate via a specially designed clamp. The clamp used a set screw to clamp the housing of the LVDT to enable some adjustment with respect to the reference rod.

The paving train required ten inch clearance. To accommodate this, the SLD was placed so that its top was one-half of an inch below the elevation of the finished slab. This provided ample clearance for the paving machinery. Another anticipated problem was the force of the advancing concrete pushed by the paver. To counter this force, a restrainer was used. The restrainer slipped over the top of the reference rod and attached to the housing via the LVDT clamp. It provided the housing with rotational and lateral support during paving. After the concrete had cured, the concrete was chipped away over the SLD, the restrainer was removed, and the LVDT was set into the housing. A brass cap that was flush with the surface of the pavement closed the SLD.

Chapter 3

Testing and Data Collection Procedures

3.1 Introduction

Environmental and Falling Weight Deflectometer tests were performed on this project. By combining the two tests, monitoring of the slab response was required during long and short term testing. Summary of the procedures used for each type of test is presented in this chapter.

3.2 Environmental Testing

The term "Environmental Testing" describes the series of tests conducted to monitor slab performance as a function of temperature and moisture. During each environmental test the recording equipment was moved sequentially to individually monitor concrete slabs. Five environmental tests were conducted: one each in Fall 1993; Winter, Spring, and Summer 1994; and Spring 1995. Timing of the tests was designed to allow each slab to be monitored at least once in each season. A sixth test in the Spring of 1995 provided a detailed examination at slab response during the spring, when environmental conditions cause the most severe reactions from the pavement.

Two collection devices are used during environmental testing: the Campbell System and the Real Time Multi-tasking (RTM) System.

3.2.1 The Campbell System

Soil moisture data were collected using equipment manufactured by the Campbell Scientific, Inc., of Logan, Utah. The Campbell system consists of four parts: the multiplexer, cable tester, datalogger, and laptop computer. Figure 3.1 shows how the system was set up in the field.

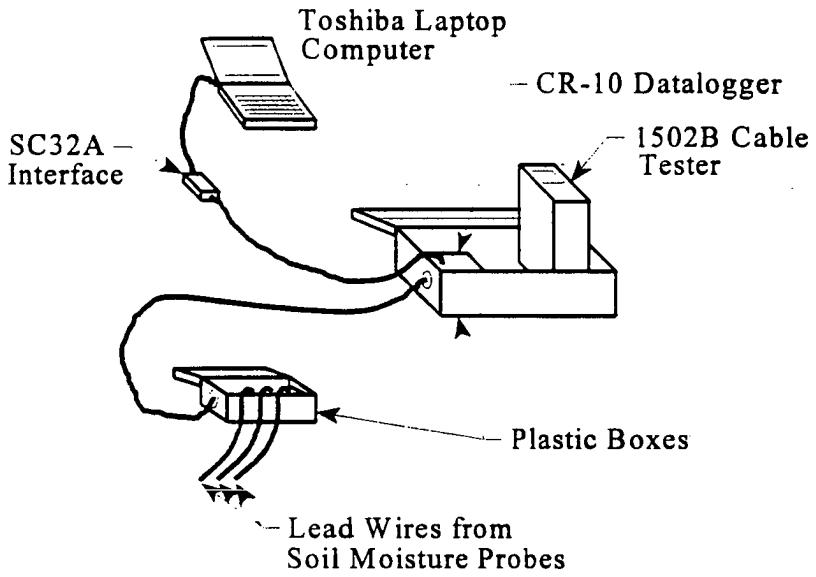

Figure 3.1 Campbell Scientific soil moisture data acquisition system.

One coaxial cable from each moisture probe connects directly to the multiplexer. A Tecktronix 1502B cable tester sends and controls a propagation wave sent along the cable to the probe. Information collected from the cable tester was recorded in the CR10 datalogger. A Toshiba 286 laptop computer running software developed by Campbell Scientific, Inc., controlled the system. Communication between the CR10 and the laptop was accomplished using a SC32A interface and the laptop's serial port.

3.2.2 The RTM System

Reaction to environmental conditions was also measured by the RTM system. This system consisted of four parts: the IMPs, external power supply, processor, and software.

IMP is an acronym for the 3595 series Isolated Measurement Pod, manufactured by

Schlumberger Industries of Buffalo, New York. Two of these pods were the backbone of the data collection system. The first IMP was a 20-channel model 35951C used to monitor the LVDTs, semi-conductor pressure cells, and thermocouples. The second IMP was a model 35951B with ten channels capable of measuring resistance. Both pods contained internal analog to digital cards. The Carson Strain Meters, and KM-100Bs strain transducers were monitored by this second IMP using full Wheatstone Bridge configurations. All lead wires connected directly into the IMPs through the plastic harnesses discussed in Section 2.2. Figure 3.2 presents a diagram of the RTM system.

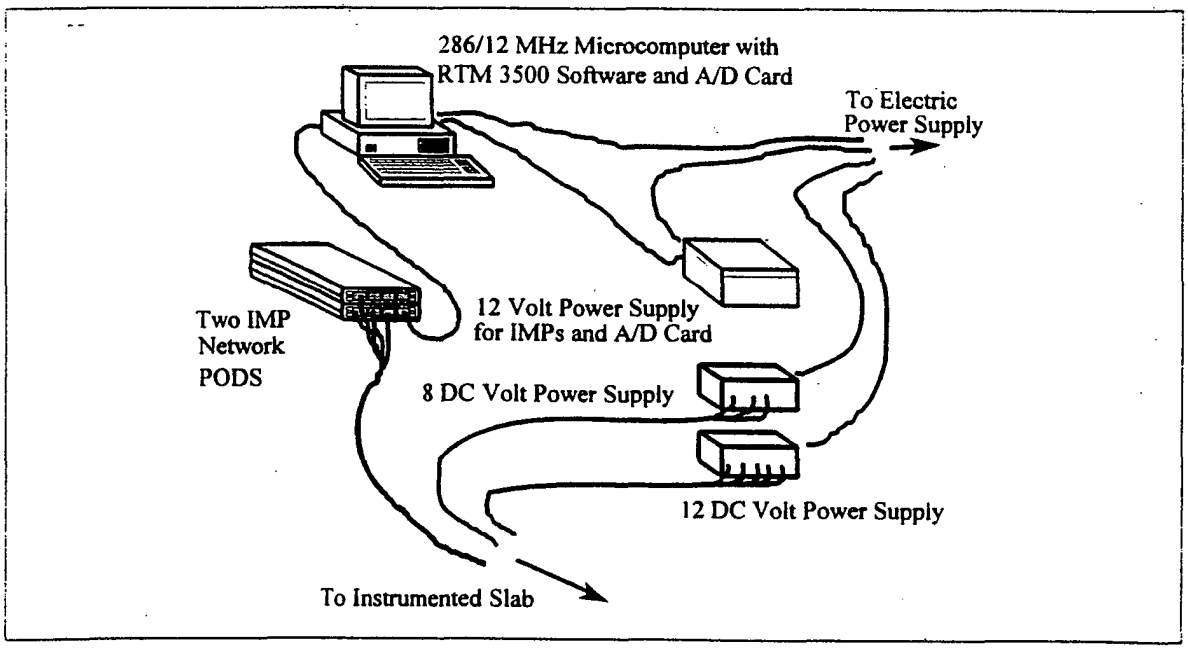

Figure 3.2 RTM data acquisition system.

LVDTs and semi-conductor pressure cells required a 12 and 8 volt DC excitation voltage, respectively. Since the IMPs were not capable of providing these voltages to the instruments directly, two external transformers were provided. An IBM 286/12 MHZ microcomputer controlled the environmental data collection system. Communications and power supply were furnished to the IMP network via a three-wire S-net cable connected to a communications card in the computer. Data

collection software used was RTM (Real Time Multitasking) 3500, developed by Microspecialty Systems, Inc., of Bethlehem, Pennsylvania. The software had two parts: the system environment program and the monitoring program. The system environment portion of the program required different configuration files to be set up for each slab since each slab has a different selection of sensors. The configuration file contained the IMP network, bridge configuration, gauge factor of each gauge, and gauge to channel assignment. Instruments were monitored in a spreadsheet format with each column in the spreadsheet containing a different channel of information, such as the strain or displacement, recorded by gauge, date, time, and an alarm signal showing when data was being saved to a file.

The software was programmed so that every half hour after system start up an alarm was triggered causing data to be saved six times, at thirty second intervals. These six points were averaged to give a value at the half hour interval. Figure 3.3 provides a time line to illustrate this process.

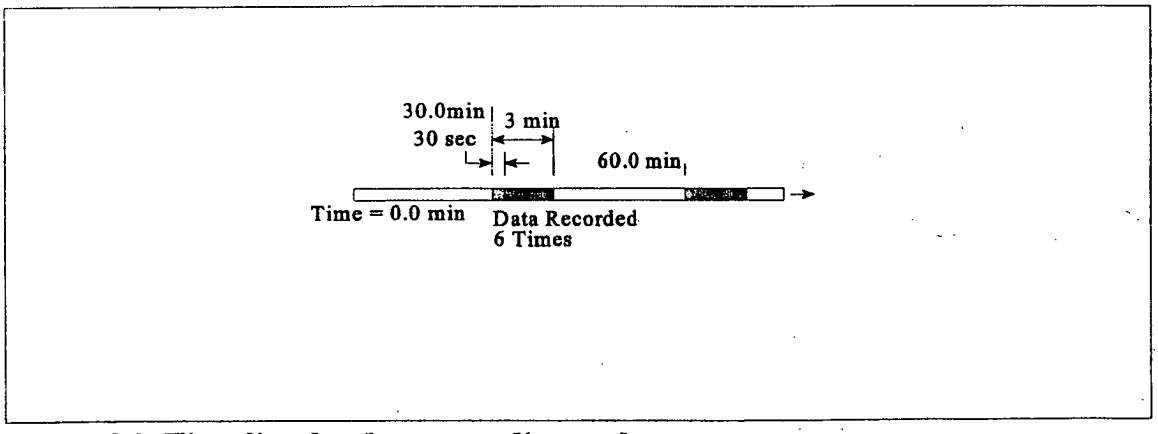

Figure 3.3 Time line for data recording cycle.

3.2.3 Environmental Testing Procedures

Environmental testing provided data on slab behavior over an extended period. All gauges, except the PML-60 embedment strain gauges and the vibrating wire pressure cells, were monitored during environmental testing. An attempt was made to record data from the PML-60s to the IMPs in the Fall of 1993. Soon after initialization, the gauges began to float from the initial readings, so these sensors were disconnected. Table 3.1 shows the dates and duration of each environmental test.

Table 3.1. Dates for environmental tests, and time on each slab.

		Number of Hours Recording on Slab #:								
Test	Dates	1	2	3	4	5	6	7	8	9
Fall '93	10/11 - 10/31	50.5	67.5	44.5	47.5	47	46.5	46.5	46	46
Winter '94	2/8 - 3/9	94.5	45	42	48.5	48.5	45.5	47	95	73.5
Spring '94	4/5 - 4/28	45	58.5	67.5	64.5	46	47	69	52.5	40
Summer '94	8/2 - 9/1	51	67.5	70	64.5	47.5	40	48	45	50.5
Spring '95	3/20 - 4/3	43	45.5	47.5	49	51	45	47	69.5	47.5

All nine slabs were monitored for each test. CGER personnel arrived on site at the beginning of the test to set up monitoring equipment on the first slab. Soil moisture readings were taken. When all connections were made and the system was activated, the RTM equipment was left running in the weatherproof cabinet for 40 to 60 hours. Data was collected at half hour intervals as described in Section 3.2.2. About two days later CGER personnel returned to shut off the system, copy recorded data to a floppy disk, and move the equipment and cabinet to the next slab. The process

was repeated until all nine slabs were monitored. The test was completed in a minimum of eighteen days.

Each slab was tested for a minimum of forty hours since this limit provided enough time for at least two day and night cycles. Data collection was limited to data storage space.

3.3 Falling Weight Deflectometer Testing

Four Falling Weight Deflectomer (FWD) tests were conducted in this project. The dates for these tests were: December 14, 1993; April 18, August 1 and 2, and November 21, 1994.

3.3.1 Testing Equipment

ODOT provided a Dynatest Model 8000 Falling Weight Deflectometer for each test. The deflectometer applied a load of 23,000 to 28,000 pounds by dropping a weight onto an 11.8 inch diameter rubber pad. Deflection of the slab was measured using geophones placed 0, 8, 12, 18, 24, 36, and 60 inches from the point of impact. This information was recorded by the FWD operator and provided to CGER personnel for comparison with IMP data.

3.3.2 The EGAA System

The equipment used to monitor the response of the slab during FWD testing consists of three main components: the microcomputer, signal amplifier, and EGAA software. Figure 3.4 provides a layout of the EGAA system.

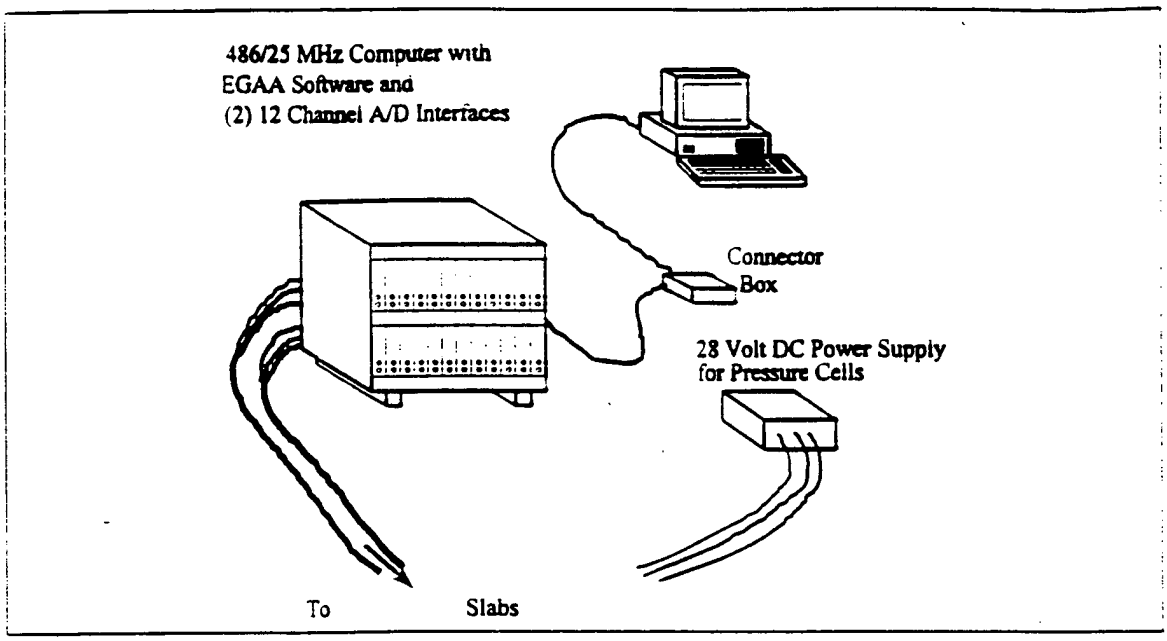

Figure 3.4 The EGAA system.

Controlling the system was a 486/25 MHz computer manufactured by Texas Measurements. To handle the enormous amounts of data created by each test, the hardware was provided with a 1 Gigabyte hard drive and two, 12 channel A/D interfaces. Loaded with the data acquisition system was the Enhanced Graphics Acquisition and Analysis (EGAA) software package developed by R.C. Electronics of Goleta, California.

High speed amplifiers magnified the input signal magnitude by a preselected gain factor. They also provided an excitation voltage to the LVDTs and KM-100B and PML-60 strain sensors. A full bridge amplifier was required for each channel when all gauges were monitored simultaneously. Each of the 24 input channels can collect up to 2000 samples per second. Two connector boxes were used in the system to simplify the wiring between the computer and the amplifiers. Excitation voltage for the pressure cells was provided by the same 28 volt power supply described in Section 3.2.2.

3.3.3 Soil Moisture and Temperature Monitoring Equipment

During FWD testing a soil moisture reading was taken for each slab, and one temperature differential reading was taken for each slab when loaded. The Campbell and RTM systems were used for these measurements.

3.3.4 FWD Test Procedures

The FWD test required cooperation of ODOT who provided the deflectometer and diverted traffic during the test. Readings from all sensors except the Carlson strain meters and the semiconductor pressure cells were recorded. Although the PML-60s tended to float when wired to the RTM system (see section 3.2.3) the short test interval of a FWD drop gave acceptable results for dynamic testing.

A software option enabled the operator to select the length of time data was recorded, which was usually one second. Another option, the graphical interface of the EGAA software, allowed the operator to instantaneously see the response of any gauge connected to the system. Thus, after confirming that the gauge response had been captured, the EGAA operator would either signal for another drop or to reposition for the next drop. Tests were repeated three times.

Chapter 4

Data Analysis

4.1 Introduction

The previous chapters described procedures used to collect data during environmental and FWD testing. This chapter discusses how instruments were calibrated, if required, and how the field data was collected and analyzed.

4.2 Temperature Differential Calculations

Thermocouples measured temperatures at several levels in the concrete. From this information, the temperature gradient was determined and the correlation to slab response was established. The *Temperature Differential* was defined as:

$$\textit{Temperature Differential} = \textit{Thermocouple @ 1"} - \textit{Thermocouple @ 10"} \quad \text{(Eqn. 4.1)}$$

4.3 Vertical Displacement Calculations

All of the LVDTs used in this project were calibrated before being placed in the pavement. Calibration involved applying a known deflection with a digital micrometer and recording the voltage change of the LVDT. Each LVDT was tested on both the RTM and EGAA data acquisition systems. For environmental testing, voltage was automatically changed to displacement by the RTM software. The same calibration was applied later for FWD testing.

4.4 Strain Calculations

Each of the strain measuring gauges, KM-100B, PML-60, or Carlson Strain Meter required

a different procedure for analyzing the output. Summary of the procedure is presented in this section. KM-100B strain transducers were the only strain gauges used during both environmental and FWD testing.

4.4.1 Strain Transducer Calculations

The strain transducers were monitored by the model 35951A IMP during environmental testing. Strain transducers were initialized immediately as the gauges were connected to the IMP, with RTM software running. Upon initialization, the IMP sends an 8mA current to the transducer and determines the initial gauge voltage, V_g. Then, the IMP reads the "out of balance" voltage value, V_o, of the transducer. For the duration of the monitoring period, the IMP registers the "out of balance" voltage, V_x, reading of the transducer. The RTM software calculates strain in microstrains from the difference in voltage readings using Equation 4.2.

$$\varepsilon = 4 * \frac{(V_o - V_x) * 4}{N * S_G * V_g} \qquad \text{(Eqn. 4.2)}$$

where ε = Strain (microstrains)
V_o = Gauge Voltage at Initialization
V_x = "Out of Balance" Voltage at Initialization
V_g = Strain "Out of Balance" Voltage
S_G = Gauge Factor of Active Gauge
N = Number of Active Gauges

The gauge factor (S_G), and the number of active gauges (N) is programmed into the RTM software environmental file before testing. Literature provided with the software recommends a gauge factor of 2.0 for all strain transducers and then corrects for the actual coefficient.

The KM-100B has four active gauges connected in a full Wheatstone Bridge configuration.

To extend the range, the manufacturer designed these transducers to read only 25% of the actual strain. Thus, to find the actual strain, the apparent value of strain must be multiplied by four, which results in Equation 4.2. When the number of active gauges of the sensor is introduced, the equation used in the field by the data acquisition system is Equation 4.3.

$$\varepsilon = 4 * \frac{(V_o - V_x)}{S_G * V_g} \qquad \text{(Eqn. 4.3)}$$

Once the test was complete and the data were returned to the laboratory, calculations were required to correct for the variance of gauge factors, for the expansion of the transducer's body, and for thermal expansion of concrete. Equation 4.4 converts measured field values for strain into stress.

$$\sigma = E_s * \varepsilon * C + E * (\varepsilon * \alpha - \Delta T * \beta) \qquad \text{(Eqn. 4.4)}$$

where σ = Stress
E_s = Young's Modulus
C = Correction Factor for Gauge Factor
ΔT = Change in Temperature at Initialization (°F)
α = Gauge Coefficient of Thermal Expansion
β = Concrete Coefficient of Thermal Expansion, 5.5x10^-6/°F

Concrete core samples of the pavement were taken for lab analysis. Compression tests gave a modulus of elasticity of the sample of about 4,000 ksi. This value was used for all calculations.

For FWD testing, the transducers were read through the EGAA system where the transducers were configured in a full bridge. A modified form of Equation 4.3 was used since amplification was necessary:

$$\varepsilon = 4 * \frac{(V_o - V_x)}{M * S_g * V_g} \qquad \text{(Eqn. 4.5)}$$

where M = Gain Factor

For FWD testing the change in voltage due to the load was measured. As signals coming from the strain transducers were extremely sensitive, the amplifiers magnified the signal to be read by the 12 Bit A/D cards. A gain factor of 10,000 was commonly used for strain transducers. Once the apparent strain was calculated, the data were multiplied by the gauge correction factor. Stress was determined by multiplying the adjusted strain by the modulus of elasticity.

4.4.2 Embedment Strain Gauge Calculations

PML-60 embedment strain gauges were used only during FWD testing. Each gauge was configured in a quarter Wheatstone Bridge configuration where bridge completion resistors were supplied with the amplifiers. The EGAA system read the change in voltage encountered by the gauge. Daily and Riley (7) use Equation 4.6 to relate the voltage differential to the resistance.

$$\Delta E = V\frac{R_1 * R_2}{(R_1 + R_2)^2} * (\frac{\Delta R_1}{R_1} - \frac{\Delta R_2}{R_2} + \frac{\Delta R_3}{R_3} - \frac{\Delta R_4}{R_4}) \qquad \text{(Eqn. 4.6)}$$

where ΔE = Change in Voltage as Read by the EGAA System
V = Input voltage
R_i = Resistance of each of the Four Arms of the Wheatstone Bridge (Ω)
ΔR_i = Change in Resistance in each of the four arms

The sensitivity of a Wheatstone Bridge is found by using Equation 4.7, also taken from Daily and Riley (7).

$$\frac{\Delta R}{R} = S_g * \varepsilon \qquad \text{(Eqn. 4.7)}$$

Since three of the resistors were provided by the amplifiers, the last three $\Delta R/R$ terms cancel in Equation 4.6. Combining equations 4.6 and 4.7 and solving for the strain results in Equation 4.8.

$$\varepsilon = \Delta E * \frac{(R_1 + R_2)^2}{R_1 * R_2 * V * S_g * M} \qquad \text{(Eqn. 4.8)}$$

A typical gain factor of 1,000 or 10,000 was used for the PML-60s. Equation 4.8 determines the strain read by the PML-60 strain gauges and does not require any calibration or adjustment. Stress was determined again by multiplying the results of Equation 4.8 by Young's modulus of the concrete.

4.4.3 Carlson Strain Meter Calculations

The Carlson strain and temperature devices were monitored only during environmental testing. The Model 35951A IMP was wired to read the two internal resistors in the gauge and the total resistance of the gauge. These values were collected by the RTM software. Temperature was measured by finding the difference between the resistance at that instant and the value recorded while the meter was at zero degrees Fahrenheit (A). The difference is multiplied by a calibration constant (B). Values for A and B, as well as Equation 4.9, are provided by the manufacturer.

$$Temp = [(R_t - A)] * B \qquad \text{(Eqn. 4.9)}$$

where Temp = Temperature (°F)
R_t = Total Resistance Across Gauge (kiliohms)
A = Meter Resistance at 0°F (ohms)
B = Calibration Factor (degrees/ohm)

Finding the stress in the gauge was a multi-step process. The first step was to determine the ratio of the two resistances using Equation 4.10.

$$Ratio = (R_2/R_1) * 100 \qquad \text{(Eqn. 4.10)}$$

where R_1 and R_2 = Resistance of the First and Second Element

On site initialization of all Carlson strain meters occurred on October 10, 1993. Values for the initial temperature and resistance ratios were recorded at that time. The initial resistance ratio was used in Equation 4.11 to find the change in the ratios. The result was expressed as a percentage by multiplying the value by 100.

$$Rchange = (Ratio - C) \qquad \text{(Eqn. 4.11)}$$

where *Rchange* = Resistance Ratio Change
C = Initial Resistance Ratio Taken on October 10, 1993

The indicated change in strain was then calculated using Equation 4.12. A calibration constant, D, was provided for each gauge by the manufacturer.

$$Indchange = D * Rchange \qquad \text{(Eqn. 4.12)}$$

where *Indchange* = Indicated Change in Strain
D = Calibration Constant

Note indicated strain is not equal to the strain in the concrete without correction. Strain is corrected for the thermal expansion/contraction of the meter frame and concrete. This is accomplished using two correction equations and modifying the strain value. Equation 4.13 adjusts the magnitude of strain for the effects of temperature on the meter frame.

$$Corrme = (Temp - T_0) * \gamma \qquad \text{(Eqn. 4.13)}$$

where *Corrme* = Correction Factor for the Gauge Frame
T_0 = Initial Temperature Reading Taken on October 10, 1993
γ = Thermal Coefficient of Expansion for the Gauge Frame, 6.7x10^-6/°F

Equation 4.14 adjusts the measured strain for the thermal effects encountered by the concrete.

$$Corrce = (Temp - T_0) * \beta \qquad \text{(Eqn. 4.14)}$$

where *Corrce* = Correction Factor for the Concrete
β = Coefficient of Expansion for the Concrete, 5.5x10^-6/°F

These correction factors (Equation 4.13 and 4.14) are then added to the results of Equation 4.12 to find the actual strain in the concretein Equation 4.15.

$$Actstrain = Indchange + Corrme + Corrce \qquad \text{(Eqn. 4.15)}$$

where *Actstrain* = Actual Strain in Concrete

The stress is found by multiplying the *Actstrain* by Young's modulus.

4.5 Slab/Base Interface Pressure Calculations

Each pressure cell was calibrated in the laboratory before field installation. All vibrating wire pressure cells were read using a Geokon GK-401. The semiconductor pressure cells were read on the EGAA and RTM systems. Semiconductor pressure cells gave a voltage differential as their output. This was multiplied by the CGER determined calibration factor to find the pressure. The RTM software was programmed to calculate pressure in the field for environmental testing. For FWD testing the calibration factors were entered manually.

4.6 Soil Moisture Calculations

Ledieu's calibration is recommended by Campbell Scientific, Inc., to find the volumetric water content. The TDR cable tester measures the velocity of the propagation wave sent through the

soil between the two probes. Software is provided that uses Equation 4.16 to calculate the volumetric water content.

$$W_v = \frac{0.1138}{v_p} * 0.1758 \qquad \text{(Eqn. 4.16)}$$

where W_v = Volumetric Water Content (V is percent value)
v_p = Propagation Wave Velocity, m/s

When the data was brought back to the lab it was converted into the more familiar soil moisture content. Lambe and Whitman (8) define soil moisture content as:

$$w = \frac{W_w}{W_s} \qquad \text{(Eqn. 4.17)}$$

where w = Soil Moisture Content (SM is percent value)
W_w = Weight of Fluids
W_s = Weight of Solids

Densities of the base and subgrade material have been determined by ODOT. For the A304 crushed limestone base, the density is 2.24 grams/cubic centimeters, and 1.72 grams/cubic centimeters for the subgrade. The derivation of Equation 4.18 gives the equation for soil moisture content used in the lab.

$$w = \frac{V_w * \gamma_w}{V_s * \gamma_s} = W_v * \frac{g * \rho_w}{g * \rho_s} = \frac{W_v}{\rho_s} \qquad \text{(Eqn. 4.18)}$$

where V_w and V_s = Volume of Water and Solids, cm^3
γ_w and γ_s = Specific Weight of Water and Solids, N/cm^3
g = Gravity, m/s^2
ρ_w = Density of Water, 1 g/cm^3
W_v = Volumetric Water Content
ρ_s = Density of Soil

4.7 Environmental Data Analysis Procedures

Data files from the RTM software were saved in ASCII format. Each file was imported into Axum 3.0, a graphing software by TriMetrix Corp. of Seattle, Washington. RTM saved six data points to a file every half hour using the process discussed in Section 3.2.2. These six points were averaged to produce a single point. This procedure ensures that vehicle loading did not affect the readings, and the responses read by the instruments were those caused by environmental changes.

Once the data were corrected and a zero reference selected (see Section 4.7.1), they were plotted as a function of time. Two graphs were created for each slab: one for the reactions of the strain transducers and Carlson gauges, and the other for deflections of the two LVDTs at the transverse centerline. For slabs with five LVDTs instead of two, a third graph showing the deflection at the west joint of the slab was also plotted. Appendix B contains complete sets of graphs for the Fall 1993 and Spring 1995 tests.

4.7.1 Reference Position for Environmental Testing

The primary source of environmental strain and displacement was slab curl. Solar radiation heats the slab during the daytime hours. At night the heat dissipates into the cool night air. Since the pavement was heated and cooled at the surface, a temperature gradient develops which caused the slab to curl. When the temperature differential was greater than zero, that is when the temperature at the top was higher than at the bottom, the slab curled concave down. Similarly, when the temperature differential is negative, the slab curled concave up. A diagram showing the effects of curling on the slab is given in Figure 4.1

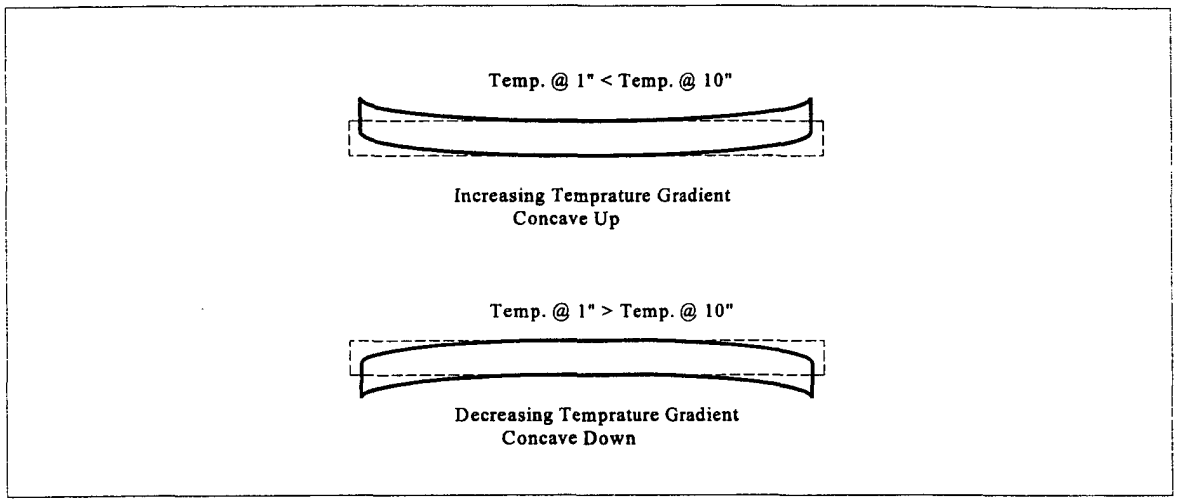

Figure 4.1 Slab warpage due to temperature gradient.

When exposed to a heat source, pavement materials experience some degree of thermal expansion. If the slab is unrestrained, it will expand and strain, but no stress will develop. The instrumented concrete slabs were restrained at the joints, and therefore, developed stress under thermal expansion. When there was no temperature gradient in the slab, i.e., the temperature was constant with depth, there was no warpage and therefore no vertical displacement.

After data were collected and brought back to the laboratory, the temperature differential was plotted and the time when temperature was approximated as zero was determined. Correction and calibration factors for LVDTs, strain transducers and Carlson gauges were applied, data were "zeroed" at that point in time.

4.8 FWD Data Analysis Procedures

The process of analyzing the data recorded in the falling weight test was different than that used for environmental testing. First, data from the LVDTs, strain transducers, and embedment strain gauges were filtered as described in Section 4.8.1. The filtered data were imported into Axum

and one "drop" was graphed for each gauge. The peak value was found and the magnitude was recorded. The peak values of deflections were compared to those determined by the geophones on the FWD trailer.

4.8.1 FWD Data Filtering

Unlike the environmental tests where data were collected for several days, the purpose of the FWD tests were to monitor the instantaneous, low level response of the gauges to an applied load. Thus, the data acquisition system must be highly sensitive. The amplifiers, at this level of sensitivity, are susceptible to picking up unwanted electrical noise. To eliminate this noise, data from the embedment strain gauges, strain transducers, and vibrating wire pressure cells were filtered using a program developed by CGER personnel. Filtering the data involved converting the binary data files created by the EGAA software into a Fast Fourier Transform (FFT). A low pass frequency routine then cleaned the data of noise at or below a user specified level, usually about 50 Hz. The final step was to run the files through a second program that converted the file back into ASCII format for use in Axum.

Figures 4.2 and 4.3 show examples of the two types of plots created from the filtered data. Plots were used to determine the induced stress or displacement for each gauge.

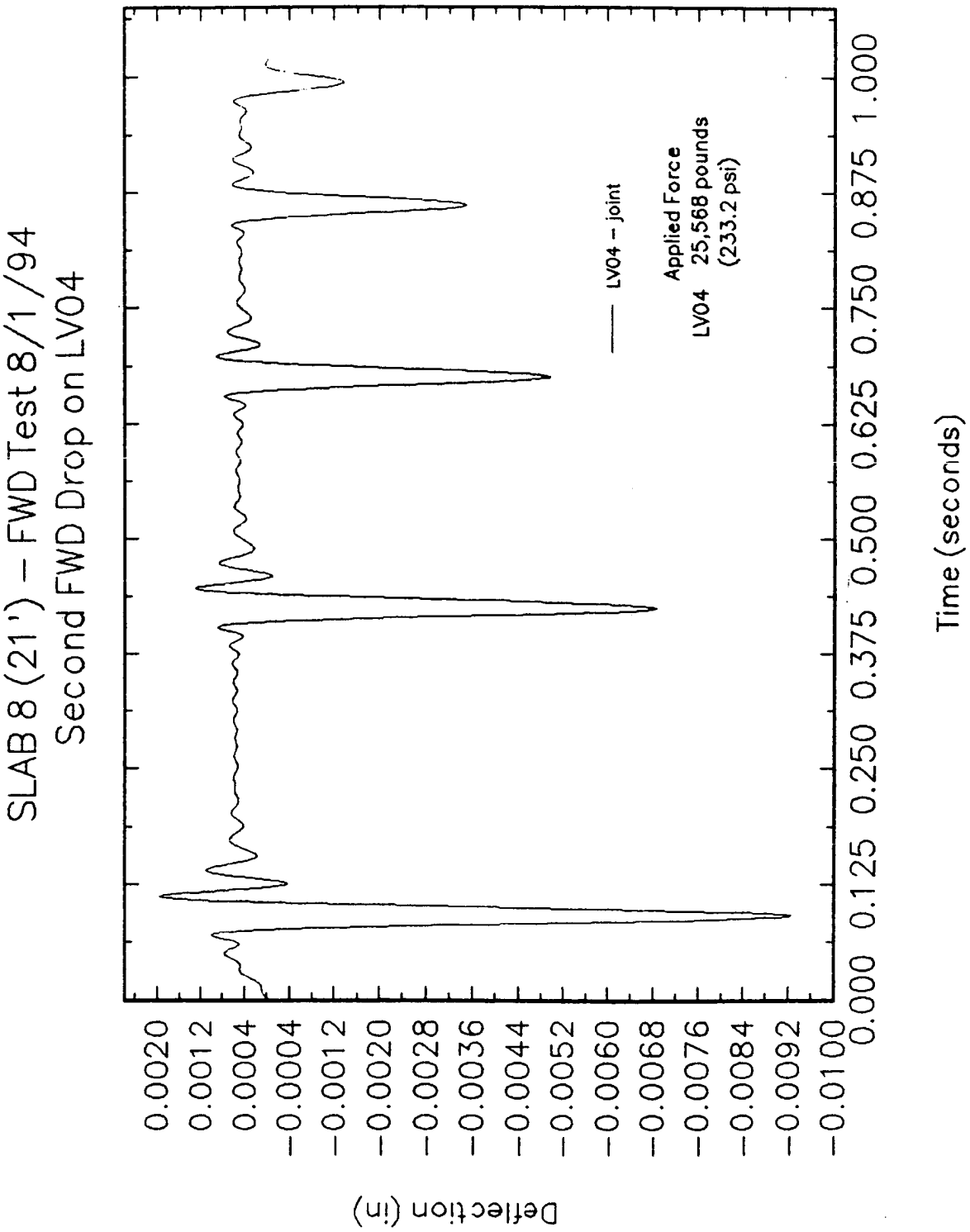

Figure 4.2 Example FWD graph for displacement.

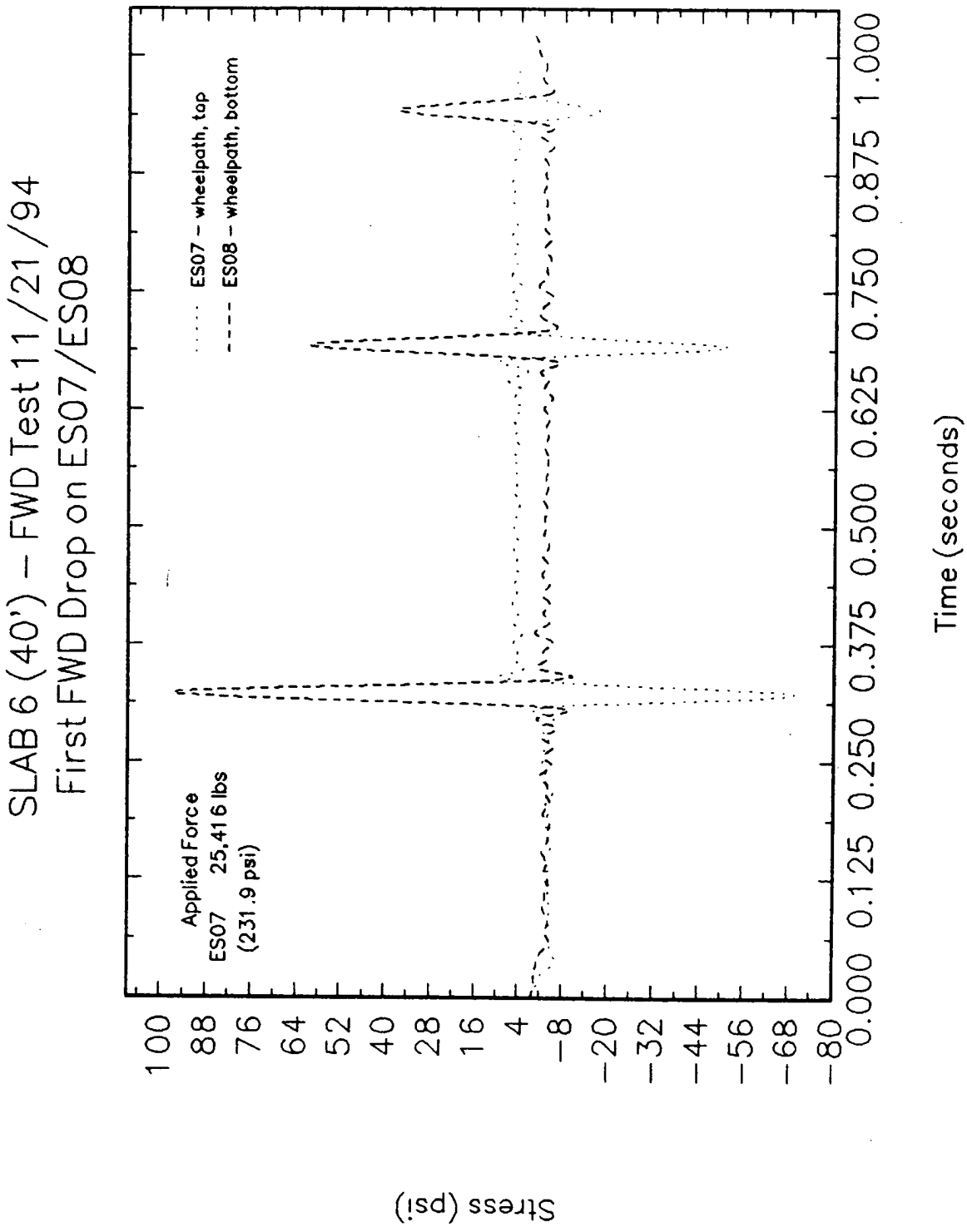

Figure 4.3 Example FWD graph for induced stress.

Chapter 5

Environmental and FWD Test Results

5.1 Introduction

Five environmental and four FWD tests were conducted in this investigation. This chapter presents the results of these tests in tabular format for comparison to slab response. A discussion about the performance of instrumentation and response of concrete slabs is also presented in this chapter.

5.2 Environmental Testing Results

Strain and movement in the concrete slabs is due to temperature and moisture gradients. Since change of moisture in the concrete along the slab was not recorded, this additional variable was not incorporated in the investigation. Figures 5.1 and 5.2 show examples of temperature distribution for the slab centerline and slab joint. Temperatures were measured at 1 in., 4 in., 7 in., and 10 in. levels, with respect to thickness of the slab. In past analyses of rigid pavement response to environmental factors, the temperature distribution was assumed to be linear, with respect to depth, and the same throughout the slab. Examination of Figures 5.1 and 5.2 reveals that the change in temperature close to the joint and away from the joint varies highly nonlinearly, with respect to depth, and there is a major difference between the temperature distributions. To analyze the environmental response of the slabs, these phenomena must be incorporated.

Data selected from that collected during environmental testing through the depth of the slab are presented in Tables 5.1 through 5.36. For each slab a curve showing the temperature differential in the depth of the slab versus time was plotted. Temperature maximum and minimum differential points were determined. Magnitude and sign of displacement or stress were recorded for each gauge

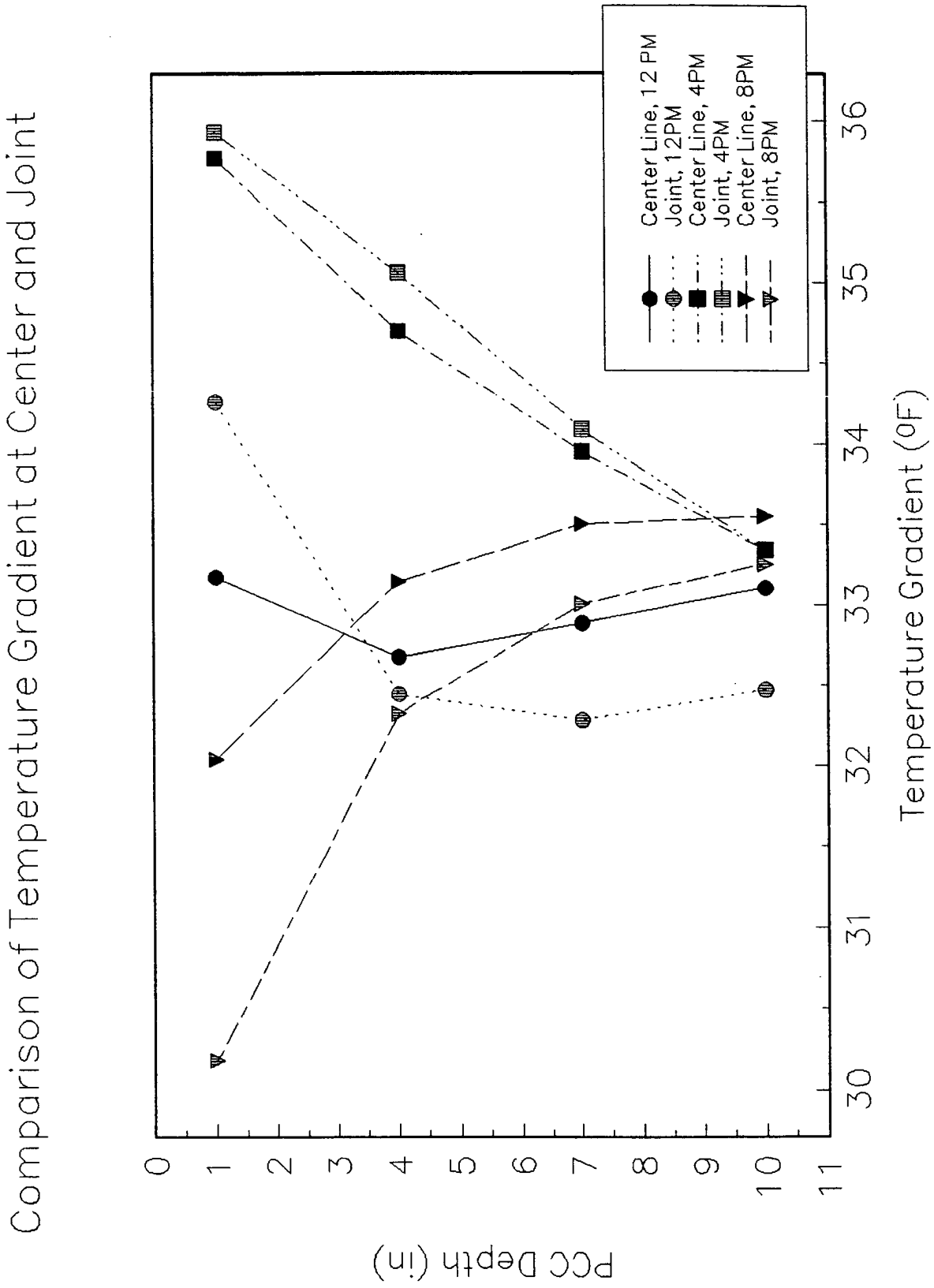

Figure 5.1 PCC Temperature Gradient for February 1994

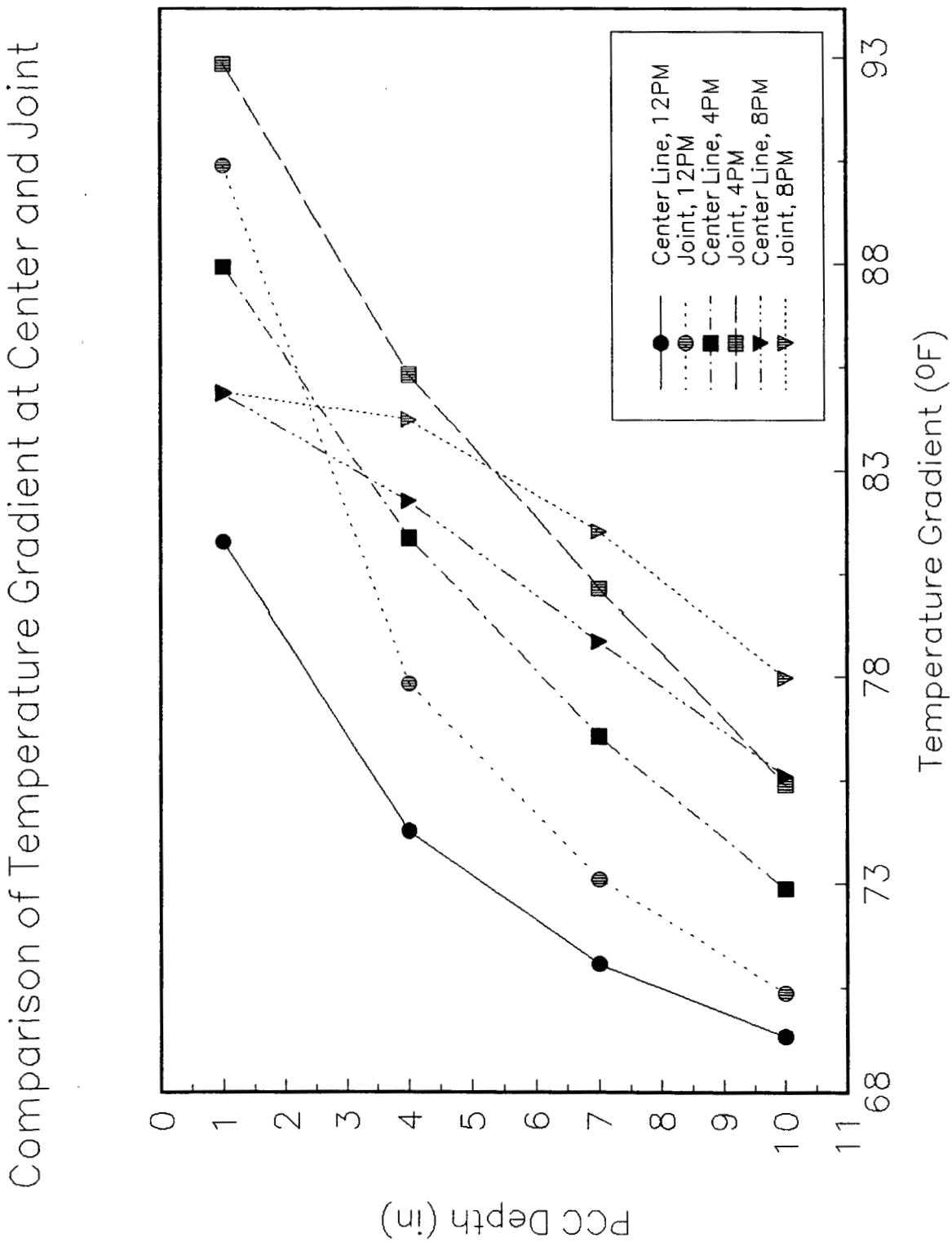

Figure 5.2 PCC Temperature Gradient for April 1994

Table 5.1 Slab 1, maximum temperature differential and associated period of time.

Change in Temperature Differential (°F) vs. Time (hrs)									
Fall '93		Winter '93		Spring '94		Summer '94		Spring '95	
ΔTd	Time	ΔTd	Time	ΔTd	Time	ΔTd	Time	ΔTd	Time
-10.2	9.5	-18.1	16.5	19.5	-18	-26	17.5	20.9	9

Table 5.2 Slab 1, volumetric water content readings and soil moisture content.

Percent Volumetric Water Content (V) and Percent Soil Moisture Content (SM)										
Probe	Fall '93		Winter '93		Spring '94		Summer '94		Spring '95	
	V	SM	V	SM	V	SM	V	SM	V	SM
MC01	14.2	6.3	7.9	3.5	18.6	8.3	-	-	27.3	12.2
MC02	44.3	25.6	19.2	11.1	46.2	26.9	-	-	23.1	13.4
MC03	19.3	8.6	9	4	24.9	11.1	-	-	25.5	11.4

Table 5.3 Slab 1, change in stress due to temperature differential.

Gauge	Change in Stress (psi)				
	Fall '93	Winter '93	Spring '94	Summer '94	Spring '95
ST01	95	77	119	119	172
ST02	76	60	113	108	150
CS01	2	45	255	-	61

Table 5.4 Slab 1, change in displacement due to temperature differential.

Gauge	Change in Displacement (milli-inches)				
	Fall '93	Winter '93	Spring '94	Summer '94	Spring '95
LV01	3	0	10	8	-
LV02	1	13	10	1	6

Table 5.5 Slab 2, maximum temperature differential and associated period of time.

Change in Temperature Differential (°F) vs. Time (hrs)									
Fall '93		Winter '93		Spring '94		Summer '94		Spring '95	
ΔTd	Time	ΔTd	Time	ΔTd	Time	ΔTd	Time	ΔTd	Time
-13.6	16	-10	15.5	-26.7	12.5	-18.1	16	-18.8	16

Table 5.6 Slab 2, volumetric water content readings and soil moisture content.

Percent Volumetric Water Content (V) and Percent Soil Moisture Content (SM)										
Probe	Fall '93		Winter '93		Spring '94		Summer '94		Spring '95	
	V	SM	V	SM	V	SM	V	SM	V	SM
MC01	17.7	7.9	15.2	6.8	22.6	10.1	27.4	12.2	-	-
MC02	46.6	26.9	18.5	10.8	-	-	-	-	-	-
MC03	13.4	6	23.5	10.5	-	-	-	-	-	-

Table 5.7 Slab 2, change in stress due to temperature differential.

Gauge	Change in Stress (psi)				
	Fall '93	Winter '93	Spring '94	Summer '94	Spring '95
ST01	100	18	288	8	33
ST02	61	65	225	32	29
CS01	8	27	205	132	104

Table 5.8 Slab 2, change in displacement due to temperature differential.

Gauge	Change in Displacement (milli-inches)				
	Fall '93	Winter '93	Spring '94	Summer '94	Spring '95
LV01	2	-	4.5	3	8
LV02	0	-	5	-	10
LV03	10	-	36	39	20
LV04	9	-	44	40	-
LV05	11	-	66	58	42

Table 5.9 Slab 3, maximum temperature differential and associated period of time.

Change in Temperature Differential (°F) vs. Time (hrs)									
Fall '93		Winter '93		Spring '94		Summer '94		Spring '95	
ΔTd	Time	ΔTd	Time	ΔTd	Time	ΔTd	Time	ΔTd	Time
18.4	14	-9.9	14	23.8	8	-18.1	16	25.2	18.5

Table 5.10 Slab 3, volumetric water content readings and soil moisture content.

Percent Volumetric Water Content (V) and Percent Soil Moisture Content (SM)										
Probe	Fall '93		Winter '93		Spring '94		Summer '94		Spring '95	
	V	SM	V	SM	V	SM	V	SM	V	SM
MC01	11.9	5.3	13	5.8	15.1	6.7	18.3	8.2	19.5	8.7
MC02	17.4	7.8	16.6	9.6	18.2	10.6	23.3	13.5	20	11.6
MC03	13.6	6.1	18.1	8.1	23.4	10.4	21.7	9.7	20.2	9

Table 5.11 Slab 3, change in stress due to temperature differential.

Gauge	Change in Stress (psi)				
	Fall '93	Winter '93	Spring '94	Summer '94	Spring '95
ST01	116	38	44	161	197
ST02	72	55	119	146	208
CS01	55	27	112	153	205

Table 5.12 Slab 3, change in displacement due to temperature differential.

Gauge	Change in Displacement (milli-inches)				
	Fall '93	Winter '93	Spring '94	Summer '94	Spring '95
LV01	4	18	12	3	13
LV02	0	-	9	-	-
LV03	8	-	24	37	31
LV04	9	-	33	42	-
LV05	16	-	49	58	48

Table 5.13 Slab 4, maximum temperature differential and associated period of time.

Change in Temperature Differential (°F) vs. Time (hrs)									
Fall '93		Winter '93		Spring '94		Summer '94		Spring '95	
ΔTd	Time	ΔTd	Time	ΔTd	Time	ΔTd	Time	ΔTd	Time
12.6	7.5	15.2	9	28.4	7.5	-23	18.5	25.8	11.5

Table 5.14 Slab 4, volumetric water content and soil moisture content.

Percent Volumetric Water Content (V) and Percent Soil Moisture Content (SM)										
Probe	Fall '93		Winter '93		Spring '94		Summer '94		Spring '95	
	V	SM	V	SM	V	SM	V	SM	V	SM
MC01	13	5.8	7.6	3.4	16	7.1	26.5	11.8	-	-
MC02	26.8	15.5	13.8	8	26.1	15.2	-	-	-	-
MC03	17	7.6	8	3.6	27.8	12.4	23.4	10.4	-	-

Table 5.15 Slab 4, change in stress due to temperature differential.

Gauge	Change in Stress (psi)				
	Fall '93	Winter '93	Spring '94	Summer '94	Spring '95
ST01	111	130	235	216	83
ST02	135	129	317	241	106
CS01	53	49	135	-	95

Table 5.16 Slab 4, change in displacement due to temperature differential.

Gauge	Change in Displacement (milli-inches)				
	Fall '93	Winter '93	Spring '94	Summer '94	Spring '95
LV01	1	0	2	6	13
LV02	1	1	1	2	12

Table 5.17 Slab 5, maximum temperature differential and associated period of time.

Change in Temperature Differential (°F) vs. Time (hrs)									
Fall '93		Winter '93		Spring '94		Summer '94		Spring '95	
ΔTd	Time	ΔTd	Time	ΔTd	Time	ΔTd	Time	ΔTd	Time
17.4	22	-22.8	8.5	-28.6	30	18.2	11.5	27.2	8

Table 5.18 Slab 5, volumetric water content readings and soil moisture content.

Percent Volumetric Water Content (V) and Percent Soil Moisture Content (SM)										
Probe	Fall '93		Winter '93		Spring '94		Summer '94		Spring '95	
	V	SM	V	SM	V	SM	V	SM	V	SM
MC01	11.8	5.3	11.5	5.1	9.2	4.1	17.6	7.9	24.2	10.8
MC02	24.7	14.3	14.1	8.2	21.4	12.4	27.9	16.2	14.1	8.2
MC03	15.5	6.9	12.6	5.6	14.6	6.5	29.6	12	33.1	14.8

Table 5.19 Slab 5, change in stress due to temperature differential.

Gauge	Change in Stress (psi)				
	Fall '93	Winter '93	Spring '94	Summer '94	Spring '95
ST01	102	178	-	155	-
ST02	141	192	303	240	-
CS01	45	-	230	-	152

Table 5.20 Slab 5, change in displacement due to temperature differential.

Gauge	Change in Displacement (milli-inches)				
	Fall '93	Winter '93	Spring '94	Summer '94	Spring '95
LV01	3	5	7	8	9
LV02	3	2	4	1	7
LV03	7	13	27	17	40
LV04	13	22	42	23	-
LV05	21	30	59	35	52

Table 5.21 Slab 6, maximum temperature differential and associated period of time.

Change in Temperature Differential (°F) vs. Time (hrs)									
Fall '93		Winter '93		Spring '94		Summer '94		Spring '95	
ΔTd	Time	ΔTd	Time	ΔTd	Time	ΔTd	Time	ΔTd	Time
18.6	10.5	16.5	11.5	-16.3	14	25	7	18.2	11

Table 5.22 Slab 6, volumetric water content readings and soil moisture content.

Percent Volumetric Water Content (V) and Percent Soil Moisture Content (SM)										
Probe	Fall '93		Winter '93		Spring '94		Summer '94		Spring '95	
	V	SM	V	SM	V	SM	V	SM	V	SM
MC01	11.8	5	11.7	5.2	14.1	6.3	20.5	9.2	24.3	10.8
MC02	24.7	14.3	16.9	9.8	26.2	15.2	-	-	-	-
MC03	15.5	6.9	18.6	8.3	20.4	9.1	23.1	10.3	-	-

Table 5.23 Slab 6, change in stress due to temperature differential.

Gauge	Change in Stress (psi)				
	Fall '93	Winter '93	Spring '94	Summer '94	Spring '95
ST01	167	135	152	216	177
ST02	140	125	140	208	186
CS01	66	77	70	105	110

Table 5.24 Slab 6, change in displacement due to temperature differential.

Gauge	Change in Displacement (milli-inches)				
	Fall '93	Winter '93	Spring '94	Summer '94	Spring '95
LV01	1	2	4	-	8
LV02	0	0	0	7	3
LV03	8	-	11	43	37
LV04	14	-	14	74	74
LV05	19	-	20	108	61

Table 5.25 Slab 7, maximum temperature differential and associated period of time.

Change in Temperature Differential (°F) vs. Time (hrs)									
Fall '93		Winter '93		Spring '94		Summer '94		Spring '95	
ΔTd	Time	ΔTd	Time	ΔTd	Time	ΔTd	Time	ΔTd	Time
12.6	7.5	-15.2	9.5	23.2	5.5	-22.6	16.5	-19.5	7.5

Table 5.26 Slab 7, volumetric water content readings and soil moisture content.

Percent Volumetric Water Content (V) and Percent Soil Moisture Content (SM)										
Probe	Fall '93		Winter '93		Spring '94		Summer '94		Spring '95	
	V	SM	V	SM	V	SM	V	SM	V	SM
MC01	14.2	6.4	6.3	2.8	13.7	6.1	22.5	10	23.4	10.8
MC02	35	20.2	17.3	10	41.2	24	-	-	-	-
MC03	18.7	8.3	9.4	4.2	19.7	8.8	30.1	13.4	26.7	11.9

Table 5.27 Slab 7, change in stress due to temperature differential.

Gauge	Change in Stress (psi)				
	Fall '93	Winter '93	Spring '94	Summer '94	Spring '95
ST01	133	137	208	136	124
ST02	121	121	183	114	131
CS01	84	134	125	131	145

Table 5.28 Slab 7, change in displacement due to temperature differential.

Gauge	Change in Displacement (milli-inches)				
	Fall '93	Winter '93	Spring '94	Summer '94	Spring '95
LV01	8	3	18	21	17
LV02	4	1	9	10	9

Table 5.29 Slab 8, maximum temperature differential and associated period of time.

Change in Temperature Differential (°F) vs. Time (hrs)									
Fall '93		Winter '93		Spring '94		Summer '94		Spring '95	
ΔTd	Time	ΔTd	Time	ΔTd	Time	ΔTd	Time	ΔTd	Time
16.6	6.5	-19.3	8	-24.2	9	28	8	22.1	11

Table 5.30 Slab 8, volumetric water content readings and soil moisture content.

Percent Volumetric Water Content (V) and Percent Soil Moisture Content (SM)										
Probe	Fall '93		Winter '93		Spring '94		Summer '94		Spring '95	
	V	SM	V	SM	V	SM	V	SM	V	SM
MC01	-	-	7.4	3.3	9.3	4.2	15.2	6.8	21.6	12.2
MC02	-	-	-	-	-	-	-	-	-	-
MC03	-	-	11.7	5.2	3.1	1.4	21.9	9.8	27.3	12.2

Table 5.31 Slab 8, change in stress due to temperature differential.

Gauge	Change in Stress (psi)				
	Fall '93	Winter '93	Spring '94	Summer '94	Spring '95
ST01	84	148	195	140	-
ST02	81	122	166	-	-
CS01	21	69	87	129	137

Table 5.32 Slab 8, change in displacement due to temperature differential.

Gauge	Change in Displacement (milli-inches)				
	Fall '93	Winter '93	Spring '94	Summer '94	Spring '95
LV01	6	12	6	20	24
LV02	4	7	11	11	12
LV03	5	10	9	19	27
LV04	11	20	18	38	-
LV05	16	28	30	48	52

Table 5.33 Slab 9, maximum temperature differential and associated period of time.

Change in Temperature Differential (°F) vs. Time (hrs)									
Fall '93		Winter '93		Spring '94		Summer '94		Spring '95	
ΔTd	Time	ΔTd	Time	ΔTd	Time	ΔTd	Time	ΔTd	Time
-10.2	18	-20.7	16	16.4	9	-27	15	29.7	11.5

Table 5.34 Slab 9, volumetric water content readings, and soil moisture content.

Percent Volumetric Water Content (V) and Percent Soil Moisture Content (SM)										
Probe	Fall '93		Winter '93		Spring '94		Summer '94		Spring '95	
	V	SM	V	SM	V	SM	V	SM	V	SM
MC01	9.3	6.5	15.9	7.1	18.3	8.2	26.8	12	27.4	12.2
MC02	17.3	10.1	30.3	17.6	32.9	19.1	-	-	-	-
MC03	11.2	8.6	23.7	10.6	26.4	11.8	30.1	13.4	24.3	10.8

Table 5.35 Slab 9, change in stress due to temperature differential.

Gauge	Change in Stress (psi)				
	Fall '93	Winter '93	Spring '94	Summer '94	Spring '95
ST01	62	154	100	119	150
ST02	74	128	91	85	170
CS01	30	78	-	47	117

Table 5.36 Slab 9, change in displacement due to temperature differential.

Gauge	Change in Displacement (milli-inches)				
	Fall '93	Winter '93	Spring '94	Summer '94	Spring '95
LV01	3	13	7.5	9	34
LV02	1	-	-	21	-
LV03	2	17	19	18	-
LV04	3	15	23	31	-
LV05	7	48	33	38	-

at these points. The difference in the readings was calculated.

Data recorded from each slab are presented separately in four tables. Each table contains the data from five environmental tests for the slab. The first table shows the maximum temperature differential and the time period for which it occurred. A change from the maximum to the minimum temperature was considered positive, while a change from minimum to maximum was negative. The second table lists the volumetric water content readings taken at the site, and the calculated soil moisture content. Values for the change in stress are presented in the third table. Change in displacement for each LVDT on the slab is presented in the fourth table. The magnitudes are listed without regard to direction of slab movement.

Slab stress was calculated from temperature, measured close to the gauges, and strain measurement. The effect that temperature has on pavement stress is very important. A further analysis that included the complete temperature profile would greatly improve the accuracy of stress calculations because the temperature gradients result in stresses several times larger than stresses due to vehicle loads.

The maximum temperature differential occurred for slab nine during the Spring 1995 test. A temperature differential of 29.7°F was measured over an eleven hour period during the April 2 test. Slab six encountered the maximum displacement differential, at OV05, of 108 milli-inches during the Summer 1994 test. A maximum stress differential of 303 psi was encountered by T02 on slab five during the Spring 1994 test. Table 5.37 shows the maximum displacement and stress differentials encountered for each test.

Table 5.37 Maximum deflection and stress differentials for all five environmental tests.

Test	Maximum Induced Displacement				Maximum Induced Stress			
	Slab	Gauge	Displ. x10^-3 inches	Δ°F/ hour	Slab	Gauge	Stress psi	Δ°F/ hour
Fall '94	5	LV05	21	17.4/ 22	6	ST01	167	18.6/ 10.5
Winter '94	9	LV05	48	20.7/ 16	5	ST02	192	22.8/ 8.5
Spring '94	2	LV05	66	26.7/ 12.5	5	ST02	303	28.6/ 30
Summer '94	6	LV05	108	25.0/ 7	4	ST02	241	23.0/ 18.5
Spring '95	6	LV05	61	18.2/ 11	3	ST02	208	25.4/ 18.5

5.3 Discussion of Environmental Testing Results

The soil moisture data reveal that the base moisture content only slightly changed during the testing period. However, the subgrade moisture varied with season and length of concrete slab. In general, the moisture level was higher in the fall and spring than in other tests. Moisture was generally larger in the 21 ft. concrete pavement slabs and more at the joints than the center. The largest volumetric moisture level was 46.6 in Fall 1993 in slab two, a 60 ft. slab.

Deflection and stress were examined as a function of environmental temperature difference. Maximum deflections were measured at the joints of the 40 ft. slabs which appears to be sufficient length to develop large environmental deflections. The deflection in the center of these slabs experienced the least change. For all slabs, the center wheelpath deflection measured about the same magnitude. All deflections had a similar pattern: at the joint, the centerline deflection was least, the wheelpath next, and the corner experienced the maximum deflection as expected. The maximum

value of deflection was measured as in the Summer, 1994. The change in temperature differential was 25°F. The change in deflection of the corner of slab 6 (40 ft. slab) was 108 milli-inches. Deflections depend on temperature and moisture gradients. In general, Spring readings were maximum when temperature gradients were high.

The maximum stress change over the measurement period, not absolute stress magnitude, corresponded to temperature gradient and slab deflection. Absolute temperature when the concrete was placed and curing procedures followed during paving are important since the initial shape will determine joint openings and residual stresses. These initial parameters were not established, however, the change in the slab stress was very high. The maximum value for change of stress was 317 psi in slab 4 (40 ft. slab) in the Spring 1994. The temperature gradient was 28.4°F.

There was a strong correlation between stress and temperature differential. As the temperature differential change, the level of stress changes. The state of stress is indicated by considering the shape of the slab and magnitude of the temperature differential. A negative temperature differential, which generally occurs at night during the spring and fall, gives the maximum deflection and stress condition.

5.3.1 Slab Cracking Due to Environmental Loads

Careful examination of the data for slab two gives some insight into the development of cracking and the resulting stress relief. Cracks for slabs two and four occurred near the longitudinal centerline of the slabs. The crack on slab two lay 11 inches west of the centerline. The crack on slab four lay 2 inches east of the centerline. On slab three, the crack started 93 inches west of the centerline and proceeded diagonally across the slab.

Strain transducers were positioned to measure the bending stresses caused by the curling of

the slab. Temperature differentials of 13.6 and -26.7°F were measured in the Fall 1993 and Spring 1994 tests. The strain transducer at the transverse centerline of the slab, ST01, read a change in stress of 100 psi in the Fall, and 299 psi in the Spring. ST02, which lies in the wheelpath, read a change in stress of 61, and 225 psi for the two tests. During the Summer 1994 test, with a temperature differential of 18.1°F in the concrete, stresses measured by ST01 and ST02 were only 33 and 29 psi.

One possible explanation for the drastic reduction of induced bending stress would be the development of a crack near the center of the slab. Slab two must have cracked between April 28 and August 30, 1994, the dates marking the end of the Spring and the beginning of the Summer test. Note that the Carlson Strain Meter, which measures the axial stress as described in Section 2.6.4, still read significant axial strain (see Table 5.7). Similar results are apparent from examination of the data in Table 5.15 for slab four. Also, notice that the magnitude of stress measured by ST01 and ST02 drops drastically from the Summer 1994 test to the Spring 1995 test, even though the temperature differentials are approximately the same. Slab three developed a similar crack during the Spring 1995 environmental testing period. Photographs of cracks are given in Figure 5.3 through 5.5.

5.3.2 Problems Encountered During Environmental Testing

During the Summer 1994 test, frequent thunderstorms caused short breaks in the supply of electricity. Because of the power outage, the computer would shut down and have to be restarted when CGER personnel arrived. Wiring used to complete the bridge for the Carlson strain meters became loose during the Summer 1994 test. The problem was not found and corrected until after three slabs of data had been recorded. These problems were easy to correct and resulted in minimal loss of data.

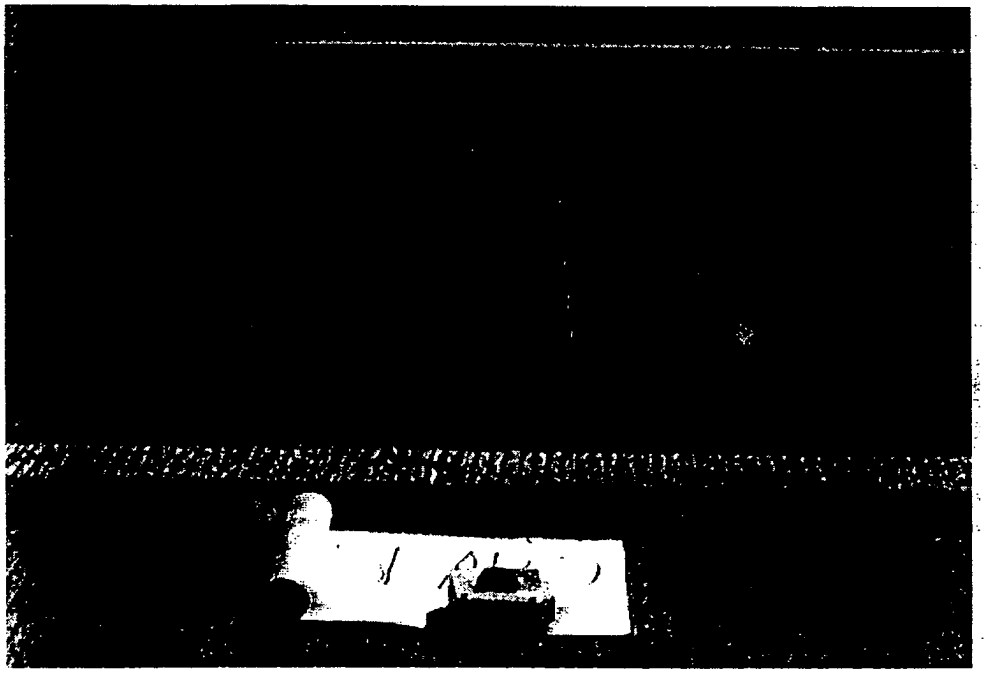

Figure 5.3: Transverse Crack in Slab 2

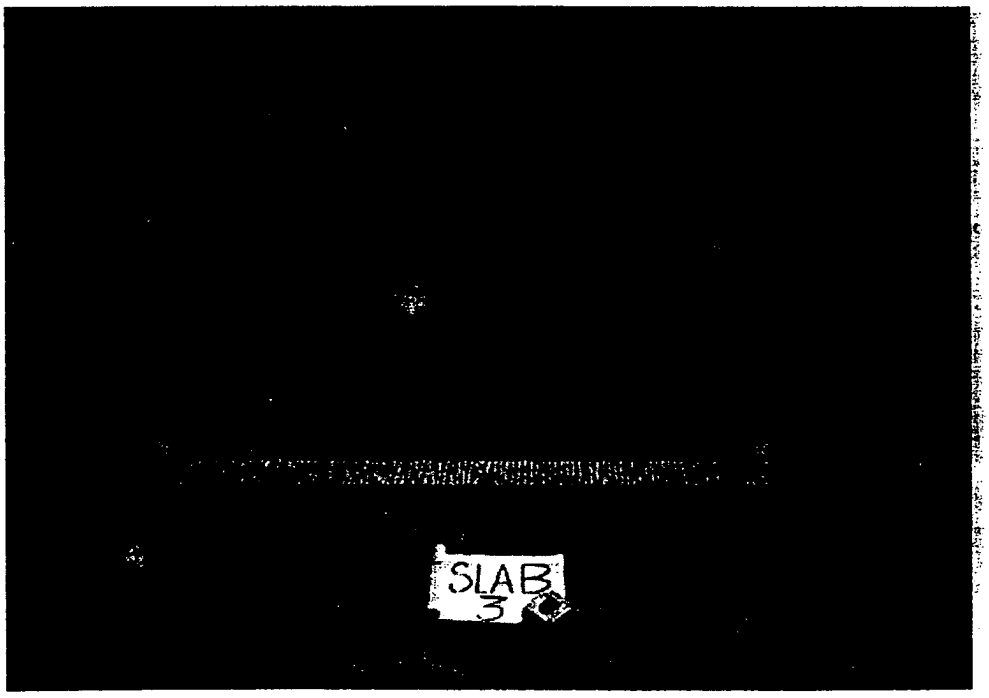

Figure 5.4: Transverse Crack in Slab 3

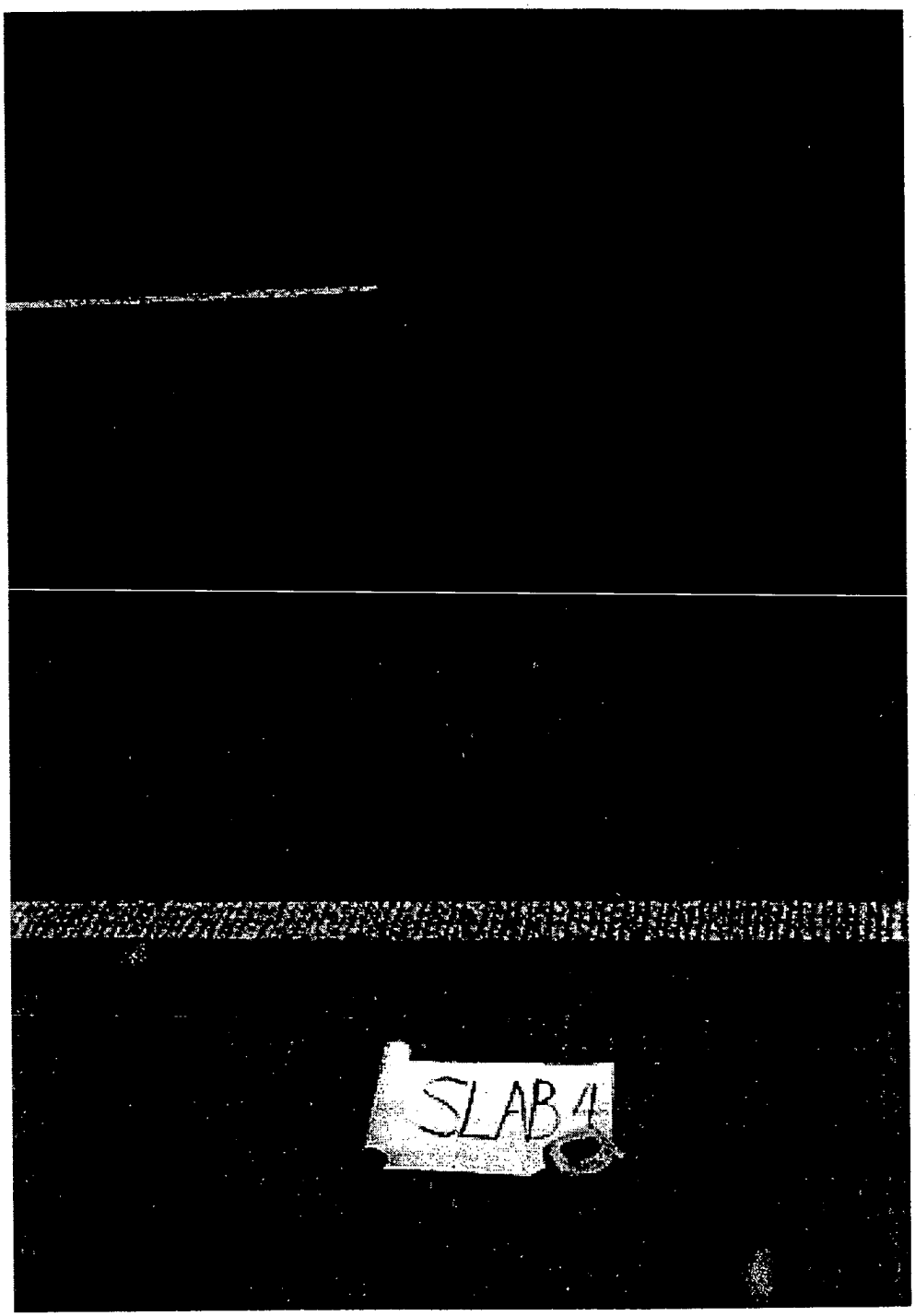

Figure 5.5: Transverse Crack in Slab 4

More serious problems occurred with the LVDTs, soil moisture probes, and the strain transducers: Environmental problems arose with the LVDTs when water and dirt penetrated the SLD. The movable core of the LVDT was exposed when the LVDT was compressed. Freezing temperatures during the winter test caused water clinging to the shaft to freeze, and so restrict the movement of the core. Once thawed, the LVDTs performed normally. A displacement versus time plot for a frozen LVDT appears to drift without regard for the change in temperature differential.

CGER personnel took the opportunity during the August and November 1994 FWD test to clean several of the LVDTs. As the accumulation of dirt on the core prevented smooth movement, the displacement versus time curve became choppy with unreliable readings. The LVDTs performed normally after cleaning. Data from frozen or choppy LVDTs are not presented.

Figure 5.6 presents a diagram of the connection of a soil moisture probe to a lead wire. A serious problem developed with these connections. Corrosion of the screws connecting the probes to the lead wires caused deterioration of the signal quality. The corrosion resulted from exposure to moisture. Of the probes located in the subgrade where the soil moisture content was highest, five of the eight ceased to give data by the Summer of 1994. A crack in the pavement was noted which may have allowed water infiltrate into the base and increase the local soil moisture content. Probes at the transverse contraction joint failed for three slabs by the Spring of 1995. Transverse cracks were observed in slabs two and four by the Spring of 1995. The only soil moisture probes, located directly beneath the center of the slab, to fail were those under slabs two and four.

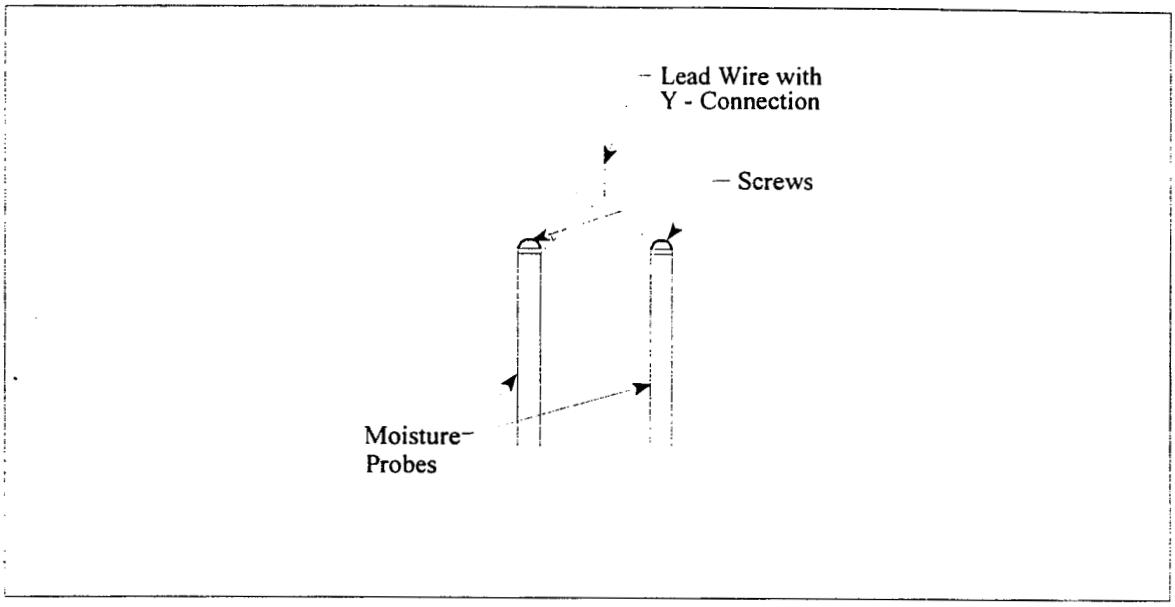

Figure 5.6 Detail of screws on a soil moisture probe.

Lead wires for a sensor must be long enough to reach the data acquisition system connections on the concrete pad. Several of the manufacturers supplied sensors that had leads of insufficient length. Splicing was required in these cases. In an attempt to protect splices from damage, all splices were covered with silicone gel and protective heat shrink wrapping. A plastic harness was used to provide further protection for splices used in the strain transducer circuit. Lead wires were buried with the splices directly beneath the berm. Ninety-nine percent of the splices on this project functioned perfectly. However, the strain transducer splices for slabs five and eight grounded out. The development of cracks may have allowed water to infiltrate. This could explain the "on again, off again" behavior of both strain transducers. A plot of strain versus time shows that strain drifts beyond an acceptable magnitude. At other times these gauges functioned normally. On April 2, 1995, three strain transducers were checked in the field. None of the gauges balanced, and three resistances were well over 350Ω. As each gauge was wired to the balance box, the magnitude of the

measured strain continually floated upwards. This indicated a defective circuit.

Ninety-two percent of the gauges survived the duration of the project. Table 5.38 provides a list of those that did not survive and a brief explanation of the cause.

Table 5.38. List of gauges that did not survive the project.

Gauge	Slab	Notes
ST01, ST02	5	Cause of failure believed to be moisture penetrating splice connection located under berm. Gauge will not zero.
ST02	8	Same as ST02 on slab 5.
LV02	2	Lead wire cracked off at joint with core. Failure caused by small crack created during installation and aggravated by vibrations caused by traffic.
LV02	3	Grounded to base plate.
MC02	8	Lead wires cut by contractor.
MC01	2, 4	Corrosion of connection due to exposure to high soil moisture content caused by seepage through a crack at the centerline.
MC02	2, 4, 6, 7, 8, 9	Corrosion of connection due to exposure to high soil moisture content in the subgrade.
MC03	2, 4, 6	Corrosion of connection due to exposure to high soil moisture content caused by seepage through the expansion joint.

5.4 Falling Weight Deflectometer Test Results

When compared to readings away from the slab centerline, a significantly smaller increase of stress occurred in the wheel path than at the slab centerline; generally of the order of 20%. In every case the top gauge measured an increase in compressive stress while the bottom gauge measured an increase in tensile stress indicating that the slab behaved as a plate in bending when subjected to the load. However, the magnitude of these changes varied for each pair of gauges.

These differences indicate that possible variations in gauge placement may have occurred during the installation process.

Despite efforts to place the gauges at consistent depths within the concrete, by the nature of the paving equipment, the thickness of the slab could have varied by up to 0.5 in. Since the depth of the gauges was controlled by the height of the stainless steel sleeve resting on the base material, if the slab thickness varied, then the depth of the gauges would also change. The thickness of the slab varies with the distance of the neutral axis to the sensors. Instead of the gauges being equidistant from the neutral axis at depths of 1.5 and 8.5 inch in a 10-inch slab, they conceivably could have ended up at depths of 1 and 8 inches in a 9.5 inch slab, in which case the top gauges would be further and the bottom gauges closer to the neutral axis, or at depths of 2 and 9 inches in a 10.5 inch slab, in which case, the top gauges would be closer and the bottom gauges further from the neutral axis. The latter was found to be the case in a core sample taken of a pair of "dummy" gauges installed to check the installation process.

The core sample was taken through the gauges to determine their depth within the slab. The sample measured about 10.25 inches thick and the gauges were located at depths of 2 and 8.5 inches, respectively. In this case, the top gauge was located 0.25 inches closer to the neutral axis than the bottom gauge, but due to the possible variation in slab thickness, this may not be the case with a sample taken from another slab.

The position of the gauges, with respect to the neutral axis, was of concern since larger stresses were expected at the extreme fibers of the cross section. Optimally, the slab thickness would have consistently been 10 inches and the top and bottom gauges would have measured equal but opposite changes in stress. Since equal but opposite changes were rarely encountered, it is logical to assume that the placement of the gauges relative to the neutral axis varied.

Further inspection of the core sample revealed that the top gauge was tilted on its transverse axis about 7 degrees and was about 15 degrees askew from the longitudinal centerline of the slab. The strains measured by this gauge would have been in error by less than 5% due to tilting and skewness.

Three drops per instrument was specified in April. The redundant test procedure showed good repeatability of the embedment gauges. However, the LVDTs consistently measured anywhere from 48% to 86% of the deflection measured by the geophones. This phenomenon tends to indicate that the support for the reference rods used in the SLD assemblies must have moved with the application of the impulse load. The accuracy of the SLD is based on the assumption that the reference rod is anchored deep enough in the subgrade to resist deflection during loading of the pavement layer.

For each gauge tested, a graph of gauge response versus time was drawn. The maximum response was located and recorded. These values are presented in Tables 5.39 through 5.58. Volumetric water content and calculated soil moisture content for each test are presented in Table 5.59. Table 5.60 summarizes the recorded values for the temperature differential during each test.

5.5 Discussion of FWD Testing Results

Tables 5.61 through 5.67 present the average values for gauge response for each FWD test. As with the environmental data in Section 5.2.3, the values are separated by slab length.

The FWD tests produced superior data. The absolute maximum displacement occurred at LV04, on slab three, during the November 11, 1994 test. A displacement of 24.5 milli-inches was recorded resulting from an applied load of 24,320 pounds. Deflection is largest at the joints for

Table 5.39 Slab 1, FWD induced stresses measured by CGER personnel.

Drop Location	Gauge Monitored	Stress (psi)			
		12/14/93	4/18/94	8/2/94	11/21/94
ES03	ES03	-47	-73	-77	-
	ES04	67	129	515	-
ES07	ES07	-67	-115	-112	-
	ES08	57	101	112	-
ES11	ES11	-54	-98	-107	-
	ES12	71	127	-	-
ST02	ST02	60	-	55	-

Table 5.40 Slab 1, FWD induced deflections monitored by CGER and ODOT personnel.

Gauge	Measured Deflection (milli-inches) (CGER Monitored LVDT Response, ODOT Monitored Geophone Response)							
	12/14/93		4/18/94		8/1/94		11/21/94	
	CGER	ODOT	CGER	ODOT	CGER	ODOT	CGER	ODOT
LV02	-	-	6	10	15	10	-	-

Table 5.41 Slab 2, FWD induced stresses measured by CGER personnel.

Drop Location	Gauge Monitored	Stress (psi)			
		12/14/93	4/18/94	8/2/94	11/21/94
ES03	ES03	-46	-70	-	-
	ES04	64	83	-	-
ES07	ES07	-30	-101	-94	-
	ES08	62	107	135	-
ES11	ES11	-37	-108	103	-
	ES12	56	-	-	-
ST02	ST02	87	-	-	-

Table 5.42 Slab 2, FWD induced deflections monitored by CGER and ODOT personnel.

Gauge	Measured Deflection (milli-inches) (CGER Monitored LVDT Response, ODOT Monitored Geophone Response)							
	12/14/93		4/18/94		8/1/94		11/21/94	
	CGER	ODOT	CGER	ODOT	CGER	ODOT	CGER	ODOT
LV02	2	9	7	12	4	10	-	-
LV03	-	-	10	14	-	-	-	-
LV04	4	12	12	20	-	-	-	-
LV05	-	-	18	26	-	-	-	-

Table 5.43 Slab 2, FWD induced vertical stresses measured by CGER personnel.

Pressure Cell Tested	Measured Vertical Stress (psi)	
	12/14/93	4/18/94
PC02	3.4	-
PC03	8.7	6.4

Table 5.44 Slab 3, FWD induced stresses measured by CGER personnel.

Drop Location	Gauge Monitored	Stress (psi)			
		12/14/93	4/18/94	8/2/94	11/21/94
ES03	ES03	-35	-40	-30	-44
	ES04	60	48	148	210
ES07	ES07	-47	-92	-19	-64
	ES08	54	102	63	37
ES11	ES11	-105	-108	-57	-
	ES12	83	85	-	-
ST02	ST02	-	-	-	-

Table 5.45 Slab 3, FWD induced deflections monitored by CGER and ODOT personnel.

Gauge	Measured Deflection (milli-inches) (CGER Monitored LVDT Response, ODOT Monitored Geophone Response)							
	12/14/93		4/18/94		8/1/94		11/21/94	
	CGER	ODOT	CGER	ODOT	CGER	ODOT	CGER	ODOT
LV02	2	9	-	-	-	-	-	-
LV03	-	-	8	14	18	11	-	-
LV04	9	11	10	15	13	11	24	13
LV05	-	-	10	19	10	14	-	-

Table 5.46 Slab 4, FWD induced stresses measured by CGER personnel.

Drop Location	Gauge Monitored	Stress (psi)			
		12/14/93	4/18/94	8/2/94	11/21/94
ES03	ES03	-51	-70	-	-
	ES04	115	118	-	-
ES07	ES07	-72	-64	-40	-
	ES08	131	128	132	-
ST02	ST02	98	-	93	-

Table 5.47 Slab 4, FWD induced deflections monitored by CGER and ODOT personnel.

Gauge	Measured Deflection (milli-inches) (CGER Monitored LVDT Response, ODOT Monitored Geophone Response)							
	12/14/93		4/18/94		8/1/94		11/21/94	
	CGER	ODOT	CGER	ODOT	CGER	ODOT	CGER	ODOT
LV02	2	7	4	8	3	9	-	-

Table 5.48 Slab 5, FWD induced stresses measured by CGER personnel.

Drop Location	Gauge Monitored	Stress (psi)			
		12/14/93	4/18/94	8/2/94	11/21/94
ES03	ES03	-23	-	-	-15
	ES04	50	93	-	346
ES07	ES07	-70	-100	-	102
	ES08	104	108	-91	-69
ST02	ST02	64	-	120	-

Table 5.49 Slab 5, FWD induced deflections monitored by CGER and ODOT personnel.

Gauge	Measured Deflection (milli-inches) (CGER Monitored LVDT Response, ODOT Monitored Geophone Response)							
	12/14/93		4/18/94		8/1/94		11/21/94	
	CGER	ODOT	CGER	ODOT	CGER	ODOT	CGER	ODOT
LV02	2	8	7	9	5	9	-	-
LV03	-	-	6	10	-	-	-	-
LV04	-	-	8	14	14	11	8	13
LV05	12	16	8	19	13	15	-	-

Table 5.50 Slab 5, FWD induced vertical stresses.

Pressure Cell Tested	Measured Vertical Stress (psi)	
	12/14/93	4/18/94
PC02	12.5	4.4
PC03	18.1	9.2

Table 5.51 Slab 6, FWD induced stresses measured by CGER personnel.

Drop Location	Gauge Monitored	Stress (psi)			
		12/14/93	4/18/94	8/2/94	11/21/94
ES03	ES03	-80	-75	-90	-55
	ES04	119	92	513	435
ES07	ES07	-78	-53	-50	-70
	ES08	102	92	107	95
ST02	ST02	108	-	87	-70

Table 5.52 Slab 6, FWD induced deflections monitored by CGER and ODOT personnel.

Gauge	Measured Deflection (milli-inches) (CGER Monitored LVDT Response, ODOT Monitored Geophone Response)							
	12/14/93		4/18/94		8/1/94		11/21/94	
	CGER	ODOT	CGER	ODOT	CGER	ODOT	CGER	ODOT
LV02	4	9	-	-	2	11	-	-
LV03	-	-	6	11	-	-	-	-
LV04	7	12	11	14	8	13	-	-
LV05	10	16	12	16	14	17	-	-

Table 5.53 Slab 7, FWD induced stresses measured by CGER personnel.

Drop Location	Gauge Monitored	Stress (psi)			
		12/14/93	4/18/94	8/2/94	11/21/94
ES03	ES03	-55	-77	-	-
	ES04	136	117	-	-
ST02	ST02	65	-	-	-

Table 5.54 Slab 7, FWD induced deflections monitored by CGER and ODOT personnel.

Gauge	Measured Deflection (milli-inches) (CGER Monitored LVDT Response, ODOT Monitored Geophone Response)							
	12/14/93		4/18/94		8/1/94		11/21/94	
	CGER	ODOT	CGER	ODOT	CGER	ODOT	CGER	ODOT
LV02	3	11	9	11	6	11	-	-

Table 5.55 Slab 8, FWD induced stresses measured by CGER personnel.

Drop Location	Gauge Monitored	Stress (psi)			
		12/14/93	4/18/94	8/2/94	11/21/94
ES03	ES03	-75	-	-20	-
	ES04	136	-	117	-
ST02	ST02	54	-	-17	-

Table 5.56 Slab 8, FWD induced deflections monitored by CGER and ODOT personnel.

Gauge	Measured Deflection (milli-inches) (CGER Monitored LVDT Response, ODOT Monitored Geophone Response)							
	12/14/93		4/18/94		8/1/94		11/21/94	
	CGER	ODOT	CGER	ODOT	CGER	ODOT	CGER	ODOT
LV02	5	10	-	-	6	10	-	-
LV03	-	-	-	-	8	11	-	-
LV04	5	13	-	-	9	20	-	-
LV05	12	18	-	-	-	-	-	-

Table 5.57 Slab 9, FWD induced stresses measured by the CGER personnel.

Drop Location	Gauge Monitored	Stress (psi)			
		12/14/93	4/18/94	8/2/94	11/21/94
ES03	ES03	-79	-118	-66	-48
	ES04	81	108	275	210
ST02	ST02	100	-	70	-

Table 5.58 Slab 9, FWD induced deflections monitored by CGER and ODOT personnel.

Gauge	Measured Deflection (milli-inches) (CGER Monitored LVDT Response, ODOT Monitored Geophone Response)							
	12/14/93		4/18/94		8/1/94		11/21/94	
	CGER	ODOT	CGER	ODOT	CGER	ODOT	CGER	ODOT
LV01	-	-	-	-	3	9	-	-
LV02	2	10	-	-	4	10	6	9
LV03	-	-	6	14	7	13	-	-
LV04	5	13	15	21	12	20	3	13
LV05	8	14	-	-	-	-	-	-

Table 5.59 Soil Moisture Probe readings in percent for the December, April and November FWD tests.

Slab	Soil Moisture Probe #	12/14/94		4/18/94		11/21/94	
		Vol. Water Content	Soil Moisture	Vol. Water Content	Soil Moisture	Vol. Water Content	Soil Moisture
1	1	14.6	6.5	18.9	8.4	-	-
	2	-	-	24.7	14.4	-	-
	3	-	-	47.6	21.3	-	-
2	1	17.1	7.6	22.4	10.0	-	-
	2	20.1	11.7	-	-	-	-
	3	36.6	16.3	-	-	-	-
3	1	12.6	5.6	15.1	6.7	18.8	8.4
	2	16.5	9.6	18.4	10.7	20.2	11.7
	3	15	6.7	24.1	10.8	-	-
4	1	13.1	5.8	17.7	7.9	-	-
	2	24.9	14.5	30	17.4	-	-
	3	17.5	7.8	21.5	9.6	-	-
5	1	12.8	5.7	17.4	7.8	23.8	10.6
	2	21.8	12.7	27.5	16	-	-
	3	16.3	7.3	29.1	16.9	-	-
6	1	11.8	5.3	14.6	13	20.1	9
	2	22.7	13.2	27.2	15.8	17.7	10.3
	3	16.4	7.3	20.7	9.2	-	-
7	1	10.8	4.8	14.5	6.5	-	-
	2	29.8	17.2	50.5	29.4	-	-
	3	15.5	6.9	20.9	9.3	-	-
8	1	12.3	5.6	16	7.1	-	-
	2	-	-	-	-	-	-
	3	14.9	6.7	23.2	10.4	-	-
9	1	14.7	6.6	18.8	8.4	23.8	10.6
	2	29.4	17.1	38	22.1	51.4	29.9
	3	19.6	8.8	26.5	11.8	-	-

Table 5.60 Temperature differential readings recorded for each slab during FWD testing.

Slab	Temperature Differential Readings Δ°F				
	12/14/93	4/18/94	8/1/94	8/2/94	11/21/94
1	0.5	-	22.1	16.6	-
2	-0.9	11.9	20.6	11.2	-
3	4.2	12.3	20.4	8.4	7.9
4	2.4	13.2	14.8	6.1	-
5	1.1	17.4	13.6	6	7.7
6	2.7	12.6	12	5.3	5.7
7	0.6	-	9.3	-0.4	-
8	7.4	18.2	6.6	2.1	-
9	-2.3	3.8	3.4	-0.4	12.7

Table 5.61 Average values for soil moisture content for 60, 40, and 21 foot slabs during FWD testing.

Probes	Soil Moisture Content [%]								
	12/14/93			4/18/94			11/21/94		
	60'	40'	21'	60'	40'	21'	60'	40'	21'
1	6.6	5.6	5.7	8.4	9.6	7.3	8.4	9.8	10.6
2	10.7	13.5	17.2	12.6	16.4	25.8	11.7	10.3	29.9
3	11.5	7.5	7.5	16.1	11.9	10.5	-	-	-

Table 5.62 Average values for induced stresses during FWD testing, 60' slabs.

Gauge	Induced Stress [psi]			
	12/14/93	4/18/94	8/2/94	11/21/94
ES03	-43	-61	-54	-44
ES04	64	87	332	210
ES07	-48	-103	-75	-64
ES08	58	103	103	37
ES11	-65	-105	-89	-
ES12	70	106	-	-
ST02	74	-	55	-

Table 5.63 Average values for induced stresses during FWD testing, 40' slabs.

Gauge	Induced Stress [psi]			
	12/14/93	4/18/94	8/2/94	11/21/94
ES03	-51	-73	-90	-35
ES04	95	101	513	391
ES07	-73	-72	-45	-86
ES08	112	109	120	82
ST02	90	-	100	70

Table 5.64 Average values for induced stress during FWD testing, 21' slabs.

Gauge	Induced Stress [psi]			
	12/14/93	4/18/94	8/2/94	11/21/94
ES03	-70	-98	-43	-48
ES04	118	113	164	210
ST02	73	-	44	-

Table 5.65 Average values for induced deflections during FWD testing, 60' slabs.

Gauge	Induced Deflection [x10^-3 in]			
	12/14/93	4/18/94	8/2/94	11/21/94
LV02	2	7	4	-
LV03	-	9	19	-
LV04	6	11	13	25
LV05	-	14	10	-

Table 5.66 Average values for induced deflections during FWD testing, 40' slabs.

Gauge	Induced Deflection [x10^-3 in]			
	12/14/93	4/18/94	8/1/94	11/21/94
LV02	3	6	4	-
LV03	-	6	-	-
LV04	7	10	11	8
LV05	11	10	14	-

Table 5.67 Average values for induced deflections during FWD testing, 21' slabs.

Gauge	Induced Deflection [x 10^-3 in]			
	12/14/93	4/18/94	8/1/94	11/21/94
LV02	3	9	5	6
LV03	-	7	8	-
LV04	5	15	11	3
LV05	10	-	-	-

FWD tests with deflections increasing toward the corner. At the joint of the 40 ft. slab, the largest average deflections for center, wheelpath, and corner were 8, 14, and 20 milli-inches. The lowest average joint deflections were recorded in the 21 foot slabs for 4, 7, 12 milli-inches. The 21 foot slab measured the highest average deflections of 4 milli-inches at the center.

Pressure cell data were only collected in December 1993 and April 1994. The highest recorded pressures were reported at the corners of the slabs when compared to the center. The maximum pressure recorded was 18.1 psi on the corner of a 40 ft. slab.

Stresses recorded on the 21 ft. slabs indicated the least difference between the induced compressive and tensile stress at the centerline, indicating no relief cracking at the bottom of these slabs. The average values recorded were -65 versus 275 psi for the 40 ft. slabs. Comparing measurement locations of the 60 ft. slabs: centerline -50 versus 173 psi; off-center -72 versus 75 psi; and joint -84 versus 88 psi. The maximum tensile stresses of 515 and 435 psi are too high to be realistic. It appears that the concrete may have developed some micro-cracks along the bottom of the slab, and thus, the modulus has been reduced. Damage of this type is observed in indirect tension tests at high loads. The effects of creep in the concrete slab were not considered. Table 5.68 contains a summary of maximum displacement and stresses for each of the four FWD tests performed. The third test was conducted over a two day period.

Table 5.68 Summary of maximum displacement and stress for each FWD test.

Test	Maximum Induced Displacement			Maximum Induced Stress		
	Slab	Gauge	Displ. x10^-3 inches	Slab	Gauge	Stress psi
12/14/93	6	LV05	12	8	ES04	136
4/18/94	2	LV05	18	1	ES04	129
8/1/94	3	LV03	18	-	-	-
8/2/94	-	-	-	1	ES04	515
11/21/94	3	LV04	24	6	ES04	435

Chapter 6

Finite Element Modeling

6.1 Introduction

This chapter discusses the use of Finite Element Modeling (FEM) software to predict the behavior of the slab under environmental and FWD loading. Results from the analysis are compared to data recorded in the field.

6.2 FEM Software

Two different FEM programs are used to model pavement in this analysis. ILLI-SLAB is used to model FWD testing. A program written by CGER personnel is used to model both FWD and environmental tests.

6.2.1 ILLI-SLAB

ILLI-SLAB was developed at the University of Illinois, Urbana-Champaign during the 1980's. The program models pavement response to live loads. It uses four node, twelve degrees of freedom quadrilateral plate elements (9). The subgrade is modeled using one of nine different methods, including Winkler, Boussinesq, and Vlasov. ILLI-SLAB allows a maximum of nine slabs in each of the horizontal directions. Slab thickness, modulus of elasticity of the slab and base material can be assumed to be constant. Load transfer can be modeled by dowels, aggregate interlock, a key way or a combination of the three modes. Multiple loads can be applied to the slabs.

For this analysis, the parameters consisted of two slabs in line with the load applied at the location of an LVDT. The base was modeled as a Winkler foundation. Most of the required material properties, such as slab thickness and Young's modulus of the concrete, were already

known. A modulus of subgrade reaction of 500 ksi/in was assumed. A different mesh was required for each test to allow a finer grid to surround the point of loading.

6.2.2 CGER Software

The FEM program developed at CGER (10) uses the same element to model all parts of the pavement system. Three dimensional, twenty node brick elements are used for the concrete slab, base, and subgrade. Each layer has its specific material properties applied to elements. Linear elastic material is assumed. Load transfer can be modeled with dowels, ties, and aggregate interlock. Ties were modeled as beam column elements to account for the bending and axial forces encountered for a rod bonded to concrete at both ends. Since one end of the dowel is theoretically considered free to slide into a socket, dowels were modeled as beam elements with no provision made for axial stresses. In addition to loads, the CGER program has the ability to model curling due to temperature changes. By inputting temperature at various points along its depth, the program can model a deflection from a reference value where the slab is assumed to be flat.

One of the advanced features of this program is that it places an interface at the slab/base juncture. The interface allows the slab and base to separate when the slab curls due to a temperature gradient. Thus, the cantilever loading, caused by concave up curling, can be modeled. Interfaces were also placed between slabs to eliminate aggregate interlock with slab shrinkage, but allow it with slab expansion.

Environmental and FWD tests can be modeled with this program. For both tests, the slab dimensions, dowel dimensions, and material properties must be entered by the user. The program automatically constructs a mesh using a mesh generator. When modeling environmental effects, the maximum, minimum, and a reference temperature for points along the depth of the cross section are

entered. For FWD loading, the magnitude and location of the load, and the temperature along the depth are required. Similar output results for both types of testing. For environmental and FWD analysis, the program determines the displacement at selected nodes, and the induced stresses at integration points.

6.3 Environmental Test Modeling

For each of the first four environmental tests, the two slabs with the maximum and minimum temperature differentials were considered for investigation. To ensure a representative sample of the site, all lengths of slabs were modeled. Some substitutions were made to those slabs originally selected to ensure that at least two each of the 21, 40, and 60 foot slabs were analyzed.

Selected data from environmental testing were compared to predictions generated by the CGER program. The program input requires the temperature magnitudes at the 0, 2.5, 7.5, and 10 inch depths. Since the thermocouples were at 1, 4, 7, and 10 inch depths, the required values are interpolated using a parabolic curve fit equation. Material properties such as the Young's modulus of concrete are known. The software has the capacity to determine stress and displacement at any point in the slab. For these tests, the program calculated maximum and minimum stress or displacement at the point where a strain gauge or LVDT was located. These values were compared to the measured maximum and minimum values recorded for each gauge.

6.3.1 Environmental Test Modeling Results

Tables 6.1 through 6.8 summarize and compare the results of the FEM analysis generated by the CGER program with data recorded in the field. The maximum value was taken at the point where the temperature differential was maximum. The minimum value was taken at the point where

Table 6.1 FEM predicted vs. actual stresses encountered during the Fall '93 environmental test.

Gauge	Slab 3 ΔT=18.4°F / 14 hrs.				Slab 4 ΔT=12.6°F / 7.5 hrs.			
	FEM Predicted Stress [psi]		Actual Stress [psi]		FEM Predicted Stress [psi]		Actual Stress [psi]	
	Max	Min	Max	Min	Max	Min	Max	Min
CS01	18	30	95	-22	12	5	6	-27
ST01	108	2	92	20	51	-44	38	-73
ST02	100	1	54	-1	47	-47	48	-87

Table 6.2 FEM predicted vs. actual displacements encountered during the Fall '93 environmental test.

Gauge	Slab 3 ΔT=18.4°F / 14 hrs.				Slab 4 ΔT=12.6°F / 7.5 hrs.			
	FEM Predicted Displacement x 10^-3 in		Actual Displacement x 10^-3 in		FEM Predicted Displacement x 10^-3 in		Actual Displacement x 10^-3 in	
	Max	Min	Max	Min	Max	Min	Max	Min
LV01	4.2	-1.2	3	-1	1.4	-2.4	0	-1
LV02	-0.1	0.6	0	0	0.4	0.9	0	1
LV03	5.4	3	-3	5	-	-	-	-
LV04	1.8	5.4	-4	5	-	-	-	-
LV05	-2.9	6.8	-8	8	-	-	-	-

Table 6.3 FEM predicted vs. actual stresses encountered during the Winter '94 environmental test.

Gauge	Slab 8 ΔT=-19.3°F / 8 hrs.				Slab 9 ΔT=-20.7°F / 16 hrs.			
	FEM Predicted Stress [psi]		Actual Stress [psi]		FEM Predicted Stress [psi]		Actual Stress [psi]	
	Max	Min	Max	Min	Max	Min	Max	Min
CS01	32	2	56	-32	60	15	76	-15
ST01	118	-42	92	-93	73	-42	107	-40
ST02	140	-30	93	-32	74	-40	89	-50

Table 6.4 FEM predicted vs. actual displacements encountered during the Winter '94 environmental test.

Gauge	Slab 8 ΔT=-19.3°F / 8 hrs.				Slab 9 ΔT=-20.7°F / 16 hrs.			
	FEM Predicted Displacement x 10^-3 in		Actual Displacement x 10^-3 in		FEM Predicted Displacement x 10^-3 in		Actual Displacement x 10^-3 in	
	Max	Min	Max	Min	Max	Min	Max	Min
LV01	22.4	-2.5	13	-22	3.8	-7.1	3	-1
LV02	7.8	-1.3	9	-14	0.8	-0.6	7	-1
LV03	9.2	5.7	9	0	-0.9	16.2	-6	8
LV04	0.8	9.3	4	4	-0.9	25	-12	8
LV05	-6	11.2	-4	12	-2	34.6	-13	10

Table 6.5 FEM predicted vs. actual stresses encountered during the Spring '94 environmental test.

Gauge	Slab 3 ΔT=23.8°F / 8 hrs.				Slab 4 ΔT=28.4°F / 7.5 hrs.			
	FEM Predicted Stress [psi]		Actual Stress [psi]		FEM Predicted Stress [psi]		Actual Stress [psi]	
	Max	Min	Max	Min	Max	Min	Max	Min
CS01	4	38	42	-23	43	31	113	-34
ST01	108	2	79	40	150	-53	137	-110
ST02	100	1	112	-1	140	-53	225	-88

Table 6.6 FEM predicted vs. actual displacement encountered during the Spring '94 environmental test.

Gauge	Slab 3 ΔT=23.8°F / 8 hrs.				Slab 4 ΔT=28.4°F / 7.5 hrs.			
	FEM Predicted Displacement x 10^-3 in		Actual Displacement x 10^-3 in		FEM Predicted Displacement x 10^-3 in		Actual Displacement x 10^-3 in	
	Max	Min	Max	Min	Max	Min	Max	Min
LV01	4.2	-1.2	11	-1	10.7	-3.3	0	-2
LV02	-0.1	0.6	2	11	5.3	1.4	-1	1
LV03	5.4	3	-12	12	-	-	-	-
LV04	1.8	5.4	-20	13	-	-	-	-
LV05	-2.9	6.8	-33	16	-	-	-	-

Table 6.7 FEM vs. actual stresses encountered during the Summer '94 environmental test.

Gauge	Slab 3 ΔT=-18.1°F / 16 hrs.				Slab 9 ΔT=-27°F / 7.5 hrs.			
	FEM Predicted Stress [psi]		Actual Stress [psi]		FEM Predicted Stress [psi]		Actual Stress [psi]	
	Max	Min	Max	Min	Max	Min	Max	Min
CS01	-52	-31	53	-108	9	-16	-	-
ST01	69	-83	108	-37	118	-45	114	-14
ST02	60	-79	108	-45	123	-42	65	-23

Table 6.8 FEM vs. actual displacements encountered during the Summer '94 environmental test.

Gauge	Slab 3 ΔT=-18.1°F / 16 hrs.				Slab 9 ΔT=-27°F / 7.5 hrs.			
	FEM Predicted Displacement x 10^-3 in		Actual Displacement x 10^-3 in		FEM Predicted Displacement x 10^-3 in		Actual Displacement x 10^-3 in	
	Max	Min	Max	Min	Max	Min	Max	Min
LV01	6	-3	10	-4	27.7	-2.9	18	-3
LV02	2.6	0.4	-	-	17.8	-1.3	8	-1
LV03	3.8	2.2	-6	31	1.2	1.5	-5	10
LV04	-0.5	6.8	-9	33	-2.9	2.8	-16	14
LV05	-5.6	11.1	-17	41	-12.2	5.5	-32	18

the temperature differential was minimum. Only limited agreement was found between the predicted and field values of displacement and stress, with some values measured at the minimum temperature gradient larger than values measured at the maximum temperature gradient. This is expected because the initial conditions are unknown. The change of shape of the slabs that occurs during

curing is unknown. Environmental conditions at the joints are unknown. The effect of the temperature on the joint behavior is unknown. For instance, for the same temperature gradient, if the total temperature is lower than the curing temperature, the joints will open slightly. On the other hand, if the curing temperature is higher, then the joints will close. Each of these conditions will have a major impact on the results predicted by FE program.

6.4 FWD Test Modeling

Both the CGER and ILLI-SLAB programs were used to model slab response under FWD loading. From each test one slab was selected for modeling with gauges giving a representative response. The CGER program required as input the magnitude of the applied load and the temperature gradient at the time of loading. Material properties inputted were the same as those used for the environmental tests. ILLI-SLAB requires an applied pressure and area of pressure application. Material properties, such as slab thickness and the Young's modulus of the concrete are known. The modulus of subgrade reaction of 500 ksi/in. was used for all tests.

6.4.1 FWD Test Modeling Results

Field recorded displacements are compared to the displacements measured by the geophone on the ODOT deflectometer and with displacements calculated with ILLI-SLAB and CGER programs. Table 6.9 summarizes the results. All units are in milli-inches.

The agreement of the magnitudes between the field data and the FEM estimated values is excellent. All predicted and recorded values are within five milli-inches, with the worst agreement between the CGER finite element program and the geophone measurement occurring in the wheelpath and at the joint for the 60 ft. section (LVDT-04). Neither program matched the actual values, but both gave results within an acceptable range.

Table 6.9 Comparison of deflection [milli-inches] recorded in the field and estimated by FEM software.

	Slab 5 Winter '93	Slab 7 Spring '94	Slab 3 Summer '94	Slab 9 Fall '94
Applied Load [pounds]	26000	25551	26112	24392
Gauge	LVDT-05	LVDT-02	LVDT-04	LVDT-02
LVDT	12	9	13	6
Geophone	16	11	11	9
ILLI-SLAB	14.0	8.0	8.2	7.6
CGER	16.6	7.7	15.3	10.8

Chapter 7

Conclusions

7.1 Instrumentation

Efforts made to secure the positioning of the LVDT housings and the stainless steel sleeves used to install the strain gauges proved successful. All the housings maintained their positions above the reference rods and all sleeves passed under the finishing machine without incident.

Strain transducers, embedment strain gauges, Carlson strain meters, thermocouples, and pressure cells functioned satisfactorily. Problems were encountered with three strain transducers and one embedment strain gauge. Since all of the leads from these sensors were spliced, problems may have occurred because of water infiltration. Soil moisture probes deteriorated over the data collection time period. It is speculated that the screws used to secure the steel probes to the lead wires were not able to withstand the corrosive environment.

No problems were encountered concerning the performance of LVDTs or the PML60 Embedment Strain Gauges. However, the LVDTs were found to be frozen during the winter session of testing. Within the housings, embedded in the concrete, condensation tended to form. The LVDTs circuitry is hermetically sealed in the body and there was no evidence of water infiltration there. However, the moveable core is not sealed within the body. Consequently, when the slab temperature became cold enough, condensation between the core and the body froze and the core became stuck at the peak points of deflection. Normal condensation collected in the housings and caused no other problems. Inspection of the LVDTs after four months of use showed no signs of loosening in the LVDT clamp screws, thus eliminating any suspicion of the rigidity of the assembly.

7.2 Environmental Factors

Some observations, consistent with expectations, can be made by examination of the environmental data. The soil moisture content is affected by pavement cracks and joints. The data collected from moisture probes at a pavement joint, when compared with data collected beneath the slab center, show an increase of moisture up to 50% once the expansion crack develops at the joint. Thermocouple data showed that the temperature gradient through the pavement cross section was not linear, and consequently, the gradient must be modeled as a second degree polynomial when analyzing slab response with a FE model. Temperatures not only vary with depth, but also with distance from joints.

Stresses within the concrete were monitored and compared with the temperature differential between the top and bottom of the concrete slab. The responses indicate that deflection and stresses due to curling of the pavement are more severe than those caused by traffic loading. When comparing environmental stresses to FWD induced stresses, no attempt was made to account for (1) moisture variations in the base and subgrade and (2) the change in modulus of concrete resulting creep and micro-cracking.

7.3 Pavement Performance

The objectives set for this project have been met. Some conclusions can be drawn from the data collected for this project:

- Deflection is largest at joints for both environmental and FWD tests. However, the twenty-one foot slabs consistently measured the highest displacement at the center and the lowest at the joint.

- Significant environmental stresses develop in all lengths of slabs. Forty foot slabs invariably developed the largest stress differentials for all seasons.

- Curling of the concrete slab as the result of temperature gradients produces significant stress. Cracks usually develop at locations of maximum stress. Cracks formed at the longitudinal center for the forty foot slabs, but away from the center for the sixty foot slabs.

- Of the three lengths of slabs instrumented for this project, only the twenty-one foot slabs did not experience any visible cracking.

- FWD test results show that the difference is least between the induced compressive and tensile stresses at the slab centerline for the 21 foot slabs, indicating no relief cracking at the bottom of these slabs.

- The results of this project suggest that the 21 foot slabs will be the most durable, based on field measurements.

- The combination of environmental plus vehicle loading creates maximum pavement stress.

- The stresses and deflections are not only affected by temperature gradient, but also total temperature.

7.4 Recommendations

The following recommendations are provided to help with future pavement research.

- More time should be scheduled to complete a FWD test. Only one test had more than one day reserved for testing. As a result, data from all sensors could not be recorded.

- Deformations can be more easily recorded if the exposed core on the LVDTs is protected from dirt and moisture.

- Because environmental curling due to temperature was found to contribute to severe stress conditions and pavement cracking, LVDTs should be placed at both joints, slab centerline, and at intervals in between to provide a complete description of slab curling.

- All three strain measuring devices, the LVDTs, and the thermocouples are essential for measuring response of concrete pavement to environmental and live load. The pressure cells and soil moisture probes were useful only as an indication of base and subgrade response.

- On a project of this size, many people need access to the data files. A simple, standardized format for naming and storing data is invaluable in eliminating confusion.

- Data collected on this project proved that significant magnitudes of deflection and stress develop in a slab because of temperature gradients. More research is needed to incorporate these factors into design procedures. Three-dimensional finite element modeling has been shown to be an effective tool and will help achieve this goal.

- When the finite element method is used to model deflection and stress due to temperature gradient, consideration must be given to variation of temperature along the slab length.

Bibliography

1. Pittman, David W., and Rollings, Raymond S., *Field Instrumentation and Performance Modeling of Rigid Pavements*, **ASCE Journal of Transportation Engineering,** (1992), pp. 365-368.

2. Armaghani, Jamshid M., Larsen, Torbjorn, J., and Smith, Lawrence L., *Temperature Response of Concrete Pavements*, **Transportation Research Record 1121,** (1986), pp. 23-33.

3. Allen, D., Harik, I.E., and Southgate, H., *Temperature Effects on Rigid Pavements*, **ASCE Journal of Transportation Engineering,** (1994), pp. 103-143.

4. Uzan, Jacob, *Rigid Pavement Evaluation Using NDT: Case Study*, **ASCE Journal of Transportation Engineering 4,** (1992), pp. 527-539.

5. Hudson, W.R. and Flannagan, Patrick R., *An Examination of Environmental Versus Load Effects on Pavements,* **Transportation Research Record 1121,** (1986), pp. 34-39.

6. Adkins, Dan F. and Merkley, Gary P., *Mathematical Modeling of Temperature Changes in Concrete Pavements*, **ASCE Journal of Transportation Engineering 3,** (1990), pp. 349-358.

7. Daily, James W. and Riley, William F., *Experimental Stress Analysis, 3rd Edition,* (New York: McGraw-Hill), 224 pp.

8. Lambe, T. William and Whitman, Robert V., *Soil Mechanics* (New York: John Wiley and Sons), 30 pp.

9. Ioannides, M.I., *Analysis of Slab-on-Grade for a Variety of Loading and Support Conditions,* diss., University of Illinois, Champaign-Urbana, (1982).

10. Bazeley, Christopher C., *Route 2 Rigid Pavement Project: Placement, Testing and Data Analysis of Instrumentation on Slabs 1 Thru 9*, M.S. Thesis (1995), Ohio University, 178 pp.

Appendix A

Instrumentation Layout

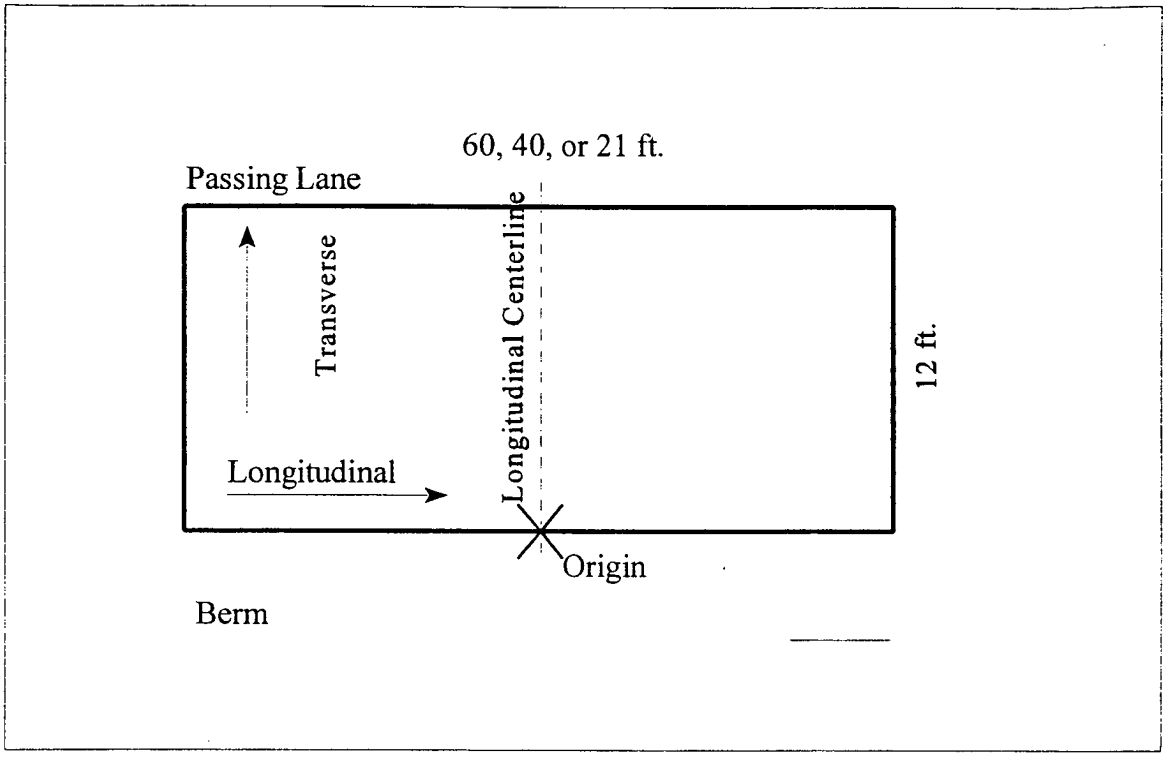

Figure A.1 Coordinate system layout.

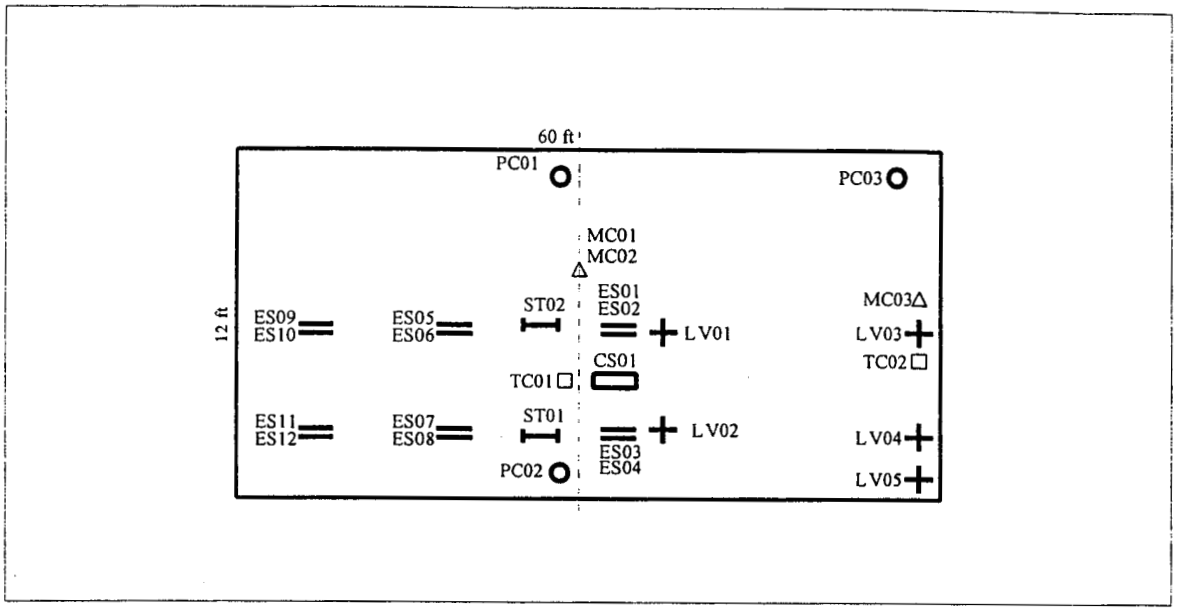

Figure A.2 Plan view of instrumentation layout for a 60 ft slab.

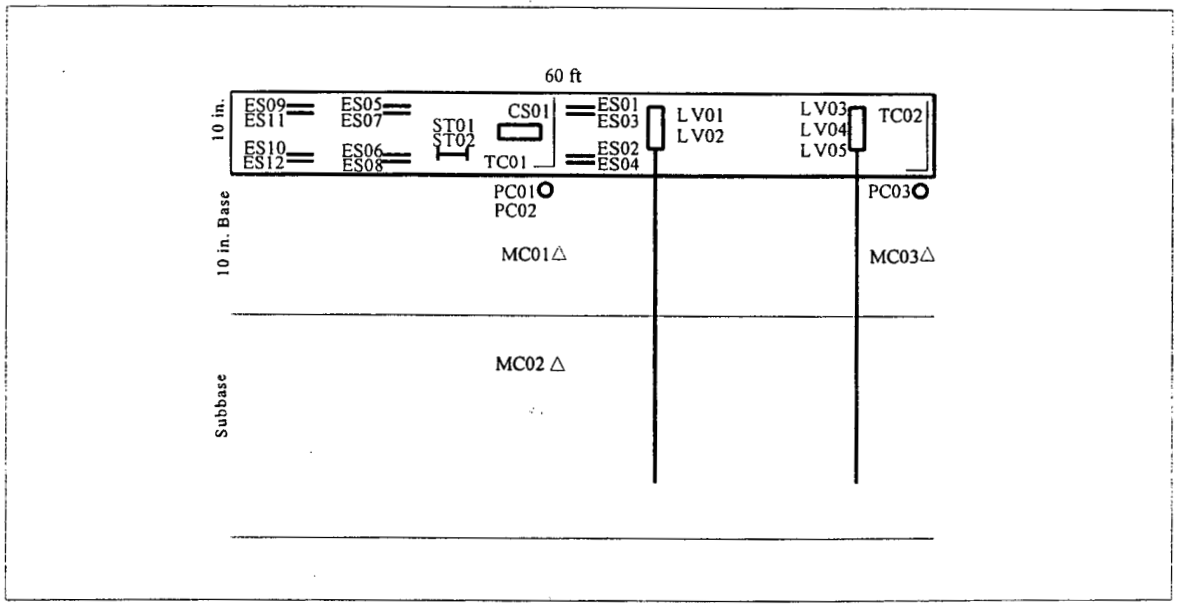

Figure A.3 Section view of instrumentation layout for a 60 ft slab.

Table A.1 Abbreviations used in instrument location coordinates.

C.L. / W.P.	Centerline / Wheelpath	LV__	LVDT
ST__	Strain Transducer	TC__	Thermocouple
ES__	Embedment Strain Gage	MC__	Soil Moisture Probe
CS__	Carlson Strain Gage	PC__	Pressure Cell

Table A.2. Instrument layout for Slab 1 - 60 Ft.

	Long.	Trans.	Vertical	Notes
ES01	5" Rt.	72"	1.5"	C.L. Top
ES02	"	"	8.5"	C.L. Bottom
ES03	"	30"	1.5"	W.P. Top
ES04	"	"	8.5"	W.P. Bottom
ES05	118" Lt.	72"	1.5"	C.L. Top
ES06	"	"	8.5"	C.L. Bottom
ES07	"	Gage	1.5"	W.P. Top
ES08	"	"	8.5"	W.P. Bottom
ES09	239" Lt.	72"	1.5"	C.L. Top
ES10	"	"	8.5"	C.L. Bottom
ES11	"	30"	1.5"	W.P. Top
ES12	"	"	8.5"	W.P. Bottom
CS01	5" Rt.	25"	5"	W.P. Middle
ST01	7" Lt.	72"	8"	C.L. Bottom
ST02	"	30"	8"	W.P. Bottom
TC01	1" Lt.	68"	-	C.L.
TC02	348" Rt.	69"	-	West Joint
LV01	17" Rt.	70"	-	C.L.
LV02	19" Rt.	30"	-	W.P.
PC01	32" Lt.	114"	10"	Semi Conductor
PC02	31" Lt.	30"	10"	Vibrating Wire
MC01	0	72"	15"	Base
MC02	0	72"	23"	Subbase
MC03	342" Rt.	80"	15"	Base

Table A.3. Instrument layout for Slab 2 - 60 Ft.

Gage	Long.	Trans.	Vertical	Notes
ES01	4" Lt.	72"	1.5"	C.L. Top
ES02	"	"	8.5"	C.L. Bottom
ES03	"	30"	1.5"	W.P. Top
ES04	"	"	8.5"	W.P. Bottom
ES05	122" Lt.	72"	1.5"	C.L. Top
ES06	"	"	8.5"	C.L. Bottom
ES07	"	30"	1.5"	W.P. Top
ES08	"	"	8.5"	W.P. Bottom
ES09	241" Lt.	72"	1.5"	C.L. Top
ES10	"	"	8.5"	C.L. Bottom
ES11	"	30"	1.5"	W.P. Top
ES12	"	"	8.5"	W.P. Bottom
CS01	4" Rt.	30"	5"	W.P. Middle
ST01	17" Lt.	72"	8"	C.L. Bottom
ST02	"	30"	8"	W.P. Bottom
TC01	2" Lt.	84"	-	C.L.
TC02	340" Rt.	98"	-	West Joint
LV01	19" Rt.	72"	-	C.L.
LV02	16" Rt.	30"	-	W.P.
LV03	344" Rt.	69"	-	C.L. @ Joint
LV04	343" Rt.	32"	-	W.P. @ Joint
LV05	343" Rt.	11"	-	Edge @ Joint
PC01	32" Lt.	114"	10"	Semi Conductor
PC02	31" Lt.	30"	10"	Semi Conductor
PC03	340" Rt.	114"	10"	Semi Conductor
MC01	0	72"	15"	Base
MC02	0	72"	23"	Subbase
MC03	342" Rt.	80"	15"	Base

Table A.4 Instrument layout for Slab 3 - 60 Ft.

Gage	Long.	Trans.	Vertical	Notes
ES01	6" Lt.	72"	1.5"	C.L. Top
ES02	"	"	8.5"	C.L. Bottom
ES03	"	30"	1.5"	W.P. Top
ES04	"	"	8.5"	W.P. Bottom
ES05	119" Lt.	72"	1.5"	C.L. Top
ES06	"	"	8.5"	C.L. Bottom
ES07	"	30"	1.5"	W.P. Top
ES08	"	"	8.5"	W.P. Bottom
ES09	239" Lt.	72"	1.5"	C.L. Top
ES10	"	"	8.5"	C.L. Bottom
ES11	"	30"	1.5"	W.P. Top
ES12	"	"	8.5"	W.P. Bottom
CS01	6" Rt.	42"	5"	W.P. Middle
ST01	6" Rt.	72"	8"	C.L. Bottom
ST02	"	30"	8"	W.P. Bottom
TC01	1" Rt.	76"	-	C.L.
TC02	344" Rt.	92"	-	Joint
LV01	19" Rt.	70"	-	C.L.
LV02	19" Rt.	30"	-	W.P.
LV03	338" Rt.	74"	-	C.L. @ Joint
LV04	341" Rt.	31"	-	W.P. @ Joint
LV05	338" Rt.	10"	-	Edge @ Joint
PC01	31" Lt.	114"	10"	Vibrating Wire
PC02	31" Lt.	30"	10"	Vibrating Wire
PC03	342" Rt.	114"	10"	Vibrating Wire
MC01	0	72"	15"	Base
MC02	0	72"	23"	Subbase
MC03	342" Rt.	80"	15"	Base

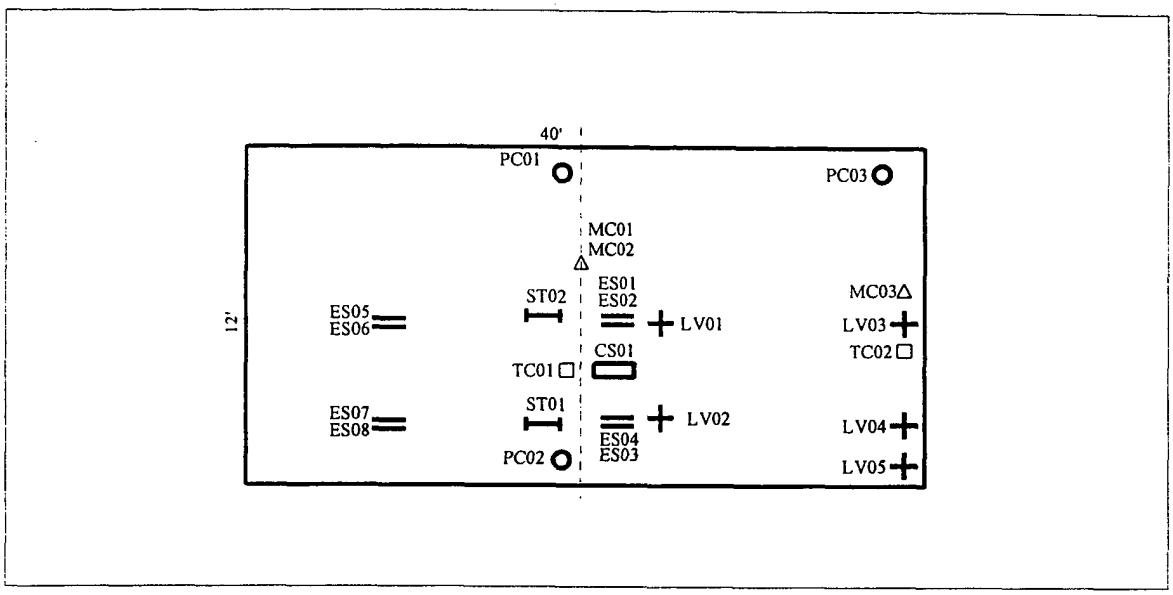

Figure A.4 Plan view of instrumentation layout for a 40' slab.

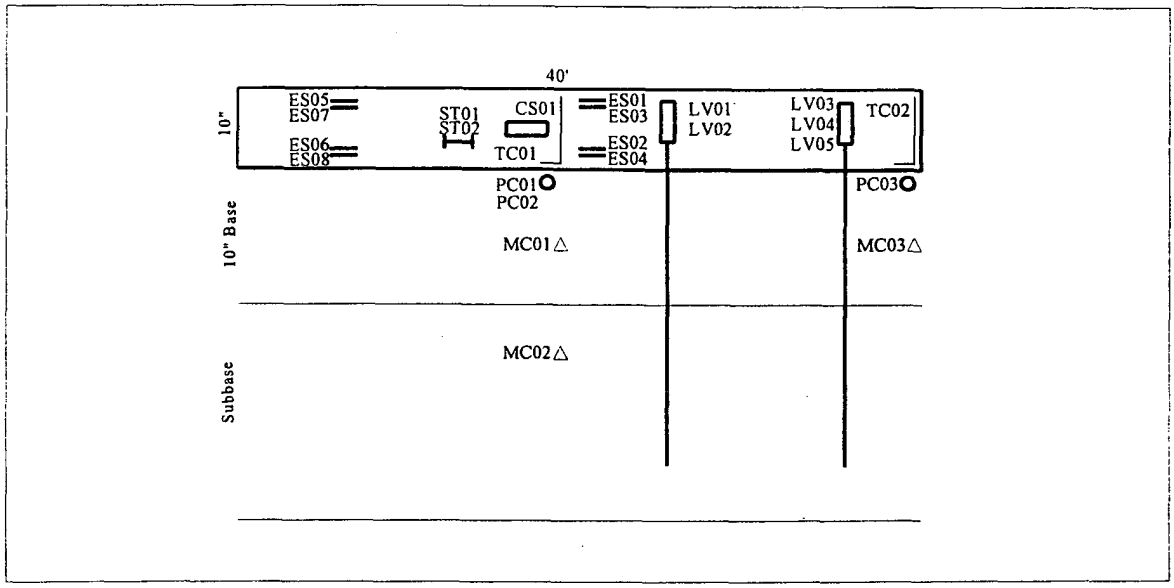

Figure A.5 Section view of instrumentation layout for a 40' slab.

Table A.5 Abbreviations used in instrument location coordinates.

C.L. / W.P.	Centerline / Wheelpath	LV__	LVDT
ST__	Strain Transducer	TC__	Thermocouple
ES__	Embedment Strain Gage	MC__	Soil Moisture Probe
CS__	Carlson Strain Gage	PC__	Pressure Cell

Table A.6 Instrument layout for Slab 4 - 40 Ft.

Gage	Long.	Trans.	Vertical	Notes
ES01	0	72"	1.5"	C.L. Top
ES02	"	"	8.5"	C.L. Bottom
ES03	"	30"	1.5"	W.P. Top
ES04	"	"	8.5"	W.P. Bottom
ES05	121" Lt.	72"	1.5"	C.L. Top
ES06	"	"	8.5"	C.L. Bottom
ES07	"	30"	1.5"	W.P. Top
ES08	"	"	8.5"	W.P. Bottom
CS01	0	30"	5"	W.P. Middle
ST01	12" Lt.	72"	8"	C.L. Bottom
ST02	"	30"	8"	W.P. Bottom
TC01	20" Lt.	81"	-	C.L.
TC02	217" Rt.	82"	-	West Joint
LV01	19" Rt.	68"	-	C.L.
LV02	19" Rt.	30"	-	W.P.
PC01	32" Lt.	114"	10"	Semi Conductor
PC02	34" Lt.	30"	10"	Vibrating Wire
MC01	0	72"	15"	Base
MC02	0	72"	23"	Subbase
MC03	228" Rt.	80"	15"	Base

Table A.7 Instrument layout for Slab 5 - 40 Ft.

Gage	Long.	Trans.	Vertical	Notes
ES01	0	72"	1.5"	C.L. Top
ES02	"	"	8.5"	C.L. Bottom
ES03	"	30"	1.5"	W.P. Top
ES04	"	"	8.5"	W.P. Bottom
ES05	121" Lt.	72"	1.5"	C.L. Top
ES06	"	"	8.5"	C.L. Bottom
ES07	"	30"	1.5"	W.P. Top
ES08	"	"	8.5"	W.P. Bottom
CS01	12" Rt.	30"	5"	W.P. Middle
ST01	13" Lt.	72"	8"	C.L. Bottom
ST02	"	30"	8"	W.P. Bottom
TC01	15" Lt.	81"	-	C.L.
TC02	226" Rt.	82"	-	Joint
LV01	14" Rt.	71"	-	C.L.
LV02	15" Rt.	29"	-	W.P.
LV03	218" Rt.	74"	-	C.L. @ Joint
LV04	221" Rt.	30"	-	W.P. @ Joint
LV05	221" Rt.	13"	-	Edge @ Joint
PC01	30" Lt.	114"	10"	Semi Conductor
PC02	30" Lt.	30"	10"	Semi Conductor
PC03	219" Rt.	114"	10"	Semi Conductor
MC01	0	72"	15"	Base
MC02	0	72"	23"	Subbase
MC03	228" Rt.	80"	15"	Base

Table A.8 Instrument layout for Slab 6 - 40 Ft.

Gage	Long.	Trans.	Vertical	Notes
ES01	3" Rt.	72"	1.5"	C.L. Top
ES02	"	"	8.5"	C.L. Bottom
ES03	"	30"	1.5"	W.P. Top
ES04	"	"	8.5"	W.P. Bottom
ES05	125" Lt.	72"	1.5"	C.L. Top
ES06	"	"	8.5"	C.L. Bottom
ES07	"	30"	1.5"	W.P. Top
ES08	"	"	8.5"	W.P. Bottom
CS01	15" Rt.	31"	5"	W.P. Middle
ST01	9" Lt.	72"	8"	C.L. Bottom
ST02	"	30"	8"	W.P. Bottom
TC01	4" Lt.	79"	-	C.L.
TC02	225" Rt.	85"	-	Joint
LV01	16" Rt.	74"	-	C.L.
LV02	16" Rt.	26"	-	W.P.
LV03	218" Rt.	73"	-	C.L. @ Joint
LV04	219" Rt.	27"	-	W.P. @ Joint
LV05	218" Rt.	12"	-	Edge @ Joint
PC01	30" Lt.	114"	10"	Vibrating Wire
PC02	30" Lt.	30"	10"	Vibrating Wire
PC03	216" Rt.	114"	10"	Vibrating Wire
MC01	0	72"	15"	Base
MC02	0	72"	23"	Subbase
MC03	228" Rt.	80"	15"	Base

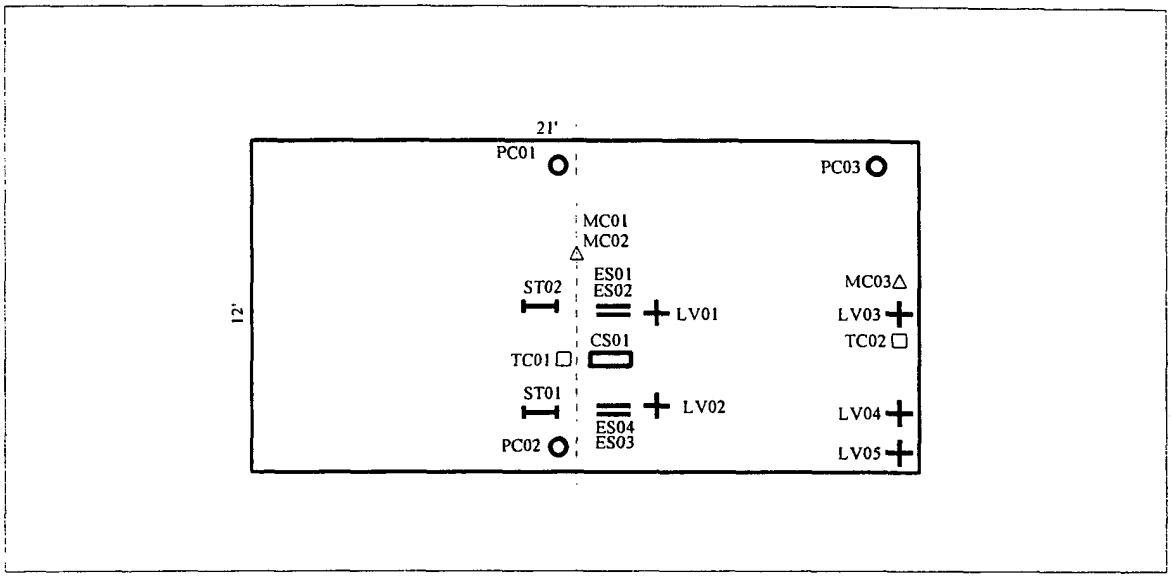

Figure A.6 Plan view of instrumentation layout for a 21' slab.

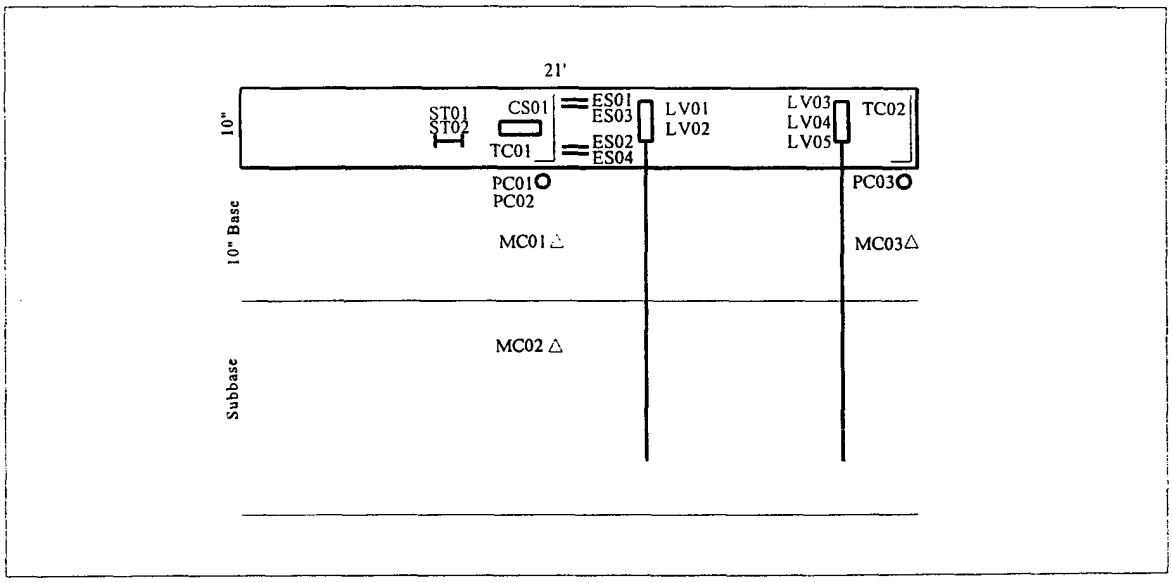

Figure A.7 Section view of instrumentation layout for a 21' slab.

Table A.9 Abbreviations used in instrument location coordinates.

C.L. / W.P.	Centerline / Wheelpath	LV__	LVDT
ST__	Strain Transducer	TC__	Thermocouple
ES__	Embedment Strain Gage	MC__	Soil Moisture Probe
CS__	Carlson Strain Gage	PC__	Pressure Cell

Table A.10 Instrument layout for Slab 7 - 21 Ft.

Gage	Long.	Trans.	Vertical	Notes
ES01	3" Rt.	72"	1.5"	C.L. Top
ES02	"	"	8.5"	C.L. Bottom
ES03	"	30"	1.5"	W.P. Top
ES04	"	"	8.5"	W.P. Bottom
CS01	0	42"	5"	W.P. Middle
ST01	9" Lt.	72"	8"	C.L. Bottom
ST02	"	30"	8"	W.P. Bottom
TC01	9" Rt.	82"	-	C.L.
TC02	121" Rt.	81"	-	Joint
LV01	18" Rt.	72"	-	C.L.
LV02	17" Rt.	28"	-	W.P.
PC01	31" Lt.	114"	10"	Semi Conductor
PC02	34" Lt.	30"	10"	Vibrating Wire
MC01	0	72"	15"	Base
MC02	0	72"	23"	Subbase
MC03	108" Rt.	80"	15"	Base

Appendix B

Environmental Graphs

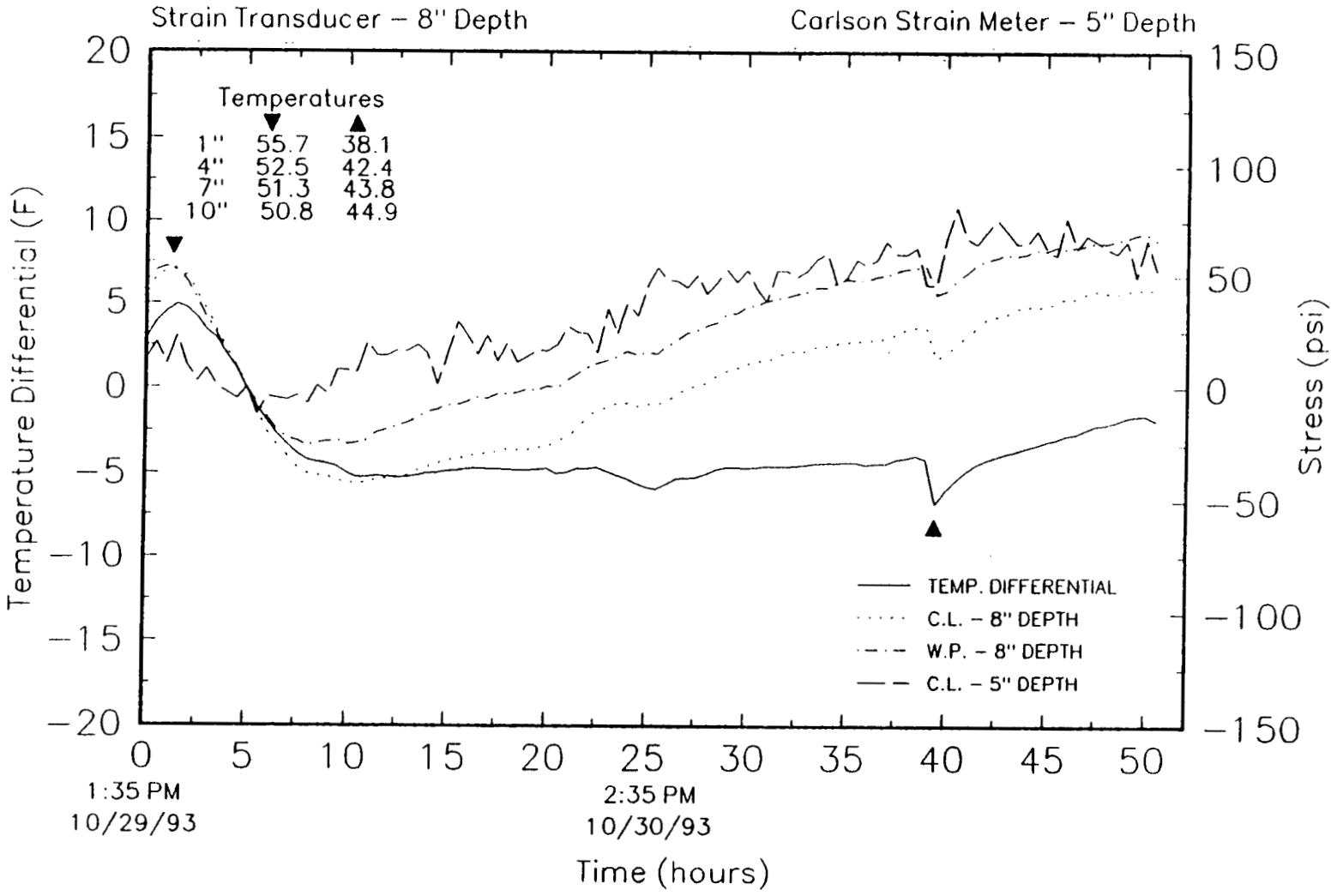

Figure B.1 Slab 1 (60 ft), change in stresses at slab centerline, Fall, '93

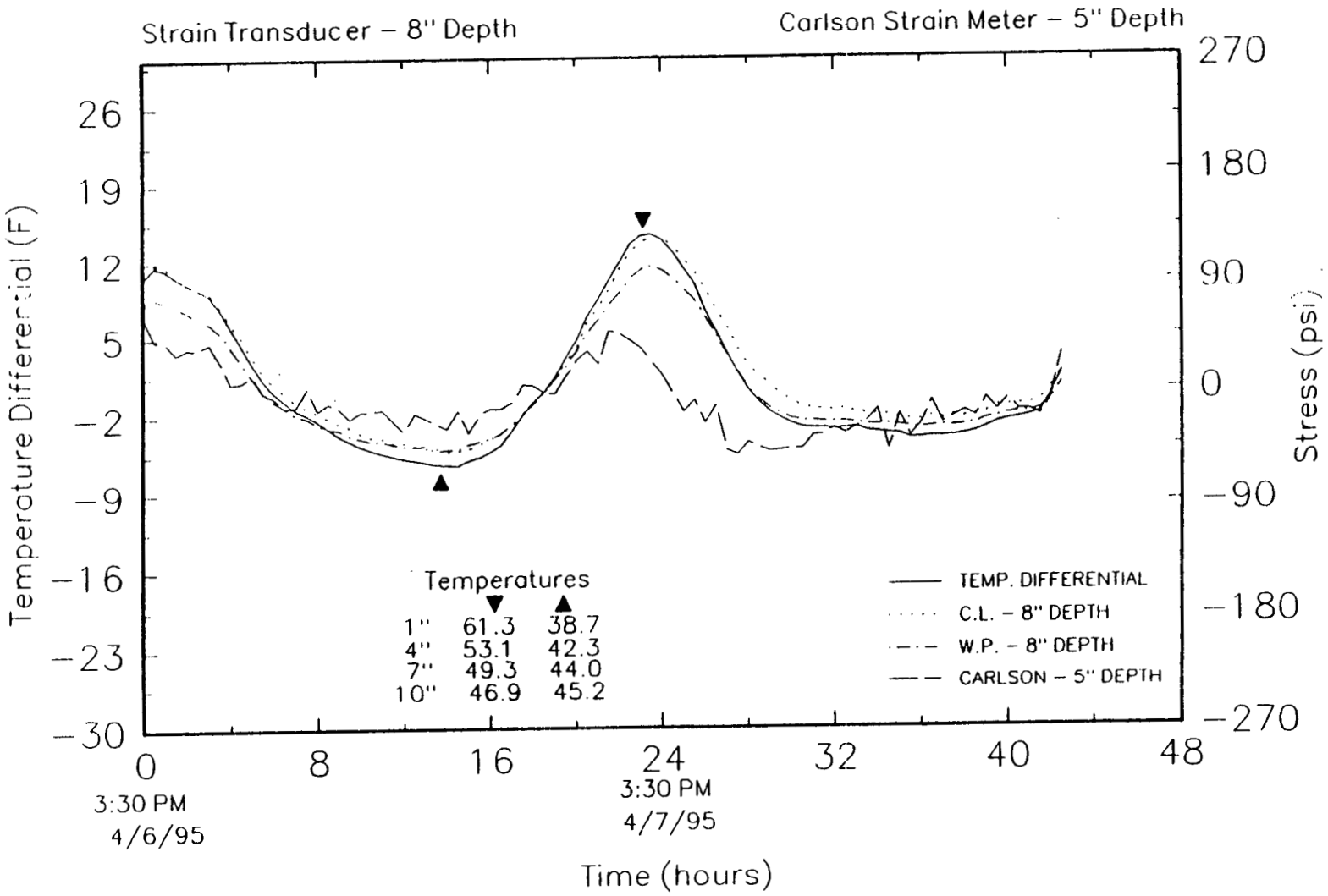

Figure B.2 Slab 1 (60 ft), change in stresses at slab centerline, Spring, '95

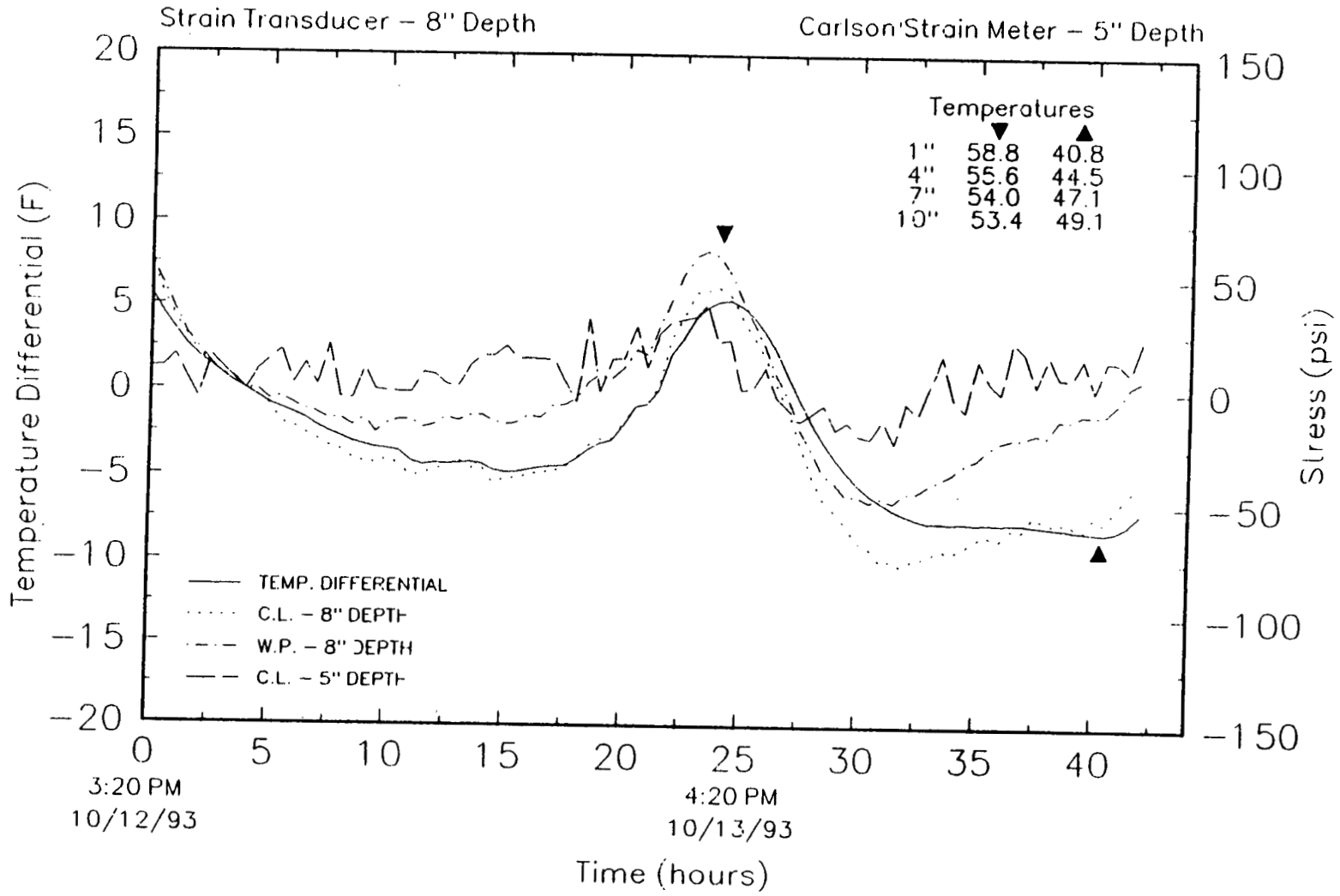

Figure B.3 Slab 2 (60 ft), change in stresses at slab centerline, Fall, '93

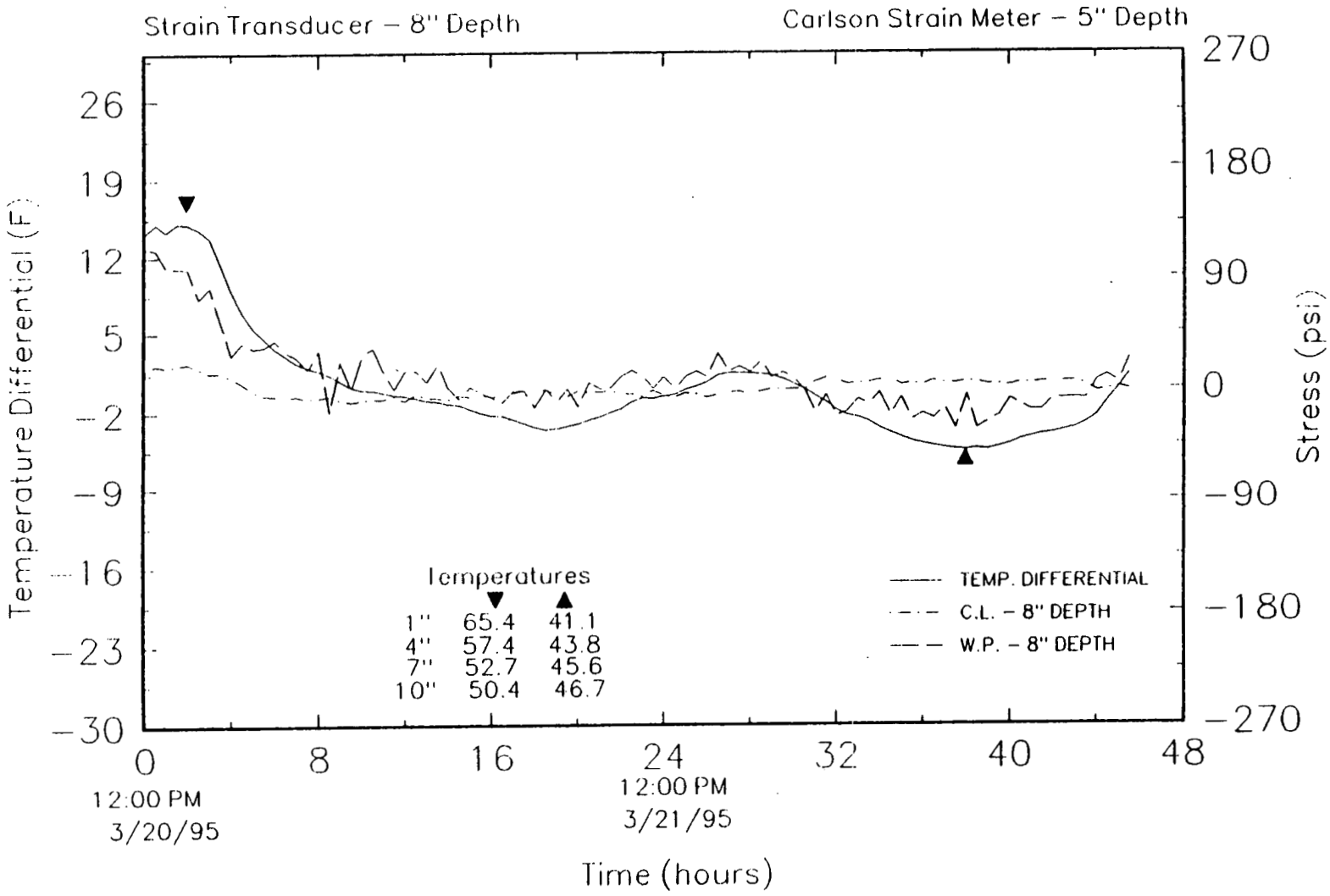

Figure B.4 Slab 2 (60 ft), change in stresses at slab centerline, Spring, '95

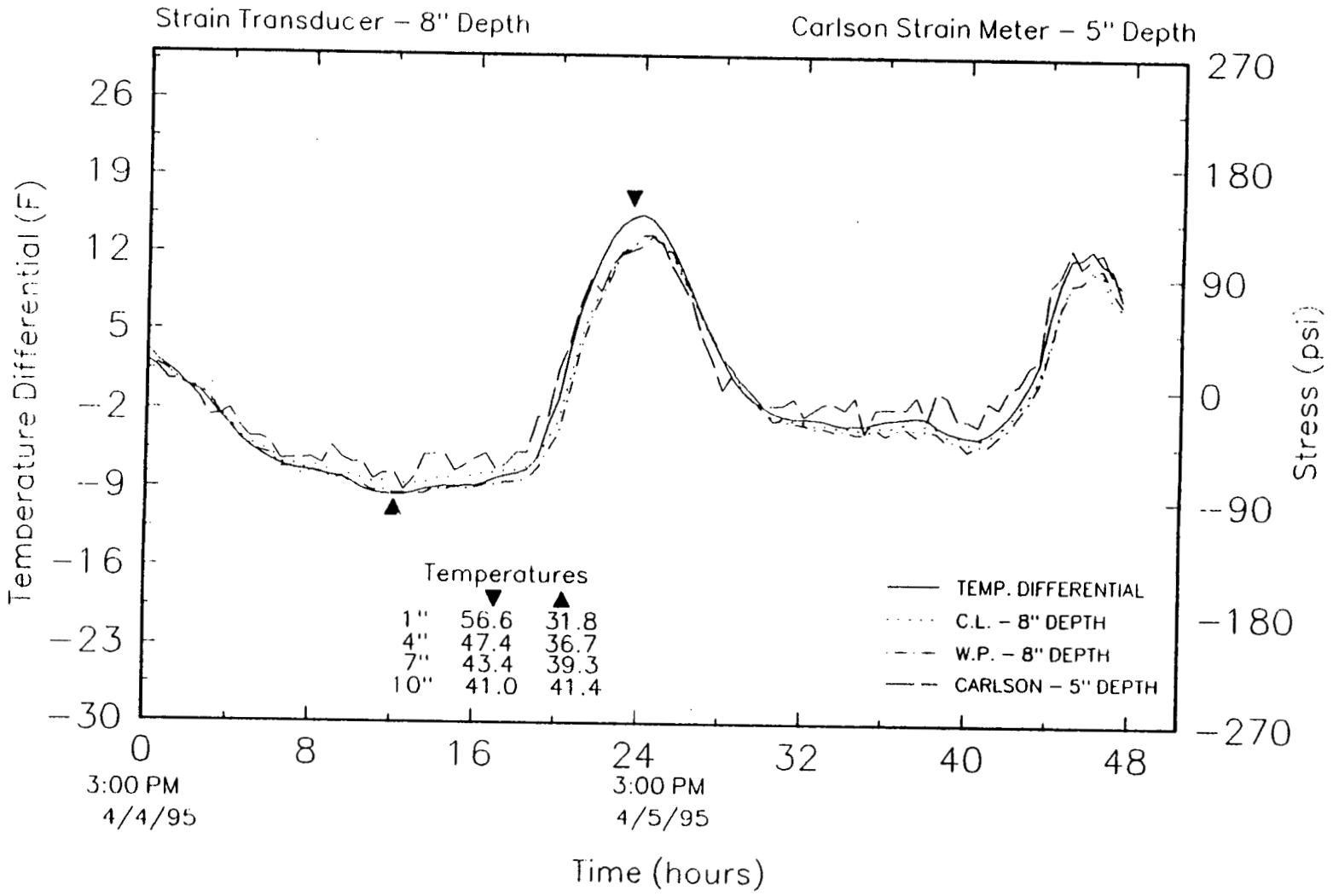

Figure B.5 Slab 3 (60 ft), change in stresses at slab centerline, Spring, '95

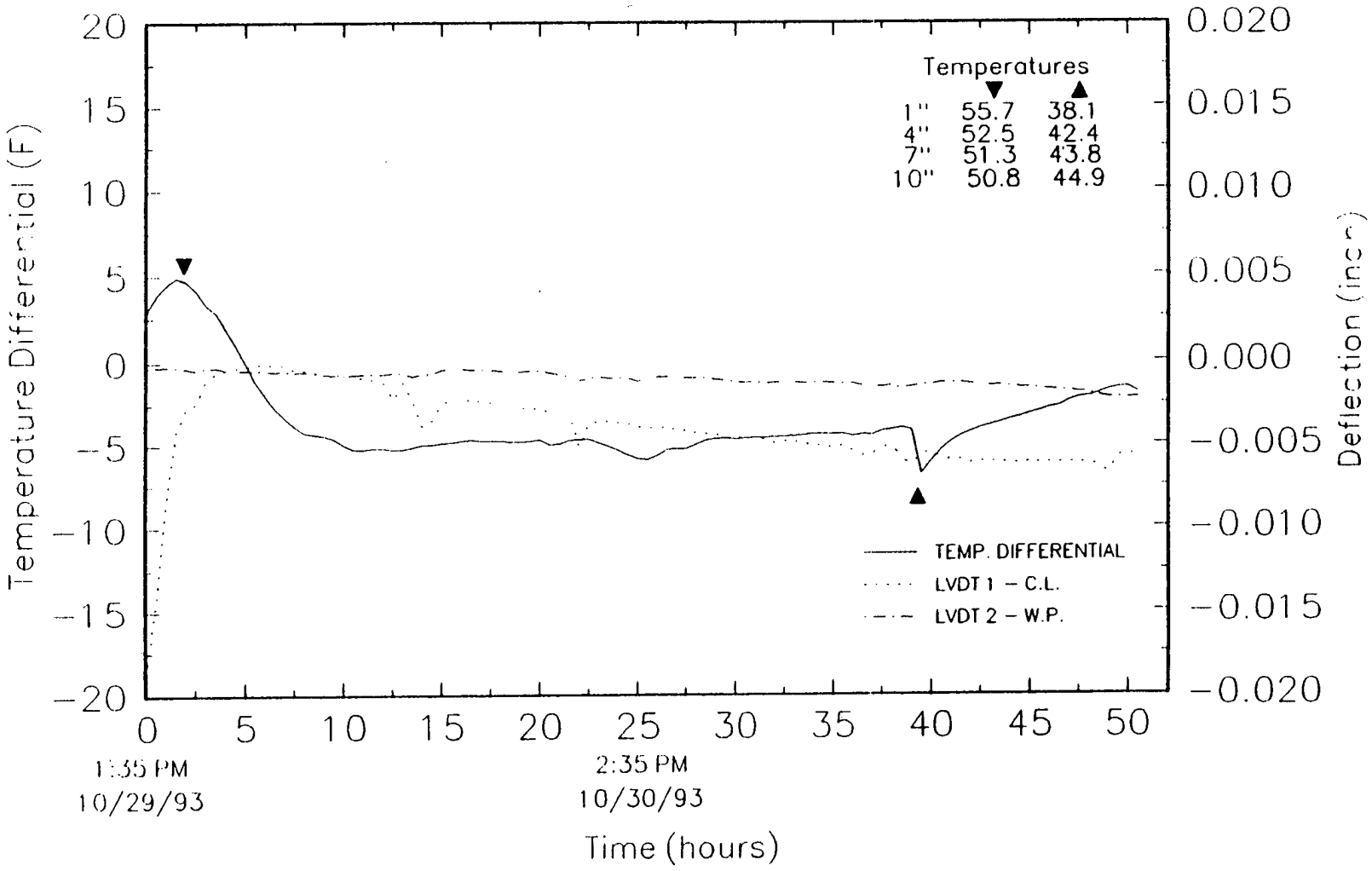

Figure B.6 Slab 1 (60 ft), deflection at transverse centerline, Fall, '93

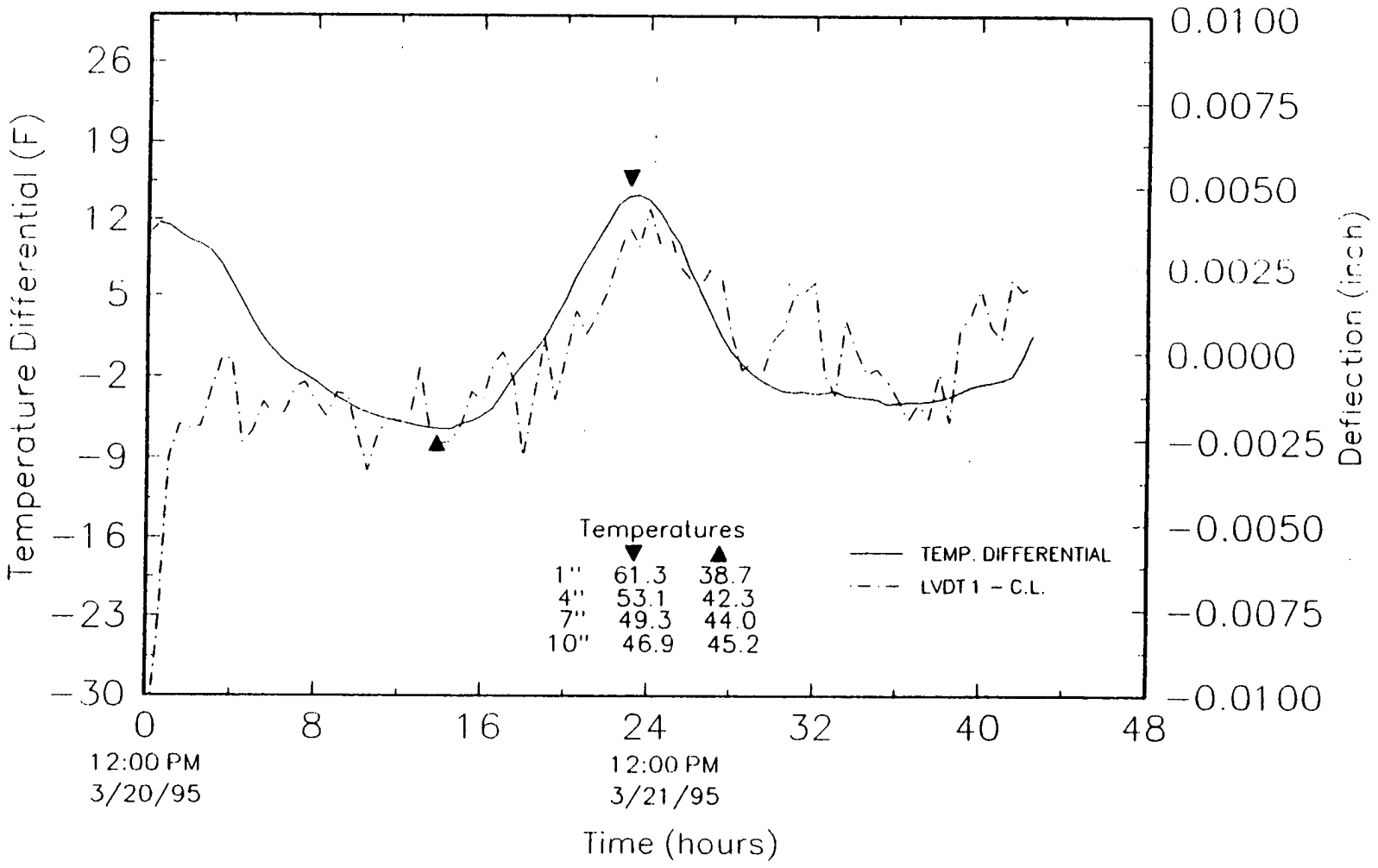

Figure B.7 Slab 1 (60 ft), deflection at transverse centerline, Spring, '95

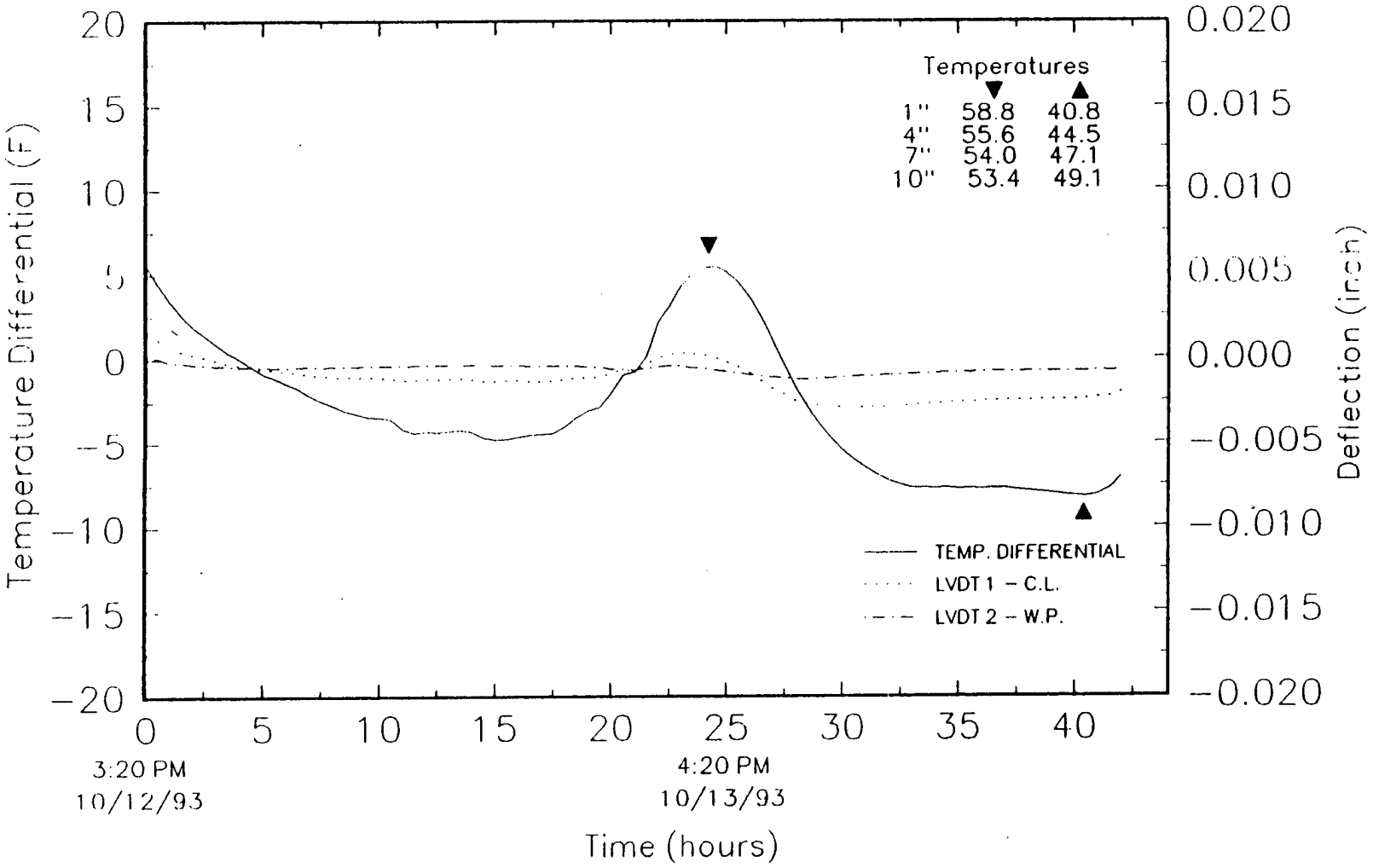

Figure B.8 Slab 2 (60 ft), deflection at transverse centerline, Fall, '93

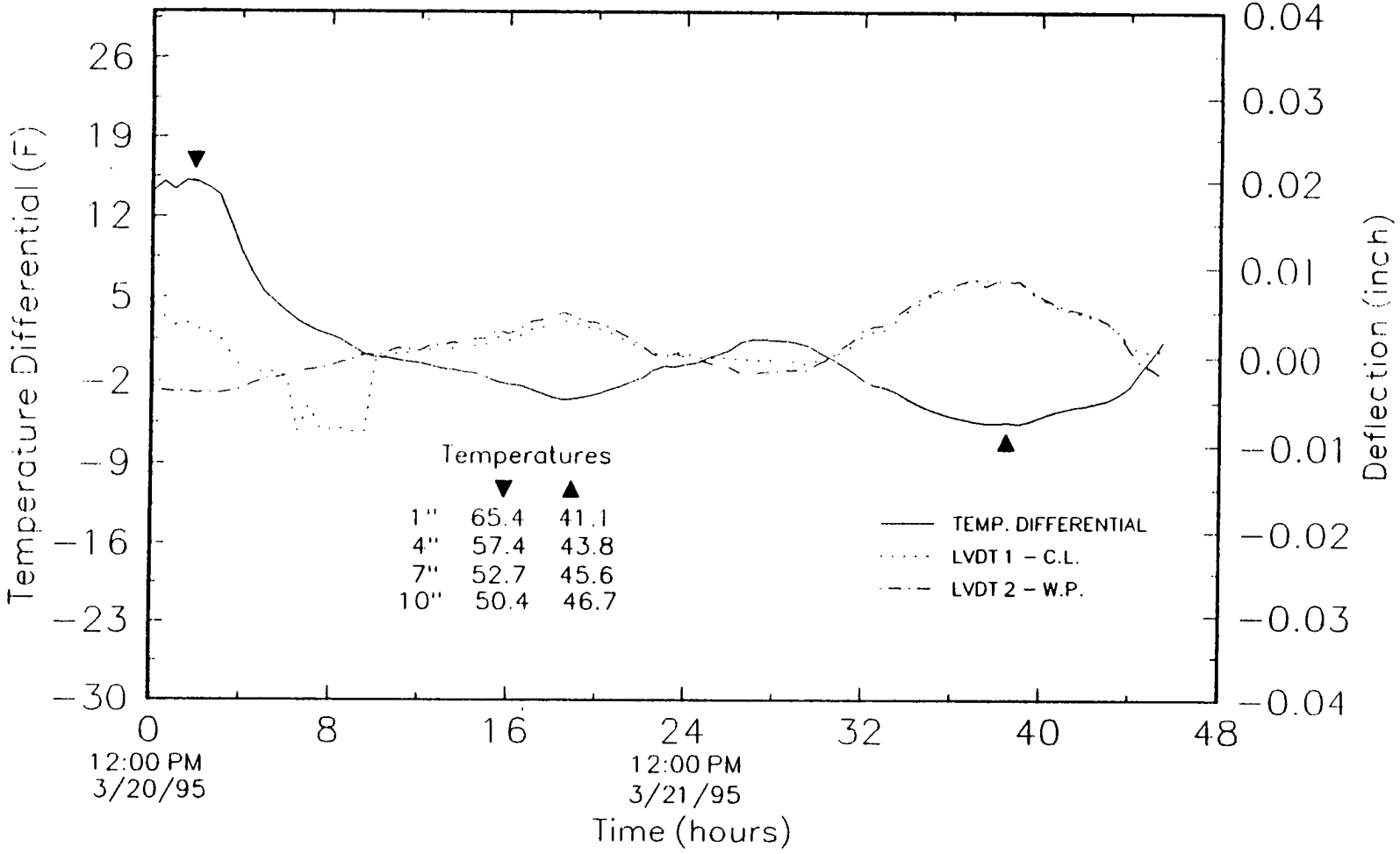

Figure B.9 Slab 2 (60 ft), deflection at transverse centerline, Spring, '95

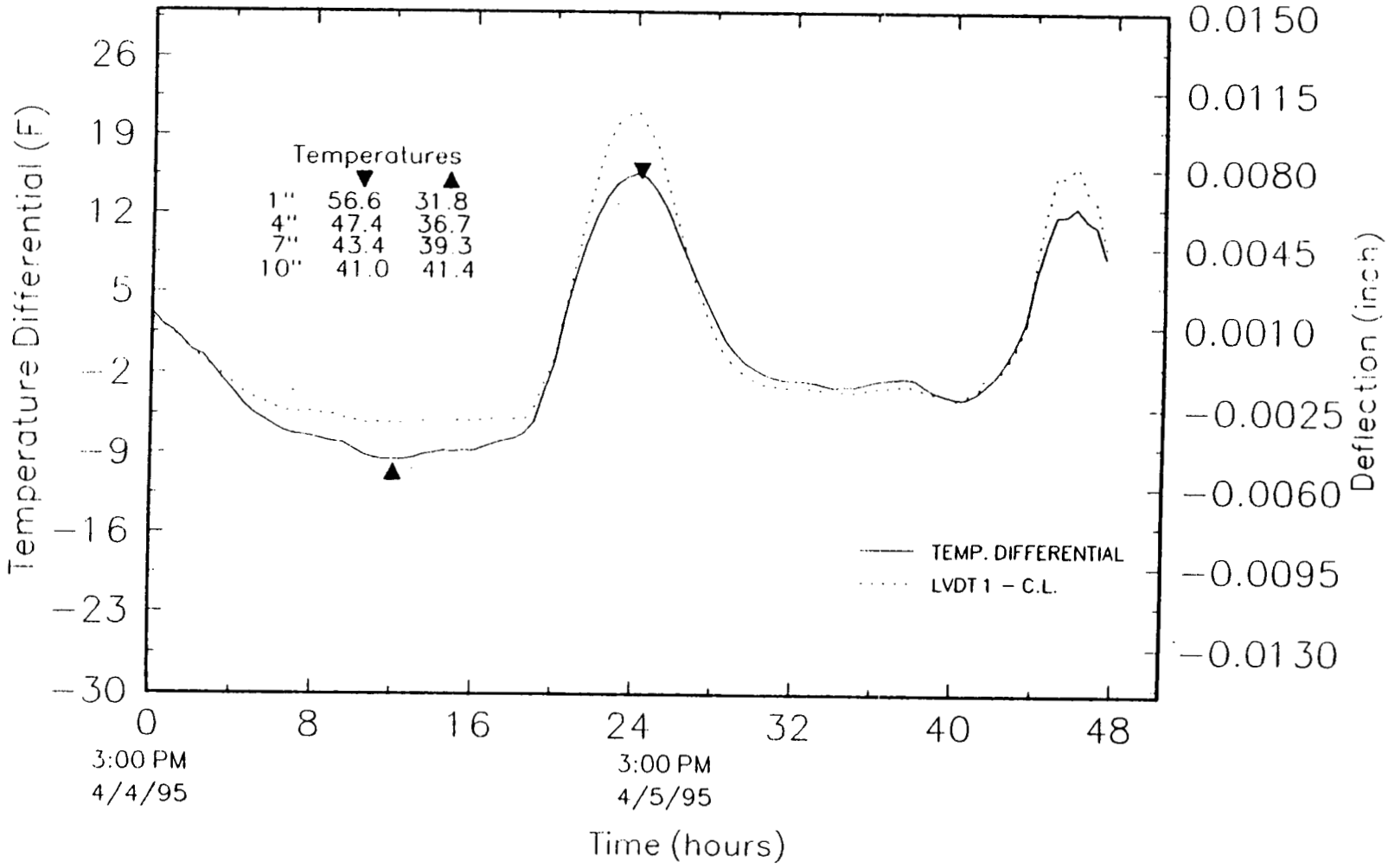

Figure B.10 Slab 3 (60 ft), deflection at transverse centerline, Spring, '95

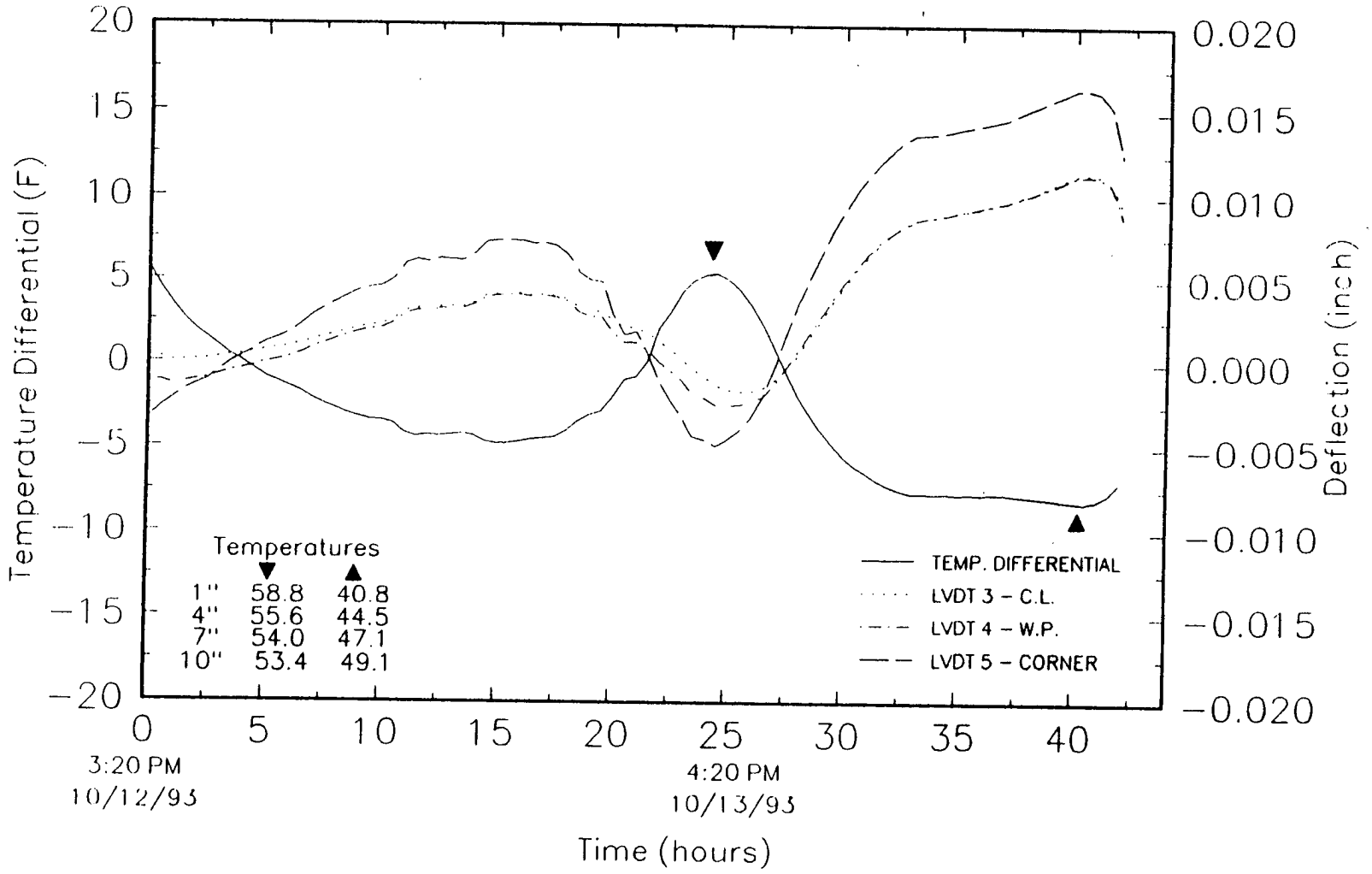

Figure B.11 Slab 2 (60 ft), deflection at joint, Fall, '93

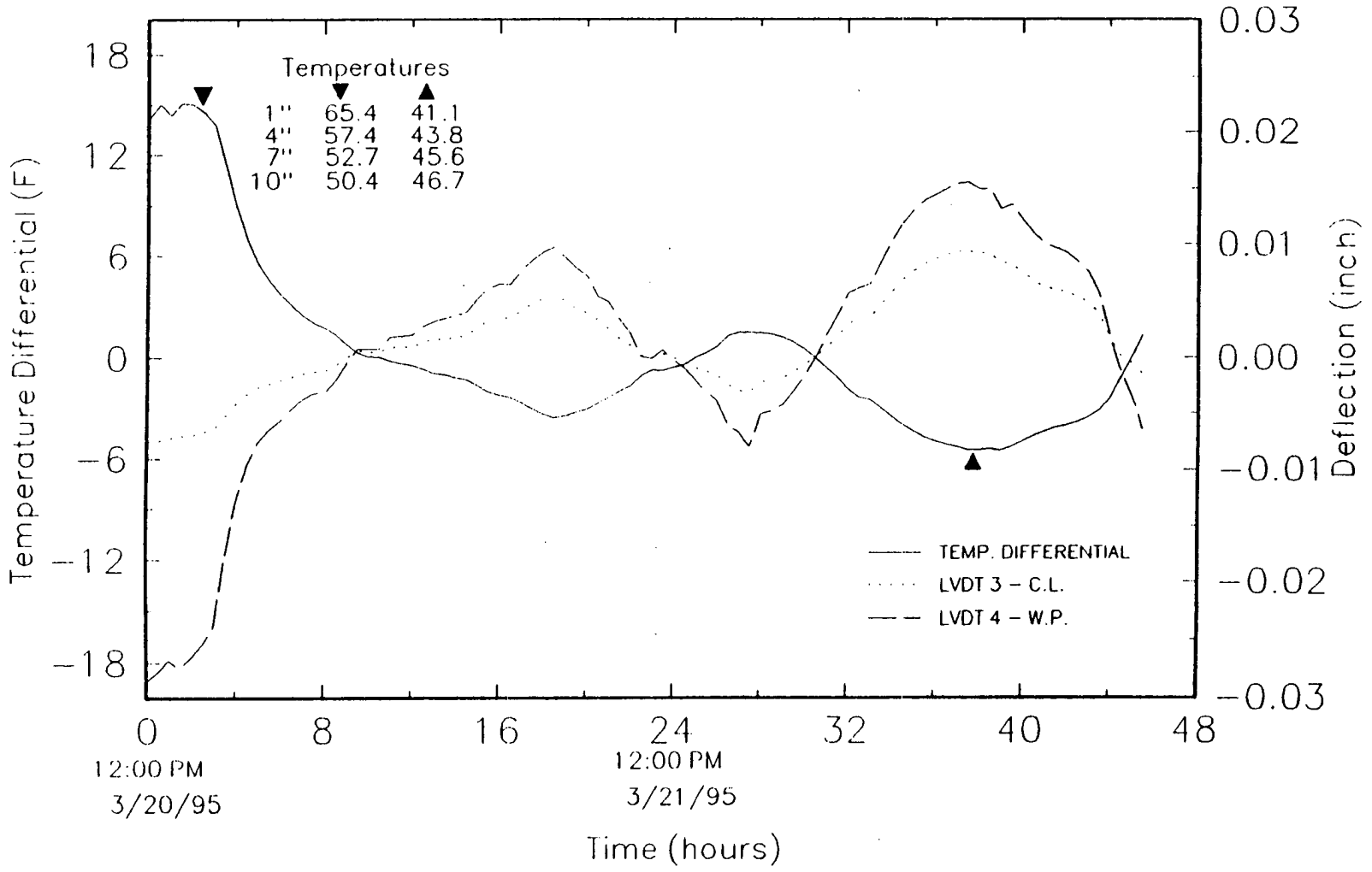

Figure B.12 Slab 2 (60 ft), deflection at joint, Spring, '95

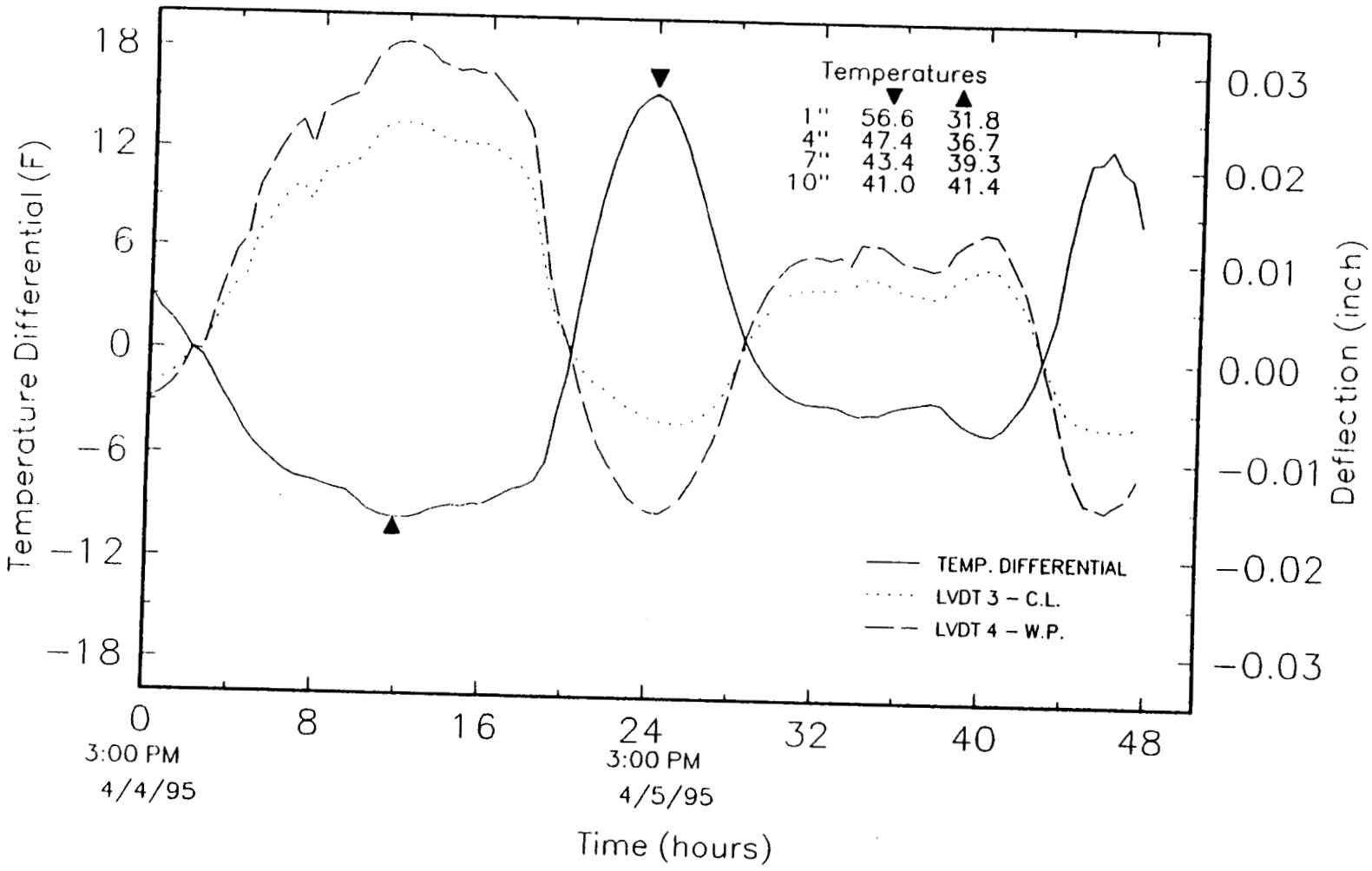

Figure B.13 Slab 3 (60 ft), deflection at joint, Spring, '95

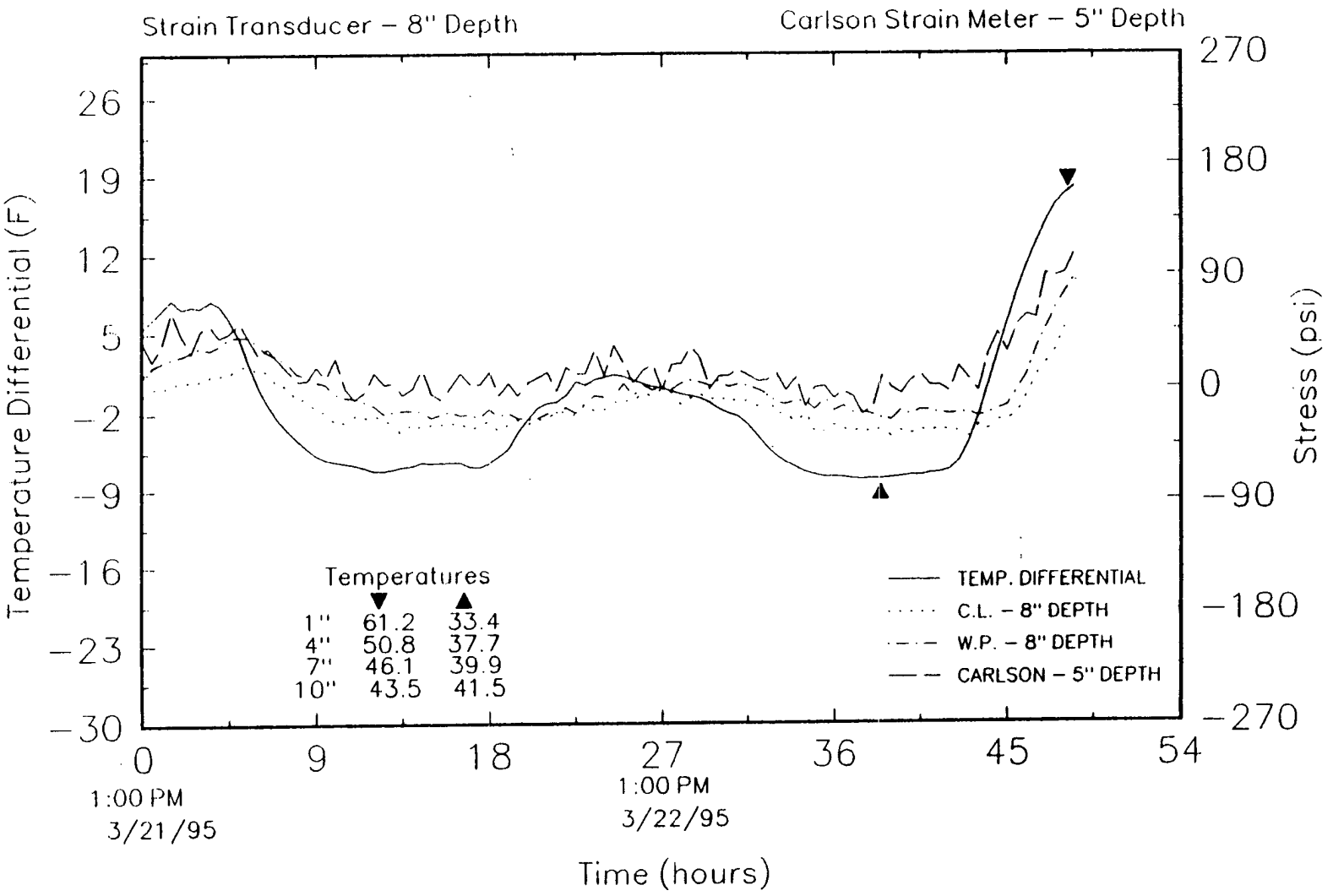

Figure B.14 Slab 4 (40 ft), change in stresses at slab centerline, Spring, '95

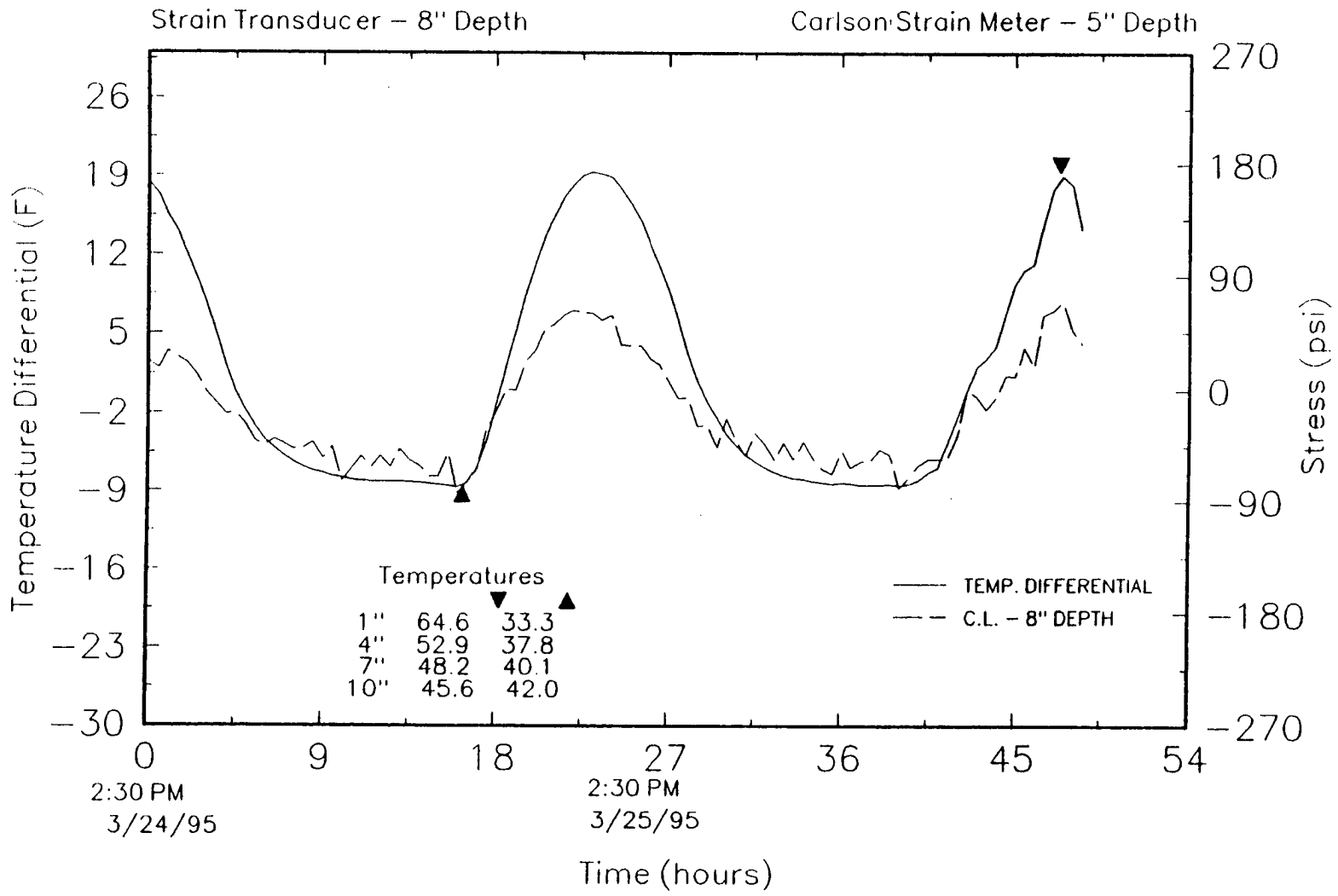

Figure B.15 Slab 5 (40 ft), change in stresses at slab centerline, Spring, '95

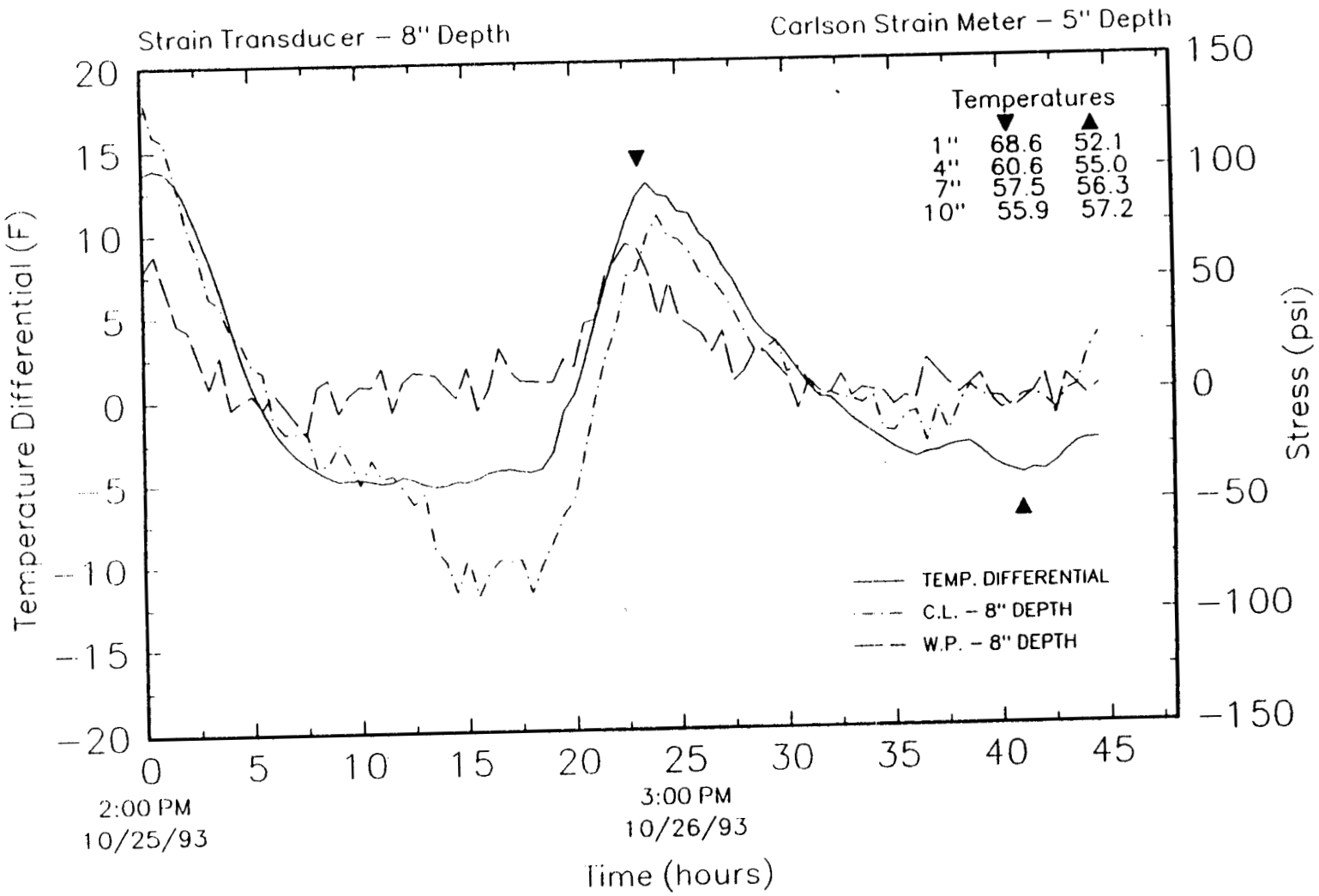

Figure B.16 Slab 5 (40 ft), change in stresses at slab centerline, Fall, '93

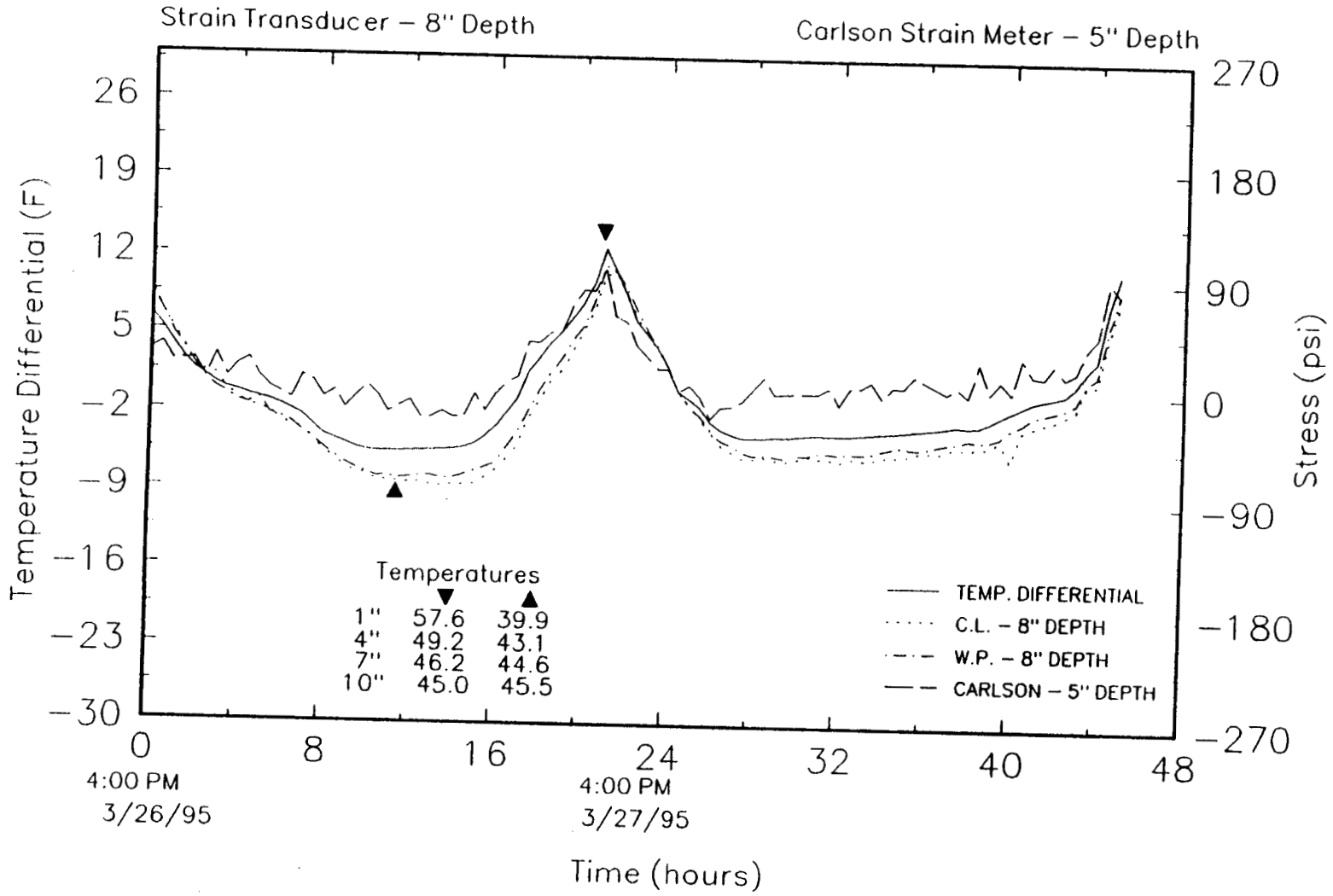

Figure B.17 Slab 6 (40 ft), change in stresses at slab centerline, Spring, '95

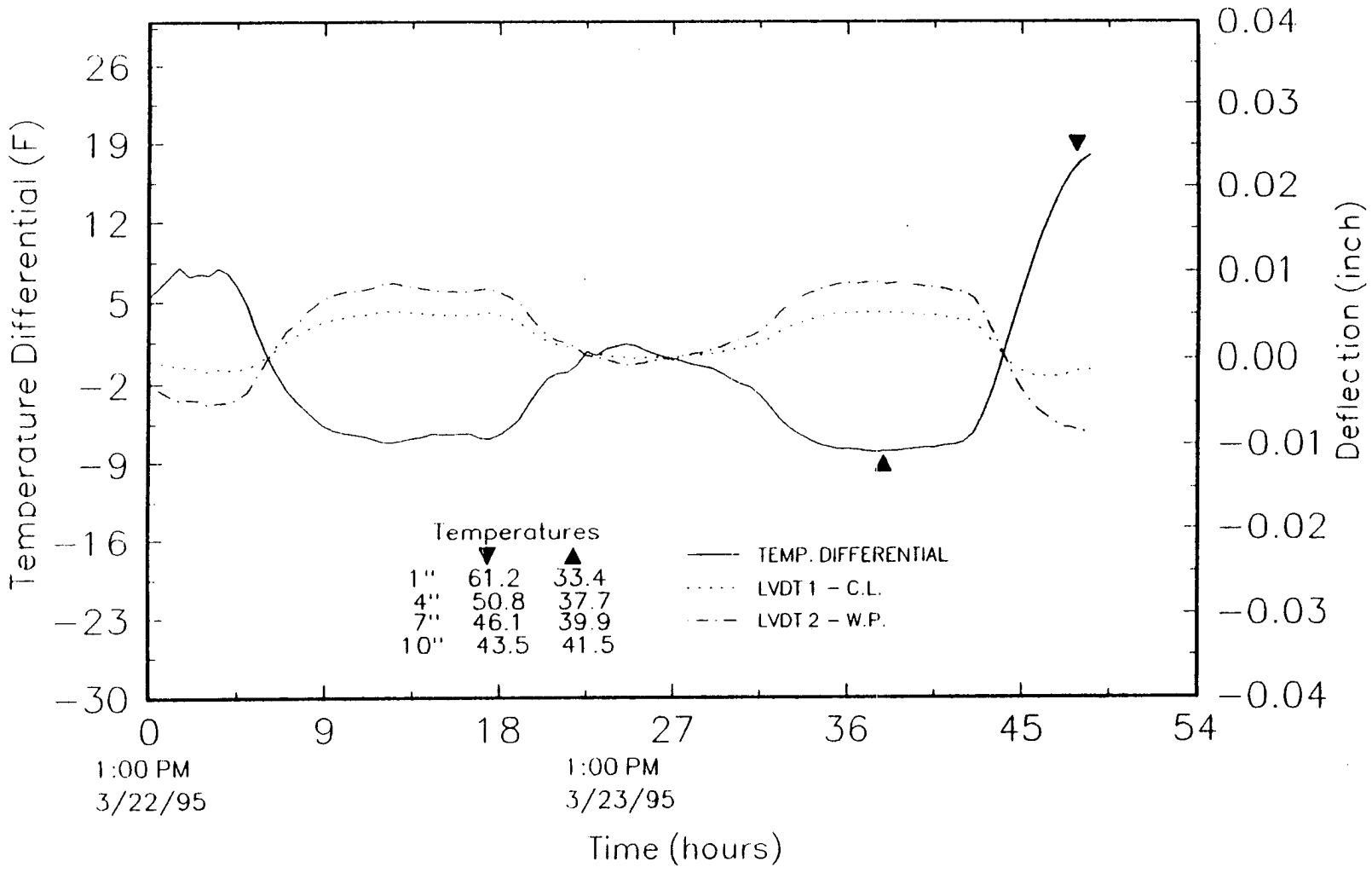

Figure B.18 Slab 4 (40 ft), deflection at transverse centerline, Spring, '95

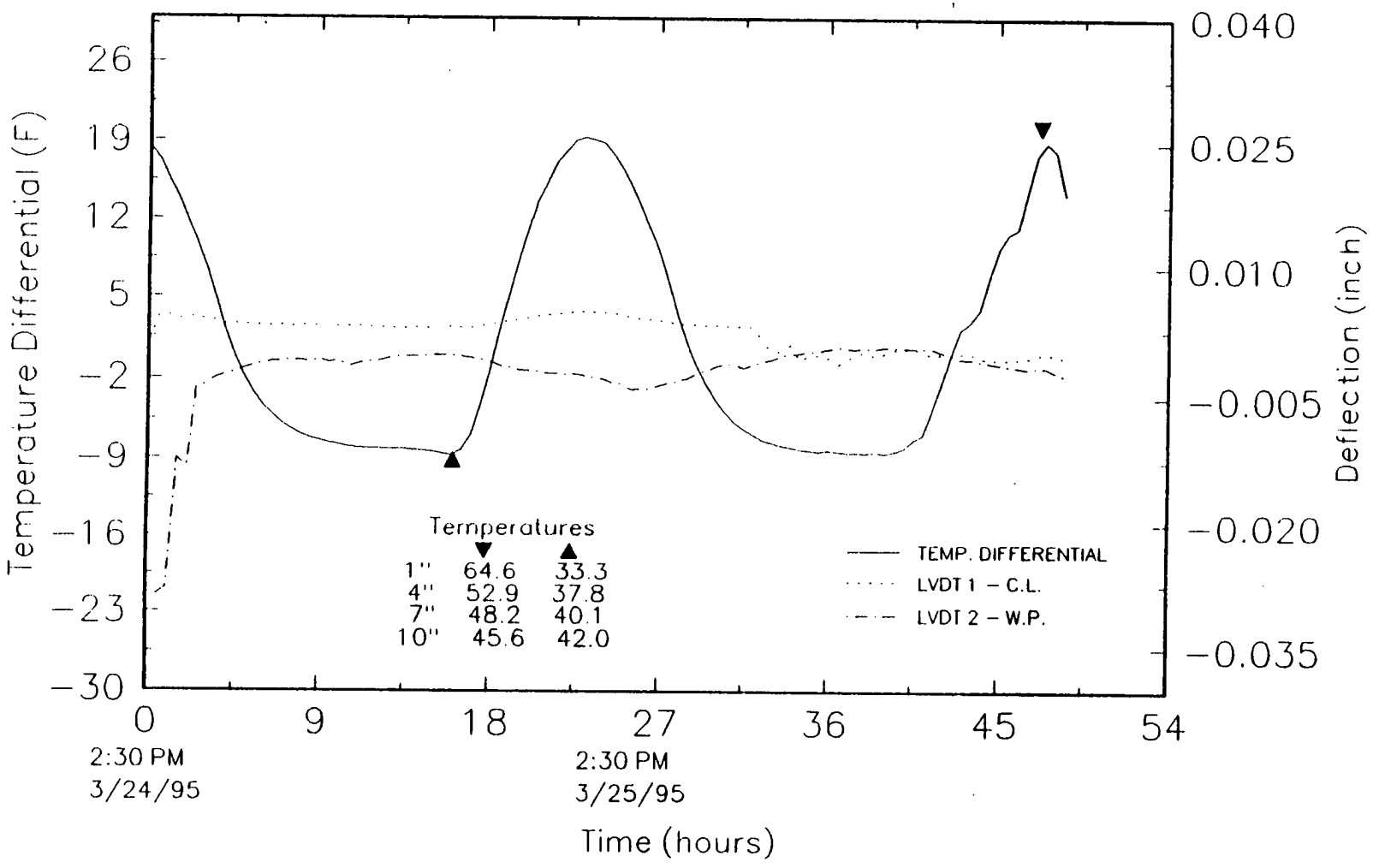

Figure B.19 Slab 5 (40 ft), deflection at transverse centerline, Spring, '95

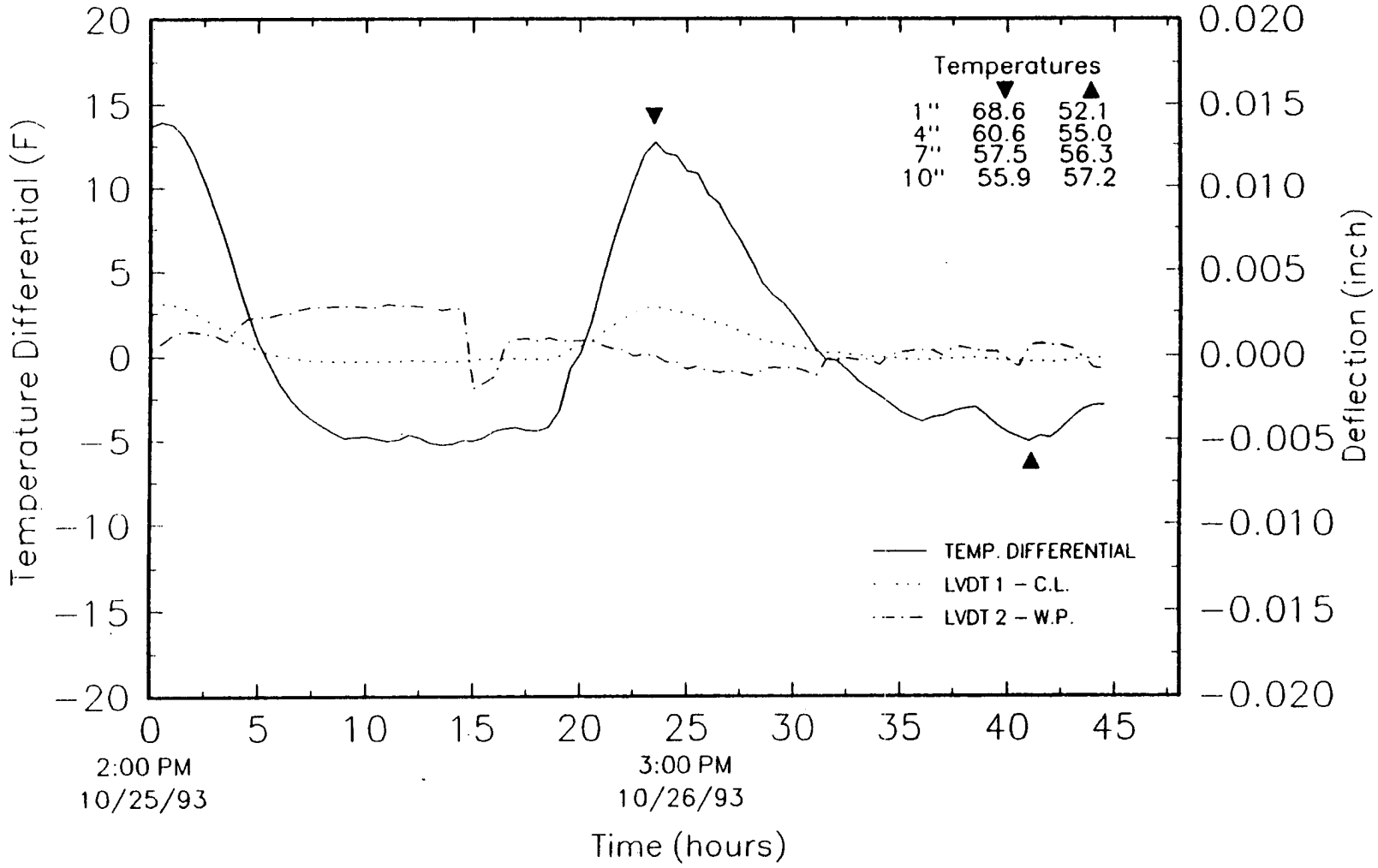

Figure B.20 Slab 5 (40 ft), deflection at transverse centerline, Fall, '93

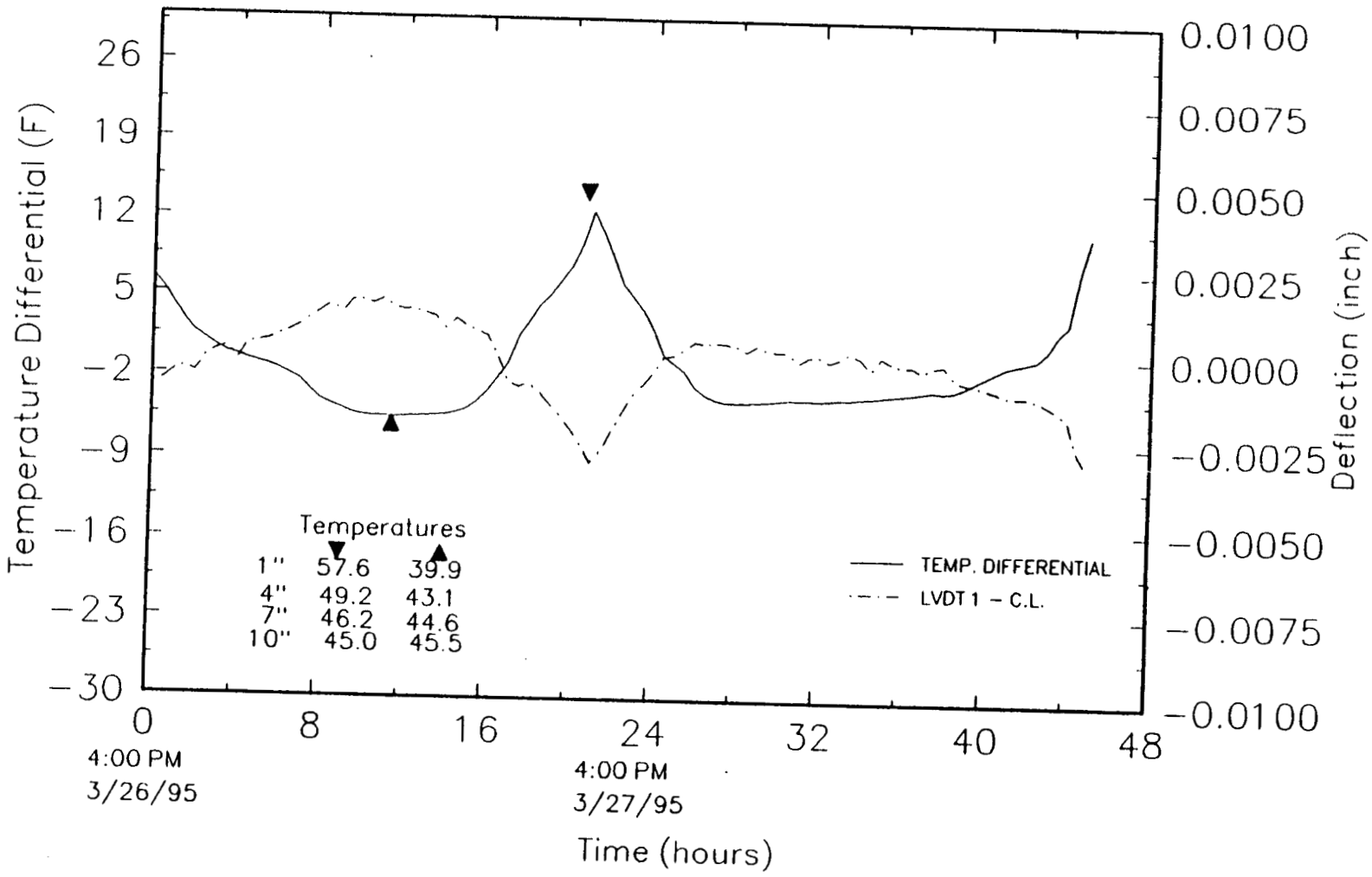

Figure B.21 Slab 6 (40 ft), deflection at transverse centerline, Spring, '95

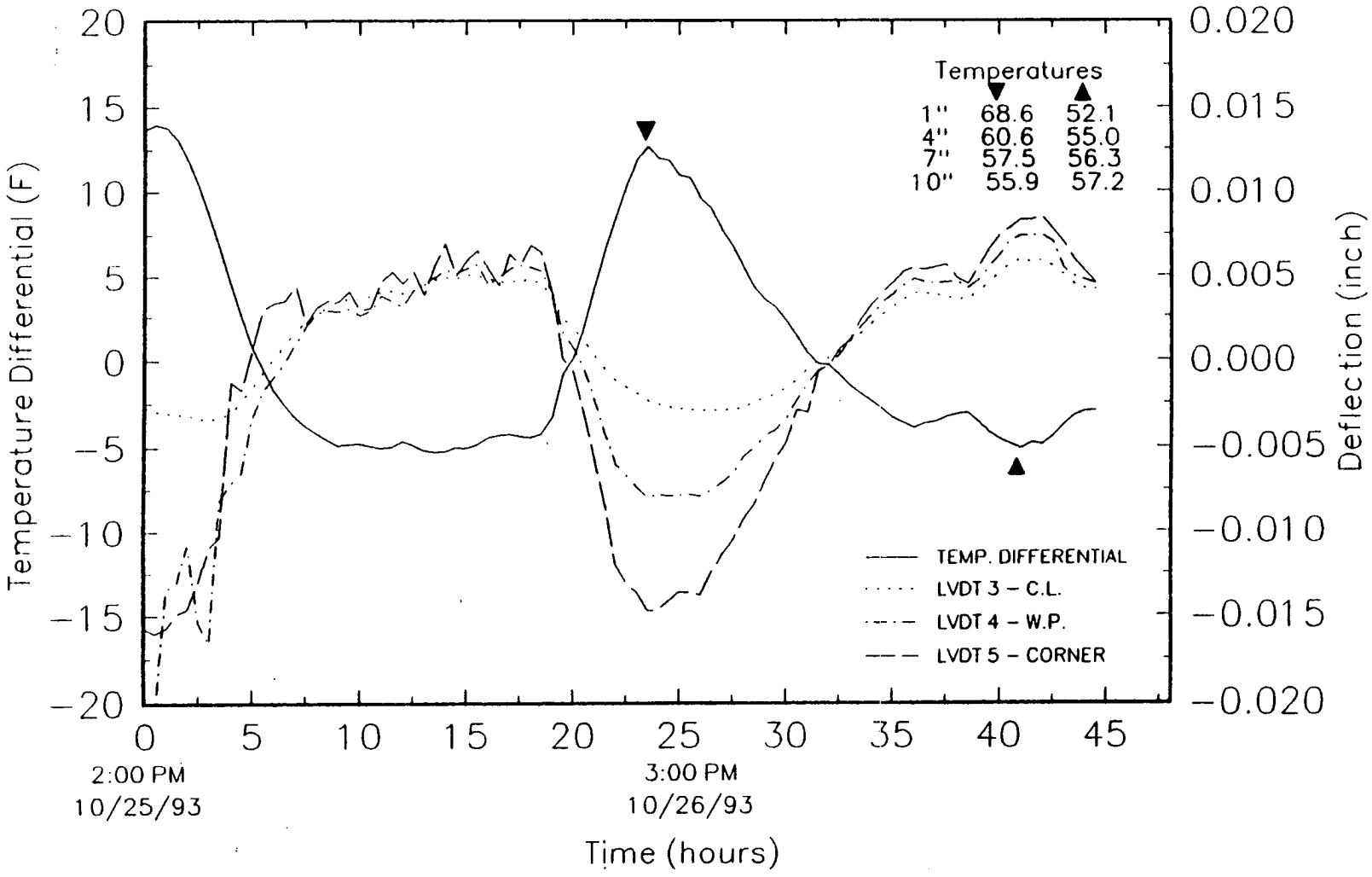

Figure B.22 Slab 5 (40 ft), deflection at joint, Fall, '93

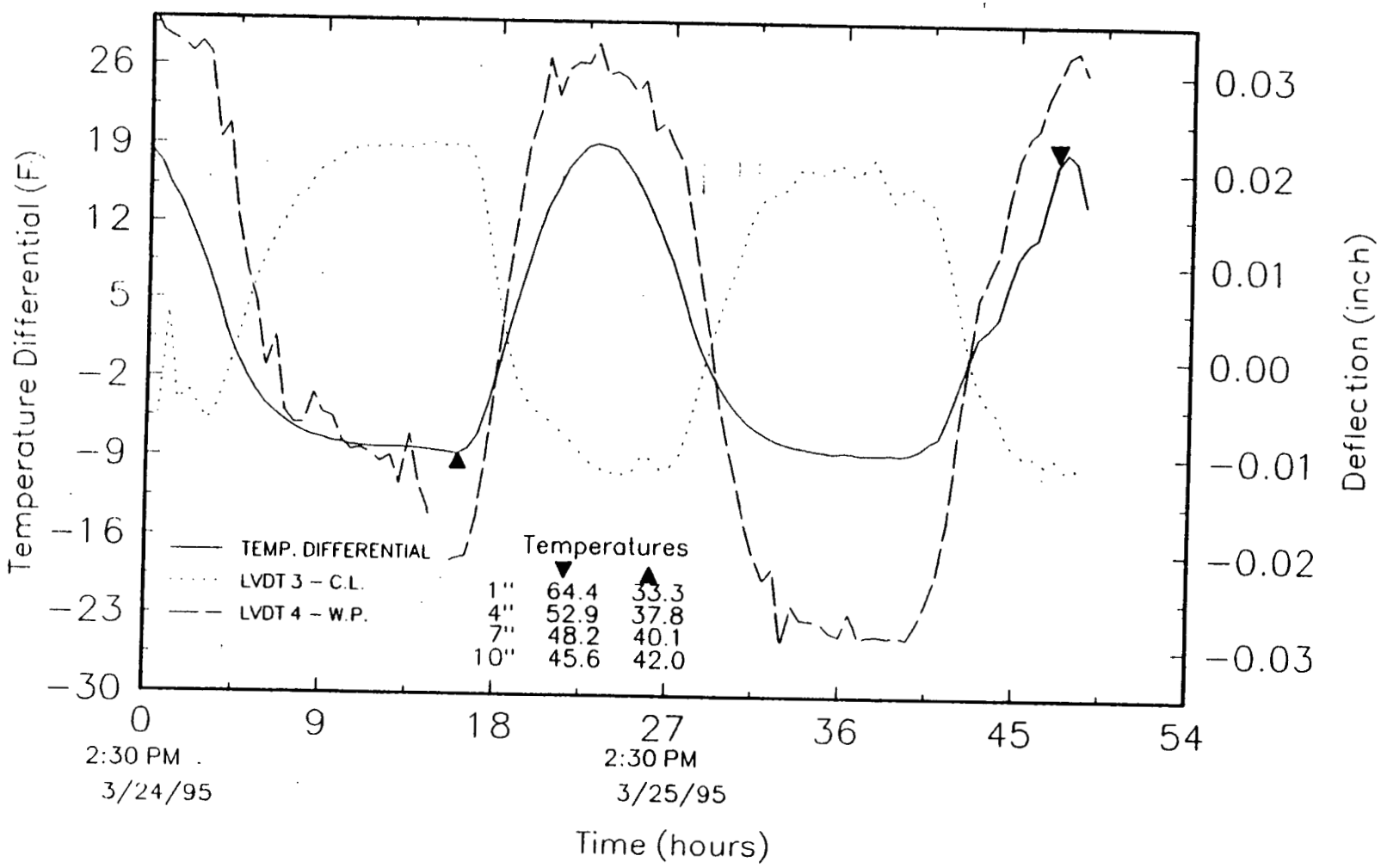

Figure B.23 Slab 5 (40 ft), deflection at joint, Spring, '95

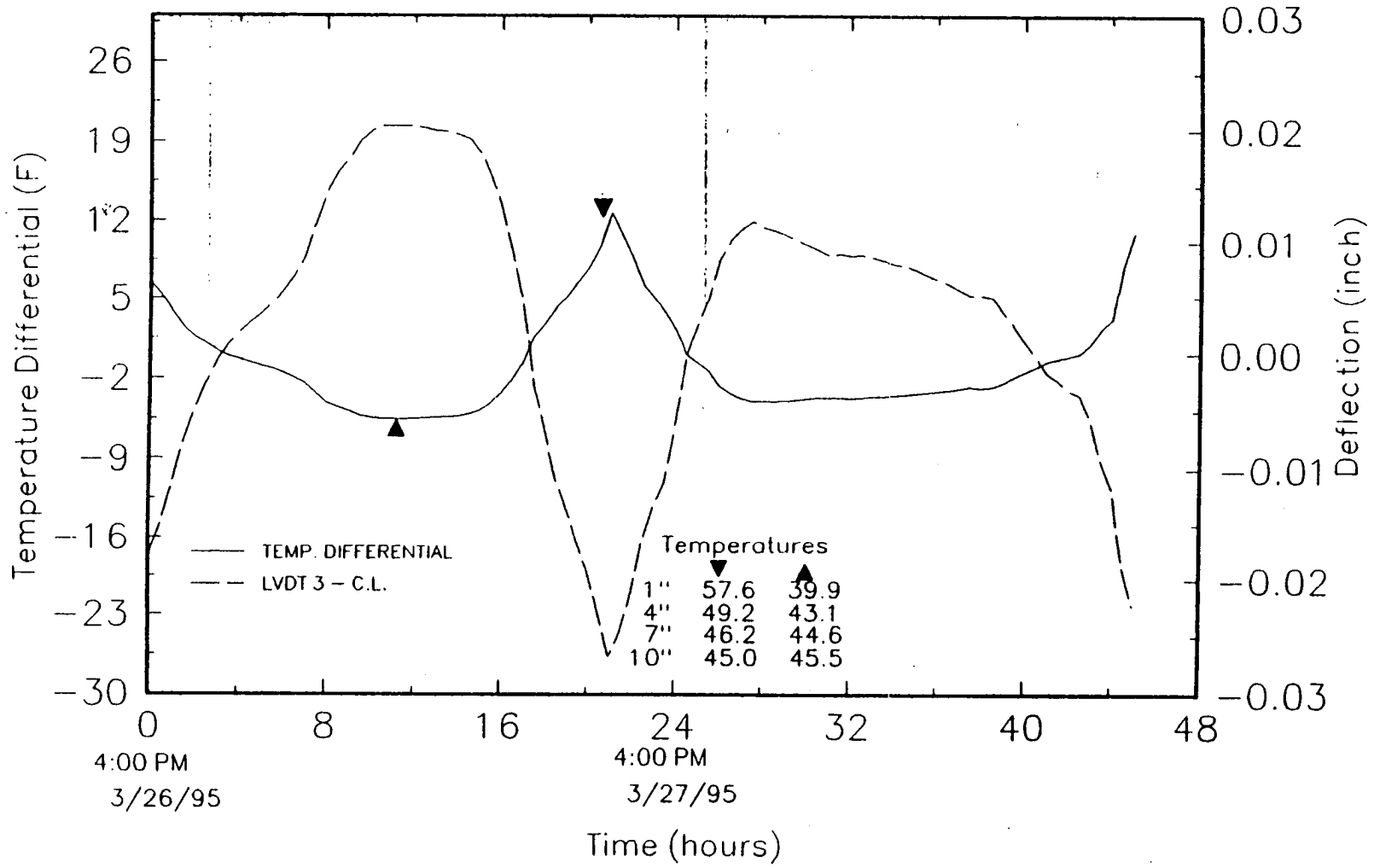

Figure B.24 Slab 6 (40 ft), deflection at joint, Spring, '95

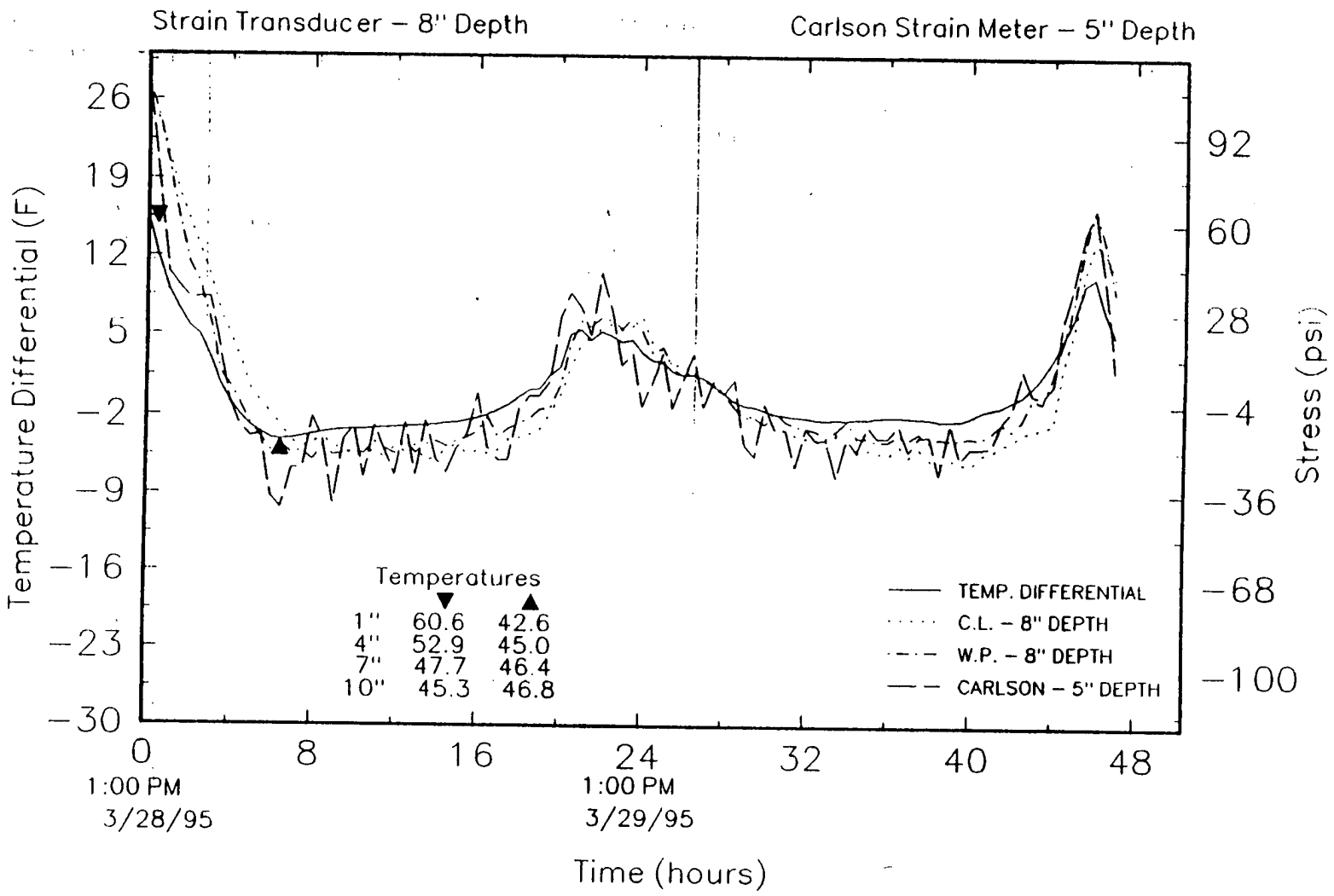

Figure B.25 Slab 7 (21 ft), change in stresses at slab centerline, Spring, '95

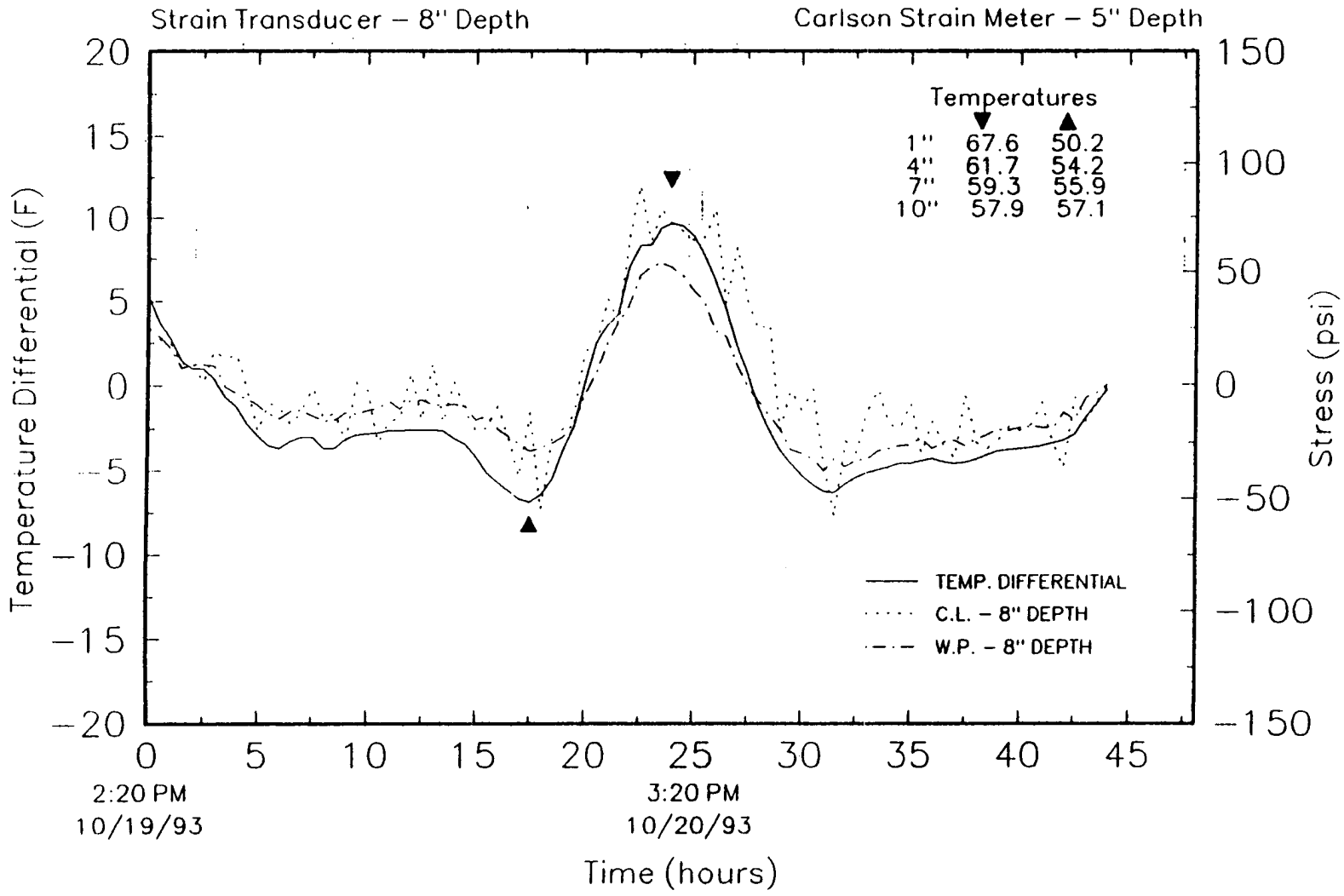

Figure B.26 Slab 8 (21 ft), change in stresses at slab centerline, Fall, '93

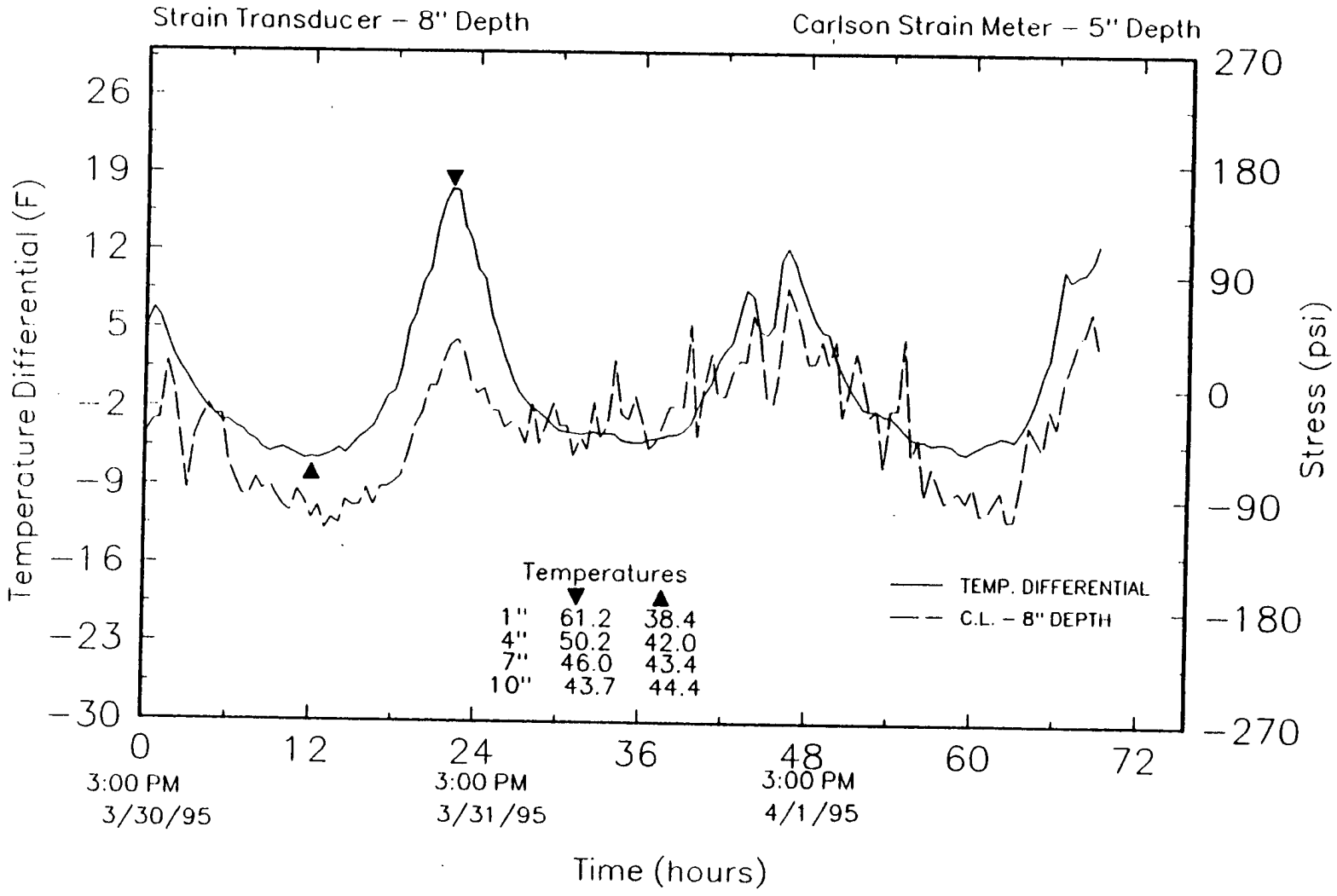

Figure B.27 Slab 8 (21 ft), change is stresses at slab centerline, Spring, '95

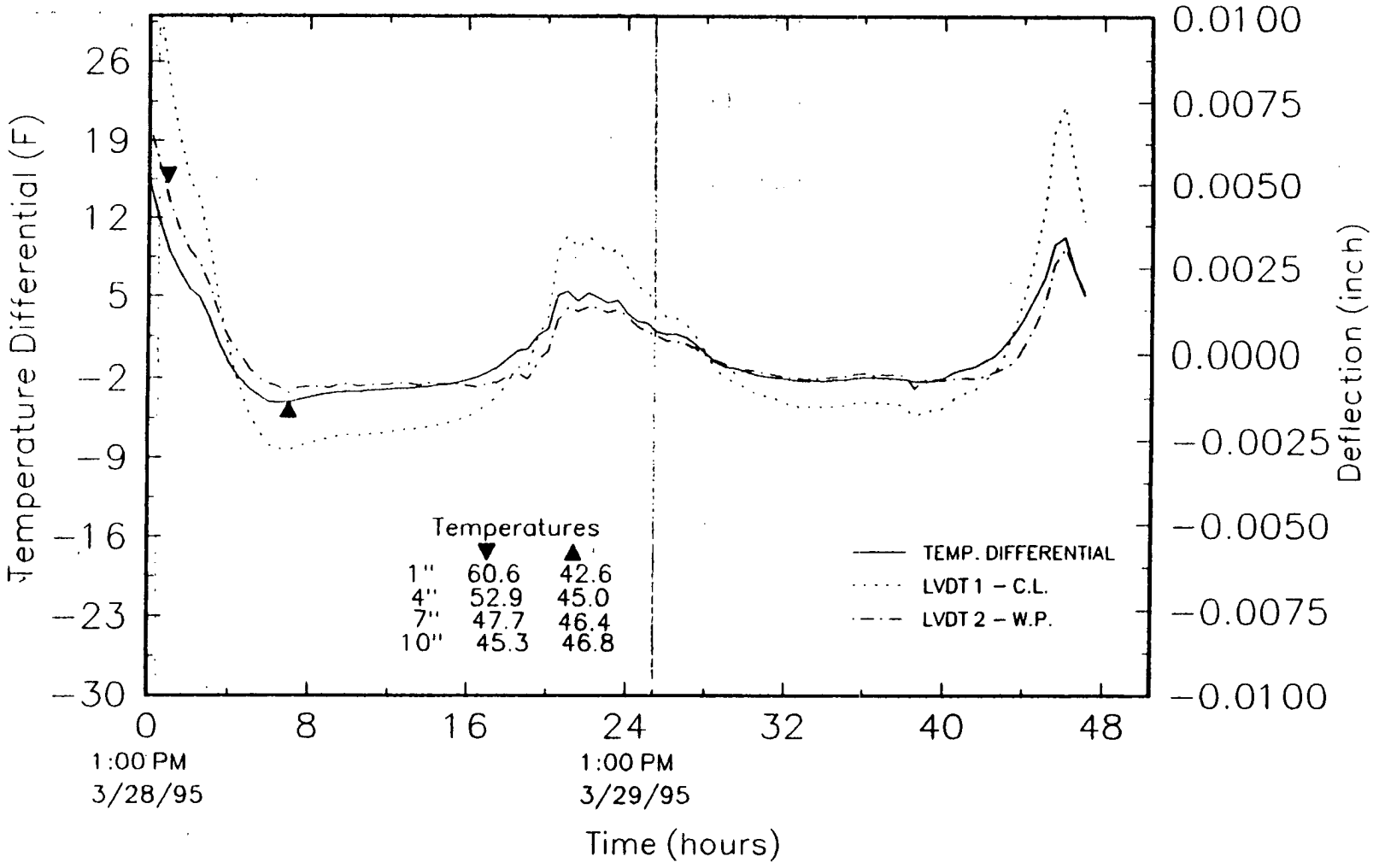

Figure B.28 Slab 7 (21 ft), deflection at transverse centerline, Spring, '95

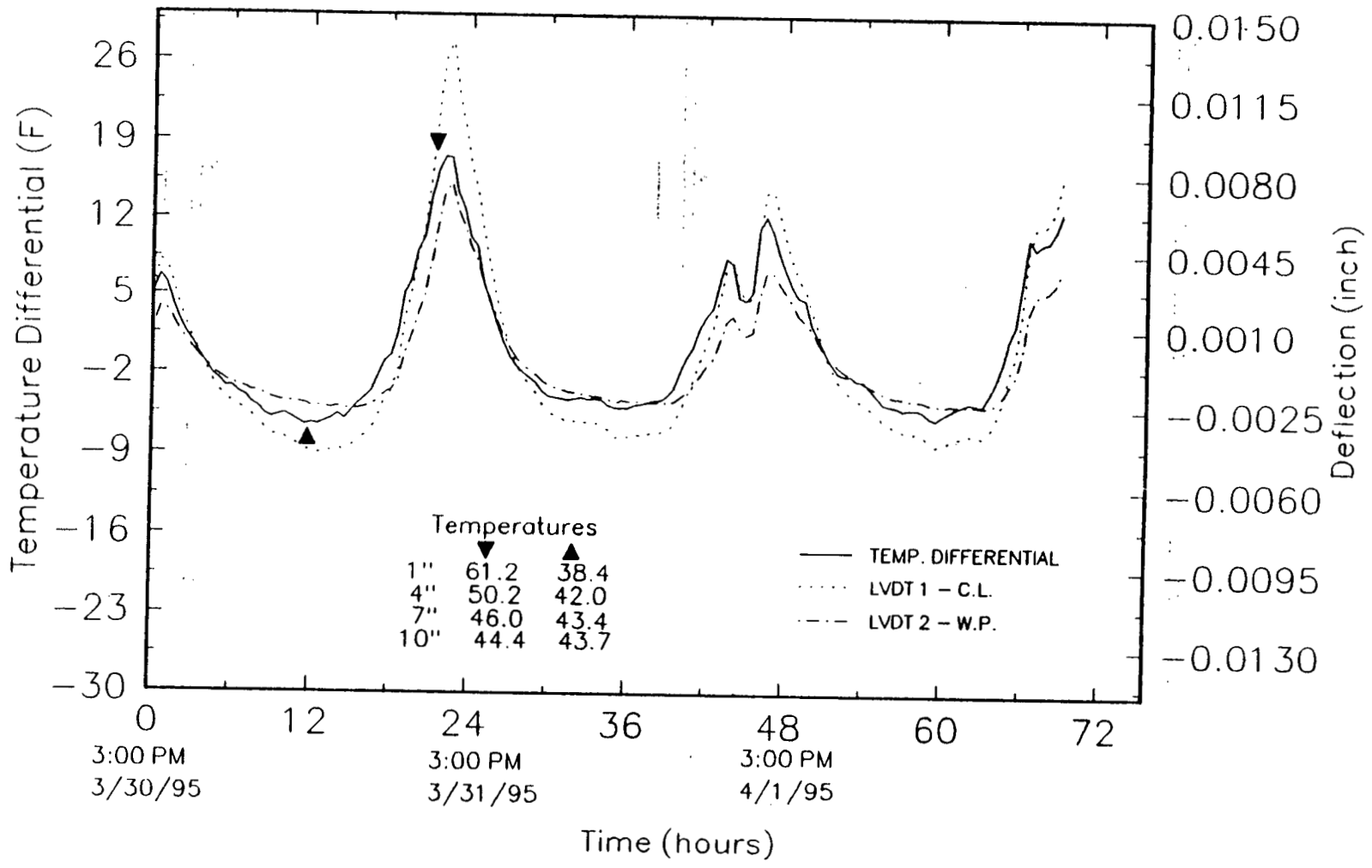

Figure B.29 Slab 8 (21 ft), deflection at transverse centerline, Spring, '95

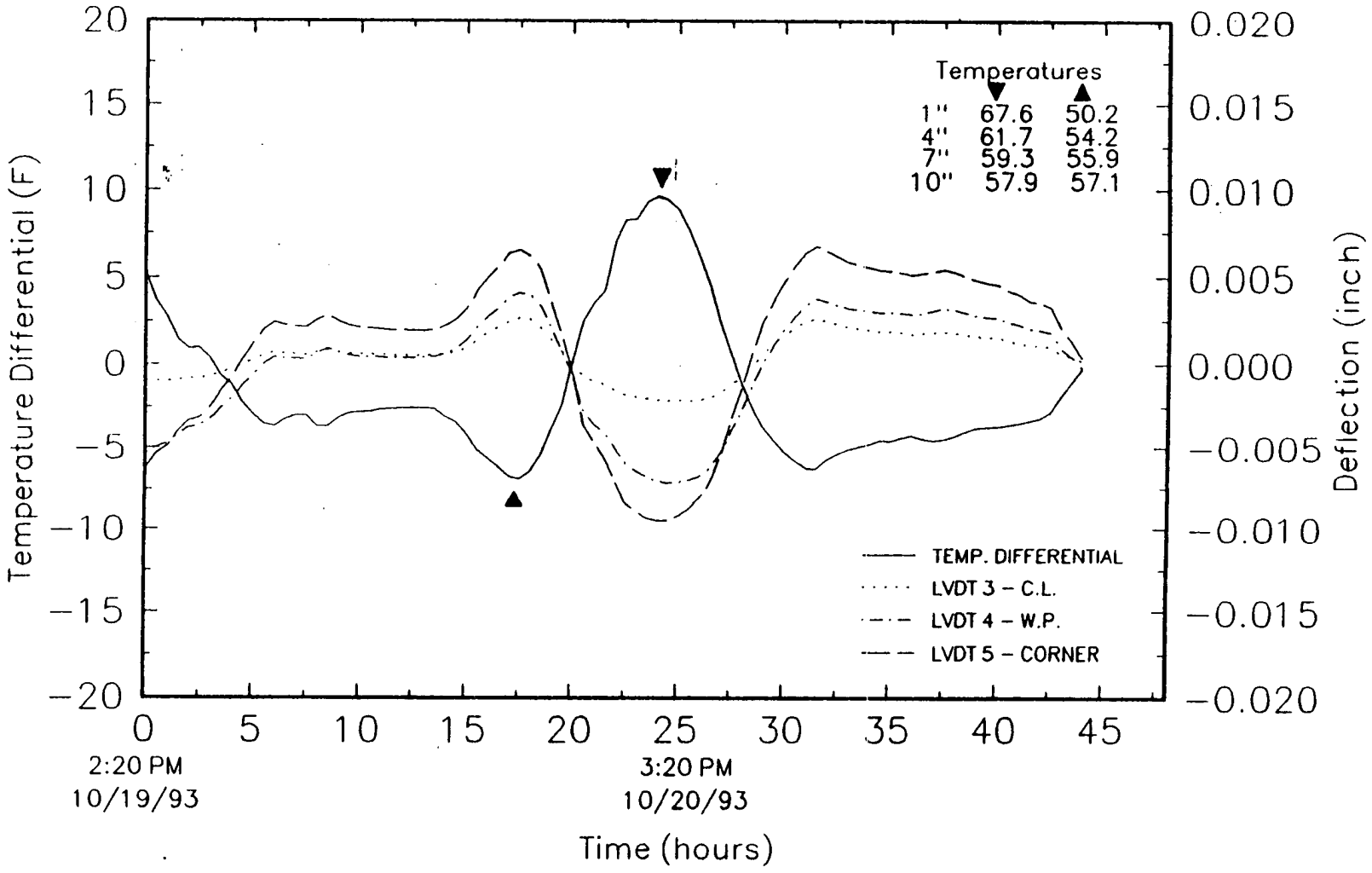

Figure B.30 Slab 8 (21 ft), deflection at joint, Fall, '93

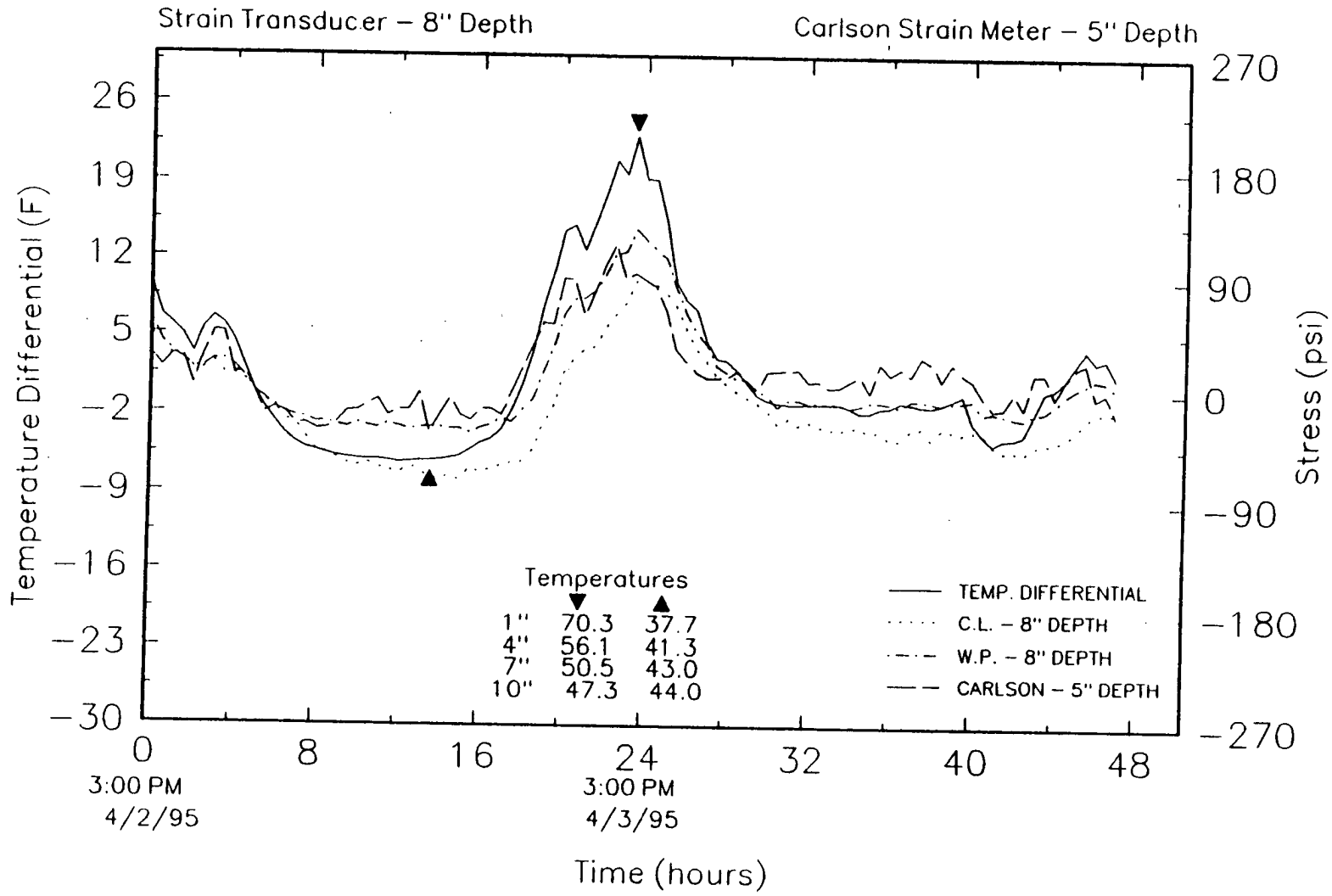

Figure B.31 Slab 9 (21 ft), change in stresses at slab centerline, Spring, '95